THEORETICAL STUDY OF DIRECT CONTACT EVAPORATION OF LIQUID DROPS IN AN IMMISCIBLE LIQUID

A THESIS
SUBMITTED TO
THE COLLEGE OF ENGINEERING
UNIVERSITY OF BASRAH
IN PARTIAL FULFILLMENT OF
THE REQUIREMENTS FOR THE DEGREE OF
DOCTOR OF PHILOSOPHY
IN
MECHANICAL ENGINEERING

By
Ammar Ali Ojimi
(M. Sc. Mech. Eng.)

August 2011

بِسْمِ اللَّهِ الرَّحْمَنِ الرَّحِيمِ

إِنَّ فِي خَلْقِ السَّمَاوَاتِ وَالْأَرْضِ وَاخْتِلافِ اللَّيْلِ وَالنَّهَارِ لَآيَاتٍ لِأُولِي الْأَلْبَابِ

{   } الَّذِينَ يَذْكُرُونَ اللَّهَ قِيَاماً وَقُعُوداً وَعَلَى جُنُوبِهِمْ وَيَتَفَكَّرُونَ فِي خَلْقِ

السَّمَاوَاتِ وَالْأَرْضِ رَبَّنَا مَا خَلَقْتَ هَذَا بَاطِلاً سُبْحَانَكَ فَقِنَا عَذَابَ

النَّارِ {   } رَبَّنَا إِنَّكَ مَنْ تُدْخِلِ النَّارَ فَقَدْ أَخْزَيْتَهُ وَمَا لِلظَّالِمِينَ مِنْ أَنْصَارٍ

{   } رَبَّنَا إِنَّنَا سَمِعْنَا مُنَادِياً يُنَادِي لِلْإِيمَانِ أَنْ آمِنُوا بِرَبِّكُمْ فَآمَنَّا رَبَّنَا فَاغْفِرْ

لَنَا ذُنُوبَنَا وَكَفِّرْ عَنَّا سَيِّئَاتِنَا وَتَوَفَّنَا مَعَ الْأَبْرَارِ {   } رَبَّنَا وَآتِنَا مَا وَعَدْتَنَا

عَلَى رُسُلِكَ وَلا تُخْزِنَا يَوْمَ الْقِيَامَةِ إِنَّكَ لا تُخْلِفُ الْمِيعَادَ {   }

العَظِيْم

آيات من سورة آل عمران المباركه

DEDICATION

Dedicated

to my family,

and

anyone looking forward completion this work.

Certification

I certify that this thesis is prepared under my supervision at the University of Basrah, as a partial requirement for the degree of Doctor of Philosophy in Mechanical Engineering.

Signature:

Name: Prof. Dr. Abdul-Muhsin A. Rageb

(Supervisor)

Data: /   /2011

In view of the available recommendations, I forward this thesis for debate by the examining committee.

Signature:

Name: Ass. Prof. Ali A. Monem

(Head of Mech. Eng. Dept.)

Data: /   /2011

Examining Committee's Report

We certify that we have read this thesis titled "**THEORETICAL STUDY OF DIRECT CONTACT EVAPORATION OF LIQUID DROPS IN AN IMMISCIBLE LIQUID**" which is being submitted by **Ammar Ali Ojimi** and as examining committee, examined the student in its contents. In our opinion it is adequate, as a thesis for the degree of Doctor of Philosophy in Mechanical Engineering.

Signature:

Name: Prof. Dr. Abdul-Muhsin A. Rageb

      (Member and Supervisor)

Data: /   /2011

Signature:

Name: Ass. Prof. Dr. Abdulwadood S. Shihab

      (Member)

Data: /   /2011

Signature:

Name: Ass. Prof. Dr. Khudheyer S. Mushatet

      (Member)

Data: /   /2011

Signature:

Name: Ass. Prof. Dr. Qais A. Rishack

      (Member)

Data: /   /2011

Signature:

Name:Prof. Dr. Haroun A. K. Shahad

      (Chairman)

Data: /   /2011

Signature:

Name: Ass. Prof. Dr. Salman H. Hammadi

      (Member)

Data: /   /2011

Approved of College of Engineering

Signature:

Name: Prof. Dr. Nabeel A. Jassim

(Dean of Engineering collage)

Data: /   /2011

ACKNOWLEDGMENTS

I

Abstract

The present work is a comprehensive theoretical investigation of the direct contact evaporation process of drops, which is growing because of change of phase, in an immiscible liquid. The attempt here is to gain fundamental understanding of the transport processes (hydrodynamic and heat transfer) that take place during the direct contact evaporation process.

A theoretical model based on continuity, motion, momentum and energy equations in addition to the energy balance equation is developed, by using cellular model. This model aims to obtain characteristics of the direct contact evaporation of a single droplet bounded by a spherical cell of continuous liquid. Furthermore, these characteristics are used in order to develop a theoretical model aims to obtain the characteristics of the direct contact evaporation of multidroplets.

The fluid dynamic associated with the growth and translation of drops was treated. The developed equations were derived and then solved simultaneously applying a numerical method. The energy equations with the potential flow velocity obtained from the fluid flow solution, taken into account the effect of the interaction between the adjacent drops, have been numerically solved using finite-difference techniques.

The calculations are performed for n-pentane drops evaporating in distilled water.

Results are presented for two cases: single and multidroplets evaporation. For the first case, the predicted results are presented in terms of the relative velocity and evaporative drobbles position, the radius

and average density ratio, the vaporizing angle (half opening angle), and the specific heat transfer coefficient. The results indicated that the main parameters affecting the evaporation process were the initial size of droplets and the degree of superheat.

For the second case, the theoretical results presented in terms of the dispersed phase holdup, the relative velocity and evaporative drobbles position, the average volumetric heat transfer coefficient, and the total time and height for complete evaporation. Also, a detailed analysis of the influence of several important parameters, such as the initial size of droplets, the degree of superheat, the column diameter and the diameter and number of holes on the evaporation characteristics were presented.

The results of the present model, for the two cases, were compared with the existing theoretical predictions; the agreement between the results was good. Also, the results were compared with the experimental results obtained by other authors and acceptable agreement was found.

Table of Contents

List of Symbols

Symbols	Description	Units
A	Cross-sectional area of the column	m^2
A_d	Droplet surface area	m^2
a	Parameter defined by equation (3.66)	
B	Dimensionless radius, R/R_0	
C_d	Drag coefficient	
C_p	Specific heat capacity	J/kg.K
D	Instantaneous diameter of drobble	m
D_0	Initial diameter of drobble	m
D_{cell}	Diameter of Spherical cell of continuous liquid	m
d_c	Column diameter	m
d_h	Hole diameter	m
DRC	Density ratio between dispersed liquid and continuous liquid, (ρ_{dl}/ρ_c)	
DRD	Density ratio between dispersed vapor and dispersed liquids, (ρ_{dv}/ρ_{dl})	

E	Non-dimensional parameter, $(1-\varepsilon)/(1-\varepsilon^{5/3})$	
Fr_0	Initial Froude number , $U_0^2/(2R_0 g)$	
G	Density ratio, (ρ_{av}/ρ_c)	
g	Gravitational acceleration	m/s^2
H	Height of liquid layer in drobble	m
h_{fg}, h_{fgd}	Latent heat of evaporation of dispersed phase	J/kg
h, h_d	Heat transfer coefficient	W/m^2.K
$h_{v,z}$	Local volumetric heat transfer coefficient	W/m^3.K
h_{mv}	Average volumetric heat transfer coefficient	W/m^3.K
h_{mvf}	Average volumetric heat transfer coefficient for complete evaporation	W/m^3.K
Ja	System Jacob number, $\rho_c C_{pc} \ T/(\rho_{dv} h_{fgd})$	
k	Thermal conductivity of continuous liquid	W/m.K
k_{dl}	Thermal conductivity of dispersed liquid	W/m.K
$\bar{m}$	Added mass	kg
m_{00}	Mass of growing drobble	kg
$\dot{m}$	Mass flow rate	kg/s
N_h	Number of holes (orifices) in the distributor	
N_d	Number density of drobbles	m^{-3}
Nu	Nusselt number , $(h\ D/k)$	
Pe	Peclet number , $(2UR/\alpha)$	
Pe	Modified Peclet number , $(2UR_0/\alpha)$	
Pe_0	Initial Peclet number , $(2U_0 R_0/\alpha)$	
Pr	Prandtl number of continuous liquid , (ν/α)	
Q	Rate of heat transfer	W
Q_c	Rate of convective heat transfer	W

q	Heat flux	W/m^2
$q_{\theta}^{''}$	Local Heat flux	W/m^2
R	Instantaneous radius of drobbles	m
R_{cell}	Radius of Spherical cell of continuous liquid	m
r	Radial coordinate	m
Re	Reynolds number , $(2\rho_c UR/\mu_c)$	
Re_0	Initial Reynolds number , $(2\rho_c U_0 R_0/\mu_c)$	
S	equilibrium spreading coefficient	
St	System Stefan number,$(C_p \; T/h_{fgd})$	
T	Temperature	K
t	Time	s
U	Instantaneous velocity of rising droplet	m/s
U_r	Instantaneous relative velocity of droplet	m/s
U_0	Initial velocity of droplet	m/s
U_d	Superficial velocity of dispersed phase	m/s
V	Volume	m^3
$\dot{V}$	Volumetric flow rate	m^3/s
$\dot{V}_d$	Volumetric flow rate of dispersed phase	m^3/s
$v_{r'}$ v_{θ}	Radial and tangential components of U_r	m/s
y	Transformed Coordinate, *(r-R)/R*	
Z	Height of evaporation (axial displacement), Column height	m
Z_f	Value of Z for complete evaporation	m

Creek Symbol

Symbols	Description	Units
α	Thermal diffusivity of continuous liquid	m²/s
$β$	Half opening angle of vapor phase in drobble	rad
T	Temperature difference(degree of superheat), $T_c - T_{ds}$	K
$ε$	Void fraction or holdup (dispersed phase volume fraction)	
$ζ$	Vaporization ratio	
$θ$	Spherical polar coordinate	rad
	Non-dimensional temperature, $((T - T_c)/(T_{ds} - T_c))$	
$μ$	Transformed coordinate,$(-cos(θ))$	
$μ_c$	Viscosity of continuous liquid	kg.m/s
$ν$	Kinematics viscosity of continuous liquid	m²/s
$ρ$	Density	kg/m³
$σ$	Surface tension	N/m
$τ$	Dimensionless time, $(αt/R_0^2)$	
$φ$	Velocity potential	m²/s

Subscript

Symbol	Description
av	Average
c	Continuous liquid
cd	Continuous/dispersed liquid interface
cell	Spherical cell of continuous liquid
d	Droplet
ds	Dispersed liquid (saturation)
dl	Dispersed Liquid phase
dv	Dispersed vapor phase
j ,k	General grid point
f	Final
0	Initial value

Superscript

Symbol	Description
+	Dimensionless
i	Time grid point

Chapter One

INTRODUCTION

Chapter One

Introduction

1.1 General:

A process in which an exchange takes place at the interface of two substances in contact with on another is called a direct contact process. One of the most common direct contact processes is heat transfer which involves the transfer of thermal energy from one material to another as the result of a temperature gradient.

Direct contact heat transfer can occur whenever two substances at different temperatures touch each other physically. The implication is that there is not an intervening wall between the two substances. Heat transfer where there is a surface between the two streams is sometimes called indirect, or the heat transfer device is one of the closed types [1].

The physical interaction of the two streams can accomplish heat transfer very efficiently. Without an intervening wall, the energy transport between the two streams can take place across small thermal resistances. In addition, the fact that a wall is not present can also allow a mass transfer process to take place. In some cases, this is a desirable phenomenon (open cooling towers), but in other cases it may be not.

The advantages of direct contact heat transfer over indirect transfer in a tubular exchanger are noteworthy. The most striking advantage is seen when overall coefficients are compared; direct contact coefficient, based on superficial liquid curtain area, may range up to 100 times greater than those for indirect transfer, based on tube heating area [2]. Thus, if rapidity of heating or cooling is a design criterion, direct contact heat exchange methods merit consideration.

Costs are often more favorable for direct contact heat transfer devices than for their closed counterparts. The thermal resistances present in closed heat exchangers result in less heat transfer than might be accomplished in direct contact, and this often translates to lower operating costs for the latter. In addition, the equipment to accomplish the direct contact processes is generally less expensive than the counterpart closed heat exchangers. Both aspects can result in considerable life-cycle cost savings for the direct contact approach over that of the closed type of heat exchanger. Some potential limitations are inherent in direct contact processes. There is a requirement that the two streams be at the same pressure. Although this requirement does not often cause significant problems, it could be very important. Also, as noted above, the mass transfer possibility in direct contact may not be desirable [1].

1.2 Direct-Contact Heat Transfer Mechanisms:

While direct-contact processes are most conveniently categorized according to the physical characteristics and phases of the fluids involved, it is sometimes of value to make distinctions also according to the details of the heat transfer mechanisms present. In all cases, it is useful to consider the physical situation to be one of a continuous fluid in direct contact with a dispersed fluid. The dispersed fluid will be assumed to be in distinct masses surrounded by a bulk, continuous phase. These masses can be approximated as spherical forms under special circumstances, but normally they are of a non-spherical geometry. They will be referred to as particles in what follows [3].

It is helpful to consider the heat transfer mechanisms and in some situations also the fluid dynamics present. This approach will give an additional way of visualizing details of the direct-contact process. To do this, we consider the external and the internal heat transfer mechanisms separately. External and internal refer here, respectively, to outside of dispersed phase particles and

inside of the dispersed phase, that is, in the adjacent continuous phase. Figure 1.1 illustrates the processes schematically.
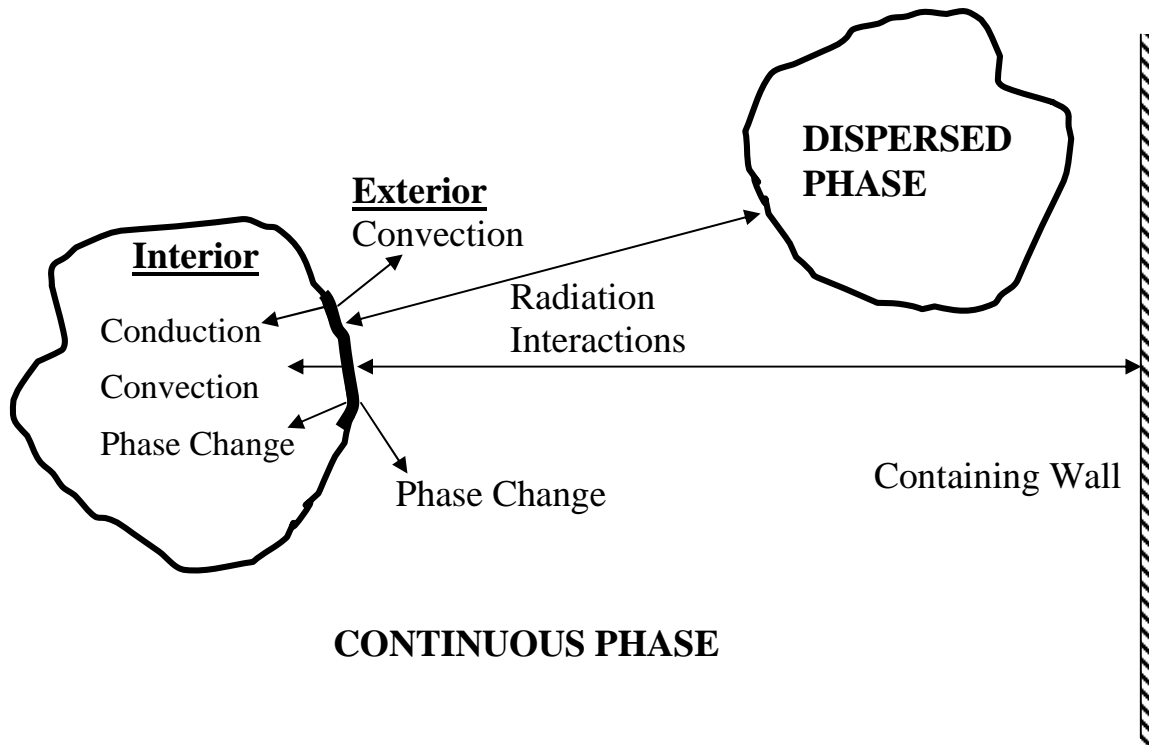
Figure 1.1: Schematic diagram for classifying direct contact processes[3].

1.2.1 The External Mechanisms of the Direct-Contact Heat Transfer Process:

These are the processes, by which the particle transmits energy to, or receives energy from, the bulk fluid or surrounding surfaces. Typically, this is a convection process, but under special circumstances, it can be by conduction, phase change, or radiation. A forced flow in fluidized beds can be accompanied by intense turbulence, but in gravity-driven systems, the external flow is usually laminar or only moderately turbulent. Conduction is dominated when fluid in the external flow is laminar and has a large thermal conductivity.

The convective process in the continuous medium, as in bubble columns, is a conventional process that has been extensively studied. To describe this transfer mechanism and, in many cases, the overall performance, it is important to understand the convection/conduction process in flow over a single particle of arbitrary shape. Consideration of the enhancement or degradation of heat transfer to the continuous phase due to the interaction of an ensemble of dispersed particles is the second most important aspect.

Radiation in the external region is a special case and it is important when the particles are at a high enough temperature to radiate appreciably to the surrounding walls and to other particles. If the continuous phase is a liquid, radiation is not important. Because of their "special case" characteristics, configurations that involve radiation as the major means of transport usually require a quite different analysis than any of the other situations[3].

Phase change of the continuous phase fluid due to heating or cooling by the particles occurs in a small percentage of cases. This includes situations where water (as the continuous fluid) evaporates into air bubbles (as the dispersed fluid) that are traveling in the water. An example of this is the injection of air streams into a cooling pond to enhance the removal of waste heat by both convection and phase change.

Evaporation is just one example of a whole group of important phenomena that involve heat and mass transfer simultaneously. As noted earlier, mass transfer operations have been the genesis for much of the equipment used in direct-contact heat transfer applications. In all cases of direct-contact heat transfer, the possible effects of mass transfer must be considered. Sometimes, mass transfer effects are negligible, and sometimes they have a profound impact on the overall process.

1.2.2 The Internal Mechanisms of the Direct-Contact Heat Transfer Process:

Inside the dispersed phase particles, one of three possible situations is found to take place during the heat transfer process: conduction, convection, and phase change. While more than one process can occur at a given time, the relative magnitudes of the heat transfer rates of the three mechanisms are usually so different which one dominates.

Conduction always is dominated inside solid particles but can also be significant in liquid and sometimes in vapor particles when the particle is small. Convection can occur inside the particle under certain condition. To have convection the particle must be liquid or vapor, and there must be a driving force for the convective flow. This driving force can be viscous shear over the particle surface due to the particle flow relative to the continuous phase, or it can be a density-driven force due to gravity or centrifugal motion acting on the particle, or it can be a gradient with interfacial tension. Usually the magnitude of the convection heat transfer is smaller in the latter situation than when the convection is driven by viscous shear when fluid particles can take on irregular shapes and can oscillate, agglomerate, or break up. The convection phenomena can become very complex under these circumstances.

Often most importantly, phase change can occur inside the particle. When evaporation or condensation occurs, these modes of heat transfer result in the highest transfer coefficients. When this fact is coupled with the high surface area implicit in direct-contact heat transfer, generally these kinds of processes are desirable for achieving high performance or low-temperature difference heat transfer.

Special attention must be given to the possible influence of heat transfer on the fluid mechanics (e.g., the relative velocities) and vice versa.

While many of the combinations of fluids and containment geometries result in an essentially constant situation throughout, the acceleration or deceleration of particles due to changes in size or shape can have a major effect on the performance in a specific application. Size effects on performance are better understood than shape effects of the dispersed phase. Also particle breakup or agglomeration is often present, but currently these are not well understood and not exploited in design [3].

1.3 Direct Contact Heat Transfer Applications:

Direct-contact heat transfer between two immiscible liquids has a lot of advantages over traditional heat exchange methods with metallic heat transfer surfaces: lower driving temperature difference (the availability to operate at relatively small temperature driving forces), simple design and scale-up procedure and no surface corrosion and fouling. The practical applications have been found in a number of engineering processes such as spray cooling tower, accumulator, water desalination, emergency core cooling system, solar, geothermal, ocean-thermal energy conversion and thermal storage systems. A recent increase in publications dealing with the direct-contact heat transfer between two immiscible liquids with change of phase evidences a growing interest in this area. Here it is suitable to refer to some of these applications.

In a spray cooling towers, which are used in conjunction with electric power generating facilities, the warm water from condenser is broken into fine droplets near the top of the structure. The droplets are then allowed to fall downward as air is blown upward over them. Both the diffusion of heat and mass from the surface of the droplets to the air reduce the liquid temperature[4].

The concept of direct contact heat transfer with a change of phase was used in Germany before time in the design of accumulators. Such accumulators are use in electric power generating plants to store energy associated with excess steam produced by the boilers during low demand periods. The accumulator is a very large tank which contained water under pressure. Excess steam from the power plant is injected into the tank in the form of bubbles which subsequently collapsed and heated the water. Later, during high demand period, the pressure in the accumulator was reduced and the water flashed into steam which was fed into a variable pressure turbine [4].

The using of direct-contact heat transfer with change of phase was stimulated by the quest for economic water-desalination units. Multiphase exchange, where latent heat is transferred between the immiscible fluids, has been effectively used in direct-contact freezing units in which a dispersed volatile fluid (e.g. drops of an organic substance) evaporates in the saline water with simultaneous freezing of part of the water forming ice crystals. The leaving vapors are then brought in contact with the withdrawn ice crystals in another unit where condensation and melting occurs simultaneously [5] (Figure 1.2).
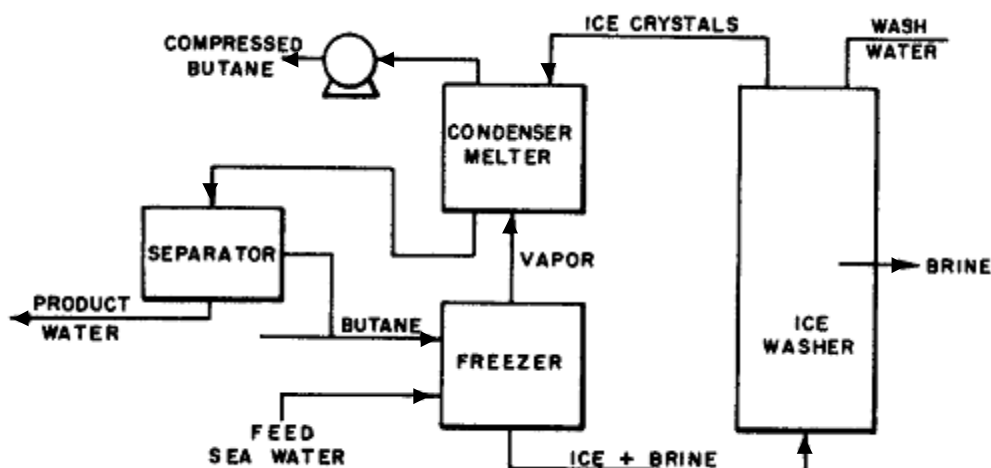
Figure 1.2: Schematic diagram of multiphase exchangers in direct-contact freezing process [5].

Another application of direct-contact heat transfer of current interest is associated with multistage flash evaporator water desalination. It is based on the difference in the vapor pressure of pure and salt water. In such process, the vapor flashed in consecutive flash chambers is brought in contact with a countercurrent stream of colder pure water. The novelty of this process lies in streamlined design of the inter-stage passages, which allows the utilization of the mechanical energy generated in each flashing stage to lift the brine upward, from stage to stage as well as in the continuous removal of noncondensables from the condensing freshwater interface. The latter procedure is claimed to increase the condensation rates by an order of magnitude, thus leading to compact evaporator-condenser stages some 70 cm long. Another interesting novelty was the concept of utilizing a solar energy pond as part of the heat recovery scheme [6].

The emergency core cooling systems (ECC), is employed in nuclear power reactors or boiling water reactors, comprises an evaporation region followed by condensation (in the downcomer region) of the generated steam on the water reflooding films. The recondensation process plays an important role, particularly in cases where the reflooding coolant is subcooled and where the wall heat flux is not sufficient to heat the subcooled films to saturation[6].

1.4 Direct Contact Evaporation of Liquid Droplets in an Immiscible Liquid:

The contact between the streams is promoted by bubbling or dropping one fluid, denominated dispersed phase, through the other, which constitutes the continuous phase. In this type of direct contact evaporation the heat transfer takes place between the continuous liquid and the droplets of a second liquid, dispersed phase, which rise, due to buoyancy or other means, through the

continuous liquid. If the temperature of the continuous liquid is greater than the saturation temperature of the dispersed phase and the nucleation set in the drops, the drops evaporate. As evaporation progresses, the droplet mass becomes a two-phase entity of liquid and vapor contained within an envelope of the surrounding immiscible second liquid. Such two-phase configurations have been referred to as a "drobbles" [7]. In this case the dispersed phase stores the heat transferred from the surrounding continuous liquid as latent heat.

Some of the terms which consider necessary in the direct contact evaporation process would be illuminated here, among them the vaporization ratio which is often used to describe the progress of evaporation, and can be defined as the ratio of the vapor mass to the total mass of the compound drop.

Also, different configurations of drobble are possible (more details in next chapter), depending on the interfacial tensions. The most common one is the "partially engulfed configuration", which consists of the liquid phase at the lower part of the two-phase drop and the vapor phase at the upper part[8, 9, 10].

Also, the shape of drobble, it has been documented that droplets and bubbles can experience a wide variety of shapes, depending on the combination of the physical properties of the bubbles and drops and of the continuous liquid, such as surface tension and viscosity. It must be pointed out that the drops may be spherical when it is carried by an inviscid continuous liquid [11]. Much work has been done on a variety of systems assuming that the droplet is spherically-shaped. A great deal of the early work was reviewed by Sideman[5].

Recently, Nucleation, as the main features of the direct contact evaporation process is the availability to operate at relatively small temperature driving forces (temperature difference between continuous and dispersed phases). But the temperature difference is not the only condition required to

start evaporation of the drops in the continuous medium. Evaporation starts only after nucleation has set in the drop. If the evaporation did not start at the nozzle, the liquid, organic, drop could rise to the top of column without evaporation [12, 13]. Vuong and Sadhal [14] described the bubble nucleation mechanism and classified the evaporation of a drop, or bubble nucleation in a drop, into two categories, homogenous nucleation and heterogeneous nucleation. Homogenous nucleation generally takes place when the liquid is purified while in heterogeneous nucleation the liquid medium contains vapor or entrapped gas that exist with impurities such as dust particles. In heterogeneous nucleation the liquid required smaller degree of superheat than the homogenous nucleation. At a given temperature difference the onset of nucleation usually depends on external disturbances and the degree of impurity of the liquids involved, hence Sideman and Taitel [15] showed that impurities in the volatile liquid and contamination normally associated with sea water, as well as very small gas bubbles introduced by mechanical mixing, are factors which retard superheating and promote nucleation. Experimentally, nucleation has been achieved by the injection of air, nitrogen, and even electrically[15,16].

Despite the large number of investigations carried out so far, the direct contact evaporation of a rising drops in another immiscible liquid is still not fully understood. The lack of understanding of the hydrodynamics and heat transfer mechanism of direct contact evaporation needs further investigation. This investigation is considered to be complementary in providing insights into the mechanism of this process.

1.5 Objectives of the Present Study:

In the face of existence of several studies about the direct contact evaporation of multidroplets in an immiscible liquid, it is noticed that there is a scarcity in the comprehensive theoretical studies of this phenomena. The available theoretical studies are based on a fundamental assumption, that using empirical correlations for specific heat transfer coefficients, for single drop, to obtain volumetric heat transfer coefficients. This may be due to the absence of theoretical model to simulate the specific heat transfer coefficients for unsteady state during the whole evaporation process. These studies become unbeneficial when the empirical correlation is not available. The present work attempt to study theoretically the direct contact evaporation of multidroplets through the following steps:

1) Development of a theoretical model for the unsteady state direct contact evaporation of drops in an immiscible liquid by using cellular model. This model aims to obtain information about the evaporation process of a drobble bounded by a cell of continuous liquid.

2) The information from above model (step 1) is used in order to develop theoretical model aims to study the unsteady state evaporation of multidroplets.

3) Study the effect of various parameters that control the direct contact evaporation process when interaction between adjacent drops is insignificant (evaporation of single drop) and compare the obtained results with that obtained from the approximated theoretical and experimental works carried out by other authors.

4) Study the effect of various parameters affecting on the direct contact evaporation performance in normal case of interaction between the drobbles and compare the obtained results with that obtained from the approximated theoretical and experimental published works done by other authors.

Chapter Two

LITERATURE REVIEW

Chapter Two

Literature Review

2.1 Introduction:

The study of direct-contact heat transfer to liquid droplets (dispersed phase) moving in a fluid medium (continuous phase) is of interest because the transfer rates with direct-contact systems are usually much higher than those with surface-type exchangers [17]. This is due to the availability of a larger surface area for a given volume. The heat transfer can also be affected with a lower potential difference (temperature).

Direct-contact heat transfer processes with moving liquid droplets may involve phase change at the drop surface. Furthermore, the process may involve single or multicomponent systems. In this chapter, we would concern with the studies of the direct-contact evaporation phenomena, rather than the other branches of the direct-contact heat transfer processes.

The literature related to the direct-contact evaporation of droplets in an immiscible liquid can be classified into three groups:

(1) The configuration of two-phase bubble (drobble) evaporating in an immiscible continuous liquid.

(2) The dynamics and heat transfer to a droplet evaporating in an immiscible liquid.

(3) Evaporation of multi-droplets in an immiscible liquid (Spray column Evaporators).

2.2 The Configuration of Two-Phase Bubble (Drobble) Evaporating in an Immiscible Continuous Liquid:

In the direct-contact heat transfer to evaporating drops in an immiscible hotter liquid, these drops take the form of two-phase bubbles (drobble) while they are undergoing the liquid-vapor phase change. The interest in the drobbles evaporation is concentrated on the configuration and the shape form of the drobble, furthermore, the heat transfer characteristics between continuous fluid and dispersed drobbles [18].

The configuration of drobbles is primarily controlled by the surface tension relation [8, 14]. This subject had been discussed early by Mori [8] (1978) who classified the possible configurations of the two–phase bubble into four types as shown in figure 2.1, assuming the drobbles are placed in a stationary liquid medium under a vanishing gravity effect.
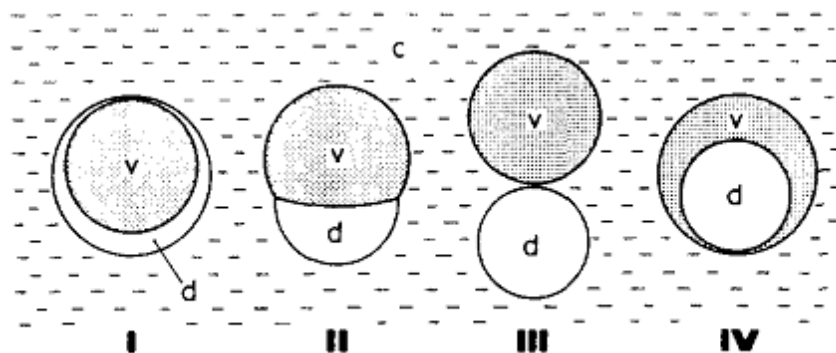
Figure 2.1 Possible types of configurations of two-phase bubbles, c: continuous-phase liquid, d: dispersed-phase liquid, v: vapor [8].

The two-phase bubble configuration is exclusively determined by the surface or interfacial tensions appropriate for vapor/dispersed-phase liquid, vapor/continuous-phase liquid and liquid/liquid interfaces: these tensions are denoted respectively by σ_d, σ_c and σ_{cd} . Conditions which permit those configuration types are represented by Mori [8] as:

$S_{d/c} > 0$, $S_{c/d} < 0$, $S_{v/cd} < 0$.   Used to configuration type I

$S_{d/c} < 0$, $S_{c/d} < 0$, $S_{v/cd} < 0$.   Used to configuration type II

$S_{d/c} < 0$, $S_{c/d} > 0$, $S_{v/cd} < 0$.   Used to configuration type III

$S_{d/c} < 0$, $S_{c/d} < 0$, $S_{v/cd} > 0$.   Used to configuration type IV

Where $S_{d/c}$, $S_{c/d}$, $S_{v/cd}$ are equilibrium spreading coefficients defined as

$$S_{d/c} = \sigma_c - (\sigma_d + \sigma_{cd})$$

$$S_{c/d} = \sigma_d - (\sigma_c + \sigma_{cd})$$

$$S_{v/cd} = \sigma_{cd} - (\sigma_d + \sigma_c)$$

In the further work by Mori [9] (1985) he noted that the configuration classification shown in figure 2.1 can not be applied directly to the case of two-phase bubbles undergoing evaporation or condensation while moving in a medium, which is a case of practical importance in relation to direct-contact evaporators or condensers. He indicated particular types of configuration (for evaporation case), as shown in figure 2.2, which are:

EI_A: A small fraction of the liquid spreads over the upper surface of bubble forming a thin film which completely envelops the vapor phase.

EI_B: The liquid film partially envelops the vapor phase.

EII: This is essentially the same as type II (in previous figure 2.1).

EIII: As the vapor phase grows it separates from the liquid phase resulting in a configuration essentially the same as type III (in previous figure 2.1).
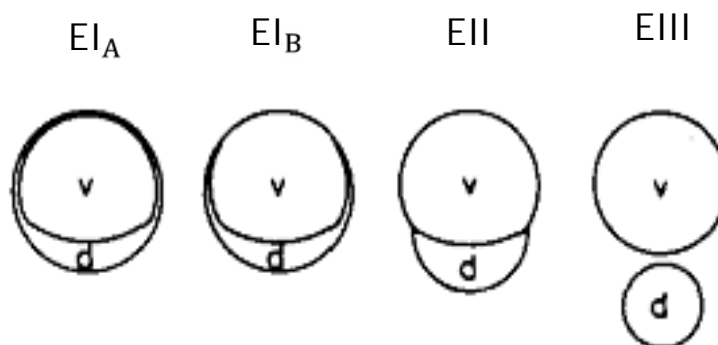
Figure 2.2 Evaporating bubble configurations, d: dispersed-phase liquid,
v: vapor [9].

In 1988 Matsubara et al.[19] presented experimental study of the surface
and the interfacial tensions of mutually immiscible liquid systems. According
to their analysis for n-pentane-water system the equilibrium spreading
coefficients ($S_{d'c}$, $S_{c'd}$, $S_{v'cd}$) have a negative sign [19], that leads to satisfy
condition II and hence type II in figure 2.1 which is represented by type EII in
figure 2.2. This type of configuration is considered the most common
configuration, which is named [14] "partially engulfed configuration" for n-
pentane-water system and other system that satisfied condition II.

The motion and the heat characteristics of a partially engulfed drobble in
an immiscible liquid has been studied experimentally and theoretically by
Sideman and Taitel [15], Sideman and Isenberg [20], Selecki and Gradon [21],
Tochitani et al. [22,16], Raina et al. [23] and other authors. The most of the
later authors have included this configuration in their theoretical models. Only
few researchers employed the configuration of drobble like type I (see figure
2.1) in their theoretical analysis such Kendosh [24], Mahood [25] and recently
Al-Jaberi [13]. Nearly all researchers assumed the drobble to be of spherical
shape in their theoretical analysis. So the spherical shape, partially engulfed
configuration, and drobbles are used in the present work to establish the motion
and heat transfer models.

2.3 The Dynamics and Heat Transfer of a Droplet Evaporating in an Immiscible Liquid:

Considerable works have been done to study the phenomenon of single drop evaporation in a column of an immiscible liquid. Among the earlier pioneering studies, Sideman and Taitel [15] (1964) developed an analytical expression for the Nusselt number by solving the energy equation assuming potential flow around the drop, considered to be a sphere, filled with vapor at the top and the unevaporated liquid at the bottom. They ignored heat transfer to the vapor and assumed that the thermal resistance was negligible inside the liquid . They obtained the following relation for the instantaneous Nusselt number

$$Nu = \left(\frac{3\cos\beta - \cos^3\beta + 2}{\pi}\right)^{0.5} Pe^{0.5} = C\, Pe^{0.5} \qquad (2.1)$$

where β is equivalent opening half-angle of the vapor phase in the two-phase drop, Pe is Peclet number and C is a function of β. By means of cine-camera, they studied the single butane and pentane drops evaporating in stagnant water, they have shown that the vapor concentrates at the upper part of the drop, while the remaining volatile liquid concentrates at the bottom part of the spheroid-like drop. Figure 2.3 shows a pentane drop evaporating in water at various evaporation ratios. They also determined experimental correlations for the parameters regarding the evaporation process, such as the instantaneous rising velocity (U), and the instantaneous heat transfer coefficient (h).

$$U = a_1[\zeta]^{a_2} \qquad (2.2)$$

$$h = \frac{a_3\, \zeta^{a_4}}{T[1 + a_5\, \zeta^{a_6}]} \qquad (2.3)$$

where a_1, a_2, a_3, a_4, a_5 and a_6 are given for different experimental conditions. Based on experimental data they suggested that, for $\beta = 135^0$, or $C = 0.27$ (in equation 2.1), the maximum average heat transfer coefficient per unit of overall drop area can be obtained.

End of evaporation

20% evaporation ratio

3% evaporation ratio

1% evaporation ratio

0.1% evaporation ratio

Nozzle outlet
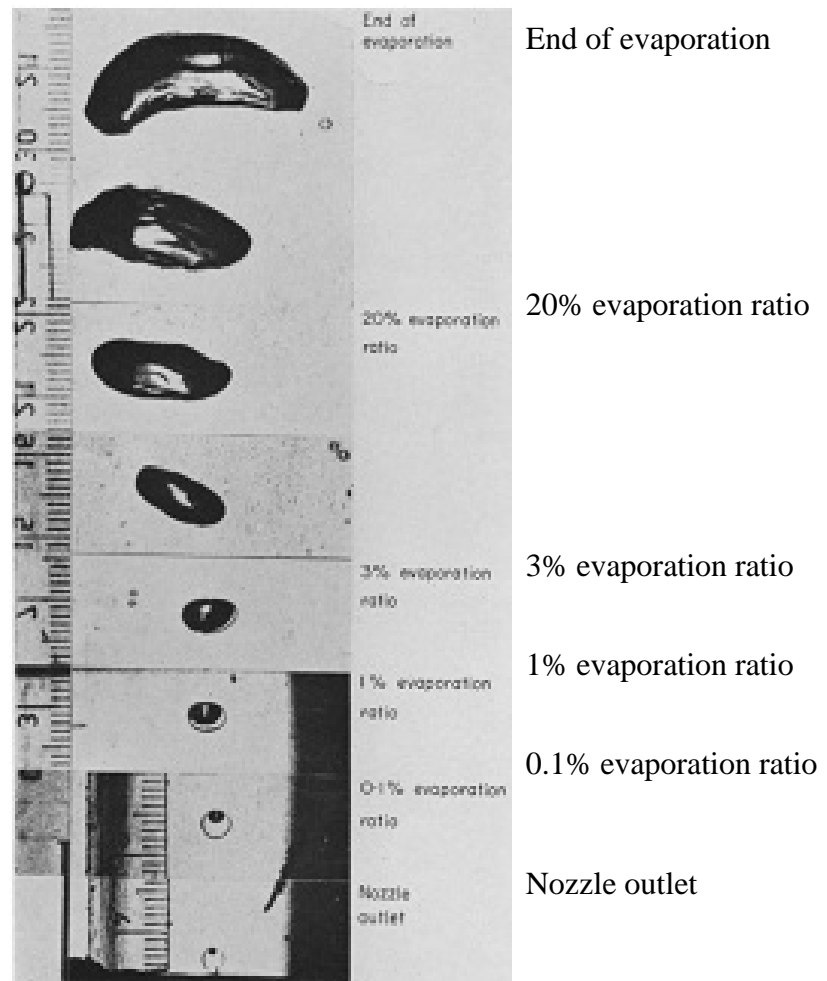
Figure 2.3 Pentane drop evaporating in water 3.5 mm initial drop diameter, Pictures taken with 16 mm Paillard-Bolex H-16 cine-camera [15].

Sideman and Isenberg[26] (1967) presented theoretical and experimental aspects of the basic mechanism of bubble growth, or collapse, and the time dependency of the heat transfer coefficients in three-phase exchangers in which freely rising volatile fluid particles evaporate or condense in another immiscible liquid. The derivation also yields an acceptable upper bound

solution for the total process time, and substantiates the postulated liquid-liquid heat transfer mechanism at the bottom of the drop. They suggested a time-average practical correlation. The theoretical value of the instantaneous heat transfer coefficient, h has the form

$$h = k \left(\frac{3\,U}{2\pi R \alpha}\right)^{1/2} \left(cos\beta - \frac{1}{3}cos^3\beta + \frac{2}{3}\right)^{1/2} \tag{2.4}$$

or, in term of B (dimensionless radius)

$$Nu_0 = \frac{hD_0}{k} = 1.128 Pe_0^{0.5} \left[\frac{m - B^3}{(m-1)B^2}\right]^{0.5} \tag{2.5}$$

where $m = \dfrac{\rho_{dl}}{\rho_{dv}}$, $B = \dfrac{R}{R_0}$.

Experimental study on a butane drop rising in brine were carried out by Simpson et al.[12] (1974). In addition to evaporation, they observed that drop oscillations induced sloshing of the inside liquid, so that a thin film effectively coated the entire interior surface of the bubble. This oscillation of the rising bubble, is probably caused by the periodic vortex shedding of the wake due to higher Reynolds number, resulting in change of shape of drop from spherical through ellipsoidal to a cap-shaped bubble.

Their experimental correlation for the instantaneous heat transfer coefficient is given as:

$$h = \frac{2.57 B^{1/6}}{1 + 0.206 B^{5/12}} \tag{2.6}$$

Equation (2.6) has been obtained using experimental data for single butane droplets about 3.75 mm initial diameter and temperature driving force T, 2 to 8 ^{0}C.

In 1976 Selecki and Gradon[27] studied theoretically and experimentally the motion of an evaporating drops in an immiscible liquid. They derived an equation describing the motion of such system and then solved this equation numerically. From experimental measurements they obtained the curve of time-dependence of drops position. Also they compared their numerical results with experimental data and they obtained good agreement.

Vaporization process of single drops of pentane or furan in an aqueous glycerol has been studied photographically by Tochitani et al.[16] (1977).Their study was in the region where the geometrically simple configuration and rectilinear motion of vaporizing two-phase bubbles were realized. The instantaneous rise velocity of the two-phase bubbles was appearing to be increase with the increasing of the initial drop diameter.

A pentane drop evaporating in highly viscous glycerol has been studied experimentally and theoretically by Tochitani et al.[22] (1977).They handled the theoretical aspects of problem by using a method and assumptions similar to these used by Sideman and Taitel[15] except that the fluid flow field was replaced by the Stokes solution for a sphere. They assumed a quasi-steady state by neglecting the transient term in the energy equation. They obtained the following relation for the average outside heat transfer coefficient

$$h = 0.291 \, k \, \alpha^{-1/3} R^{-2/3} U^{1/3} \left(\pi - \beta + \frac{sin2\beta}{2} \right)^{2/3} \tag{2.7}$$

They concluded that the heat transfer coefficient related to the total surface area of drobble decreases with the increase of temperature difference and initial drobble diameter. The influences of initial drop diameter and temperature difference on the heat transfer coefficient reduce with the progress of vaporization.

Mokhtarzadeh and El-Shirbini[28] (1979) presented a theoretical analysis of evaporation of single drops of pentane and butane in a stagnant column of distilled water. Their governing equations were derived and then solved simultaneously applying a numerical method. In their analysis they used the existing relations for the heat transfer coefficients which are the theoretical model of Sideman and Isenberg[26] and the experimental correlation by Simpson et al.[12]. Furthermore, Haberman and Morton[29] relations for the drag coefficients were employed. They examined their model for different initial droplet sizes, temperature differences and initial velocities of droplets. They compared the predicted results with experimental results of previous worker and observed that using of the existing relations for the heat transfer coefficients did not give satisfactory agreement with the experimental results under all operating conditions.

Raina and Grover[30] (1982) developed a mathematical model for the heat transfer coefficient. The model takes into account the effect of viscous shear on the spreading of dispersed liquid over the bubble surface. The predicted heat transfer coefficient was

$$h = 0.314 \, \frac{k}{R} \left[\frac{UR}{\alpha} \right]^{1/3} \left[\beta - \gamma - \frac{1}{2} (sin2\beta - sin2\gamma) \right]^{2/3} \qquad (2.8)$$

where γ is slosh contact angle(due to spread the residual mass of dispersed liquid over the upper surface, of drobble, in the form of a thin film).

Raina, Wanchoo and Grover[31] (1984) studied theoretically the motion of the vaporizing two-phase bubble. They obtained the following relation for the rise velocity based on description of a free motion of a single spherical bubble or drop

$$U = 1.91 \left\{ \left[1 - \frac{\rho_{dl}}{\rho_c} \right] \left(\frac{D_0}{D} \right)^3 \frac{\sigma_c}{\rho_c D} \right\}^{1/2} \qquad (2.9)$$

where σ_c is the surface tension at the two-phase bubble surrounding liquid boundary. Their predicted results are in reasonable agreement with experimental data for Sideman and Taitel[15].

Battya et al.[32] (1984) studied theoretically the direct contact evaporation of a drop moving in a stagnant column of an immiscible liquid. They identified the non–dimensional parameters governing the motion and heat transfer. In addition, they carried out a regression analysis using the experimental data of Sideman and Taitel[15] and obtained the following correlation

$$Nu = 0.64Pe^{0.5}Ja^{-0.35} \tag{2.10}$$

They applied the above relation in the theoretical model in order to solve the system of governing equation by numerical procedure. They studied variation the non–dimensional parameters effects. They obtained a good agreement between experimental and predicted results.

Battya et al.[33] (1985) investigated theoretically the direct contact evaporation of a drop moving in a stagnant column of an immiscible liquid. The Nusselt number was found to be a function of Peclet number, Jacob number and vapor open angle. The analysis also yields information on the temperature profile and the thickness of the thermal boundary layer surrounding the evaporating drop. The analysis was intended for evaluating the effect of bubble growth on the Nusselt number while assuming a steady heat transfer. They claimed that as Ja increases, resulting in an increase in the bubble growth rate, the thermal boundary layer around a bubble thickens, resulting in a decrease in Nu. They provided the following correlations for Nusselt number by means of a linear regression analysis of their numerical results ranging from Pe = 1000 to 50,000 and Ja =1 to 100:

$$\beta = 0^0 \qquad\qquad Nu = 0.77Pe^{0.5}Ja^{-0.443} \tag{2.11}$$

$\beta = 90^0$: $Nu = 0.68Pe^{0.5}Ja^{-0.374}$ (2.12)

Raina and Grover[34] (1985) extended the previous theoretical analysis[30] by considering the effect of sloshing. They indicated that the latter effect does not exist for the case of small drops (less than 2 mm dia.) and evaporating through high viscosity continuous liquid phase. They derived equation for instantaneous heat transfer coefficient as

$$ h = 0.2916 \frac{k_c}{R} \left[\frac{UR}{\alpha} \right]^{1/3} \left[\beta - \frac{1}{2}(sin2\beta) \right]^{2/3} \qquad (2.13) $$

It should de mentioned here that the models of Raina and Grover[30,34] are similar in many aspects to the models by Sideman and Taitel[15] and Tochitani et al.[22], with modification to the boundary conditions.

Mokhtarzadeh and El-Shirbini[35] (1986) investigated experimentally the dynamics and the associated heat transfer process of butane droplets evaporating in water. They presented a new data for the instantaneous growth, rise velocity and the heat transfer coefficient. They described and divided the behavior of the drobble, from initial to the final stages of evaporation, into four regions with reference to similarities with the behavior of a spherical droplet, spheroidal drobble, large spheroidal bubble and cap bubble. They obtained the following correlation to represent the results for the heat transfer coefficients

$$ h = \frac{1}{1000} \left[a_1 + a_2 \left(\frac{D}{D_0} \right) + a_3 \left(\frac{D}{D_0} \right)^2 + a_4 \left(\frac{D}{D_0} \right)^3 + a_5 \left(\frac{D}{D_0} \right)^4 \right] \qquad (2.14) $$

where a_1, a_2, a_3, a_4 and a_5 are given for different experimental conditions.

Tadrist et al.[36] (1987) studied the vaporization of a single droplet in a stagnant liquid medium. They provided results for evaporation and bubble growth based on an approximate momentum balance that relates compound-drop acceleration to volume and surface forces. The surface forces

are evaluated for the limits of potential and Stokes flow. Correction factors were employed for finite values of Reynolds number. The drag coefficients for air bubbles moving in water taken from Haberman and Morton[29] have been generally employed in the force balance. The Rayleigh-Plesset equation is used to determine the growth rate of the bubble. The theoretical heat transfer coefficients given by Sideman and Taitel[15] ; and later modified by Battya et al.[32] were used in their analysis. The mechanical equilibrium of the bubble droplet has been further explored in the second part of the study to determine the contact angles and the effective area available for heat transfer.

Shimizu and Mori[37] (1988) described a piece of equipment which has been specially designed to permit the study of evaporation of single liquid drops in an immiscible liquid at elevated pressures up to the order of 1 MPa. It equipped with a piezoelectric discharger for yielding nucleation in each drop and with a dilatometer for detecting the change in volume of the drop in the course of evaporation succeeding the nucleation. Some preliminary results, were obtained with the equipment, for n-pentane drops evaporating in a water medium at pressures up to 0.5 MPa (5 atm.).

Shimizu and Mori[38] (1988) obtained experimental results on evaporation of single n-pentane drops and R113 drops, both from 1.4 to 1.7 mm initial diameter, released in the medium of water under pressures of up to 0.48 and 0.39 MPa, respectively. The obtained results showed that the rise velocity of each drop taking the form of a growing drobble is held nearly constant in the course of evaporation in the whole range of experiments. They also proposed the following empirical correlations for instantaneous Nusselt number

$$Nu = 0.169Pe^{0.5} \qquad\qquad\qquad (2.15a)$$

for the n-pentane/water system, and

$$Nu = 0.121 Pe^{0.5} \tag{2.15b}$$

for the R113/water system.

Shimizu and Mori[39] (1989) described a numerical analysis to re-examine the same problem as that studied by Battya et al.[33] considered. They examined the possible deviation of the instantaneous heat transfer to a growing spherical bubble from the quasi-steady heat transfer to a non-growing bubble. The results deduced from the analysis showed that the heat transfer coefficient, or Nusselt number, is indeed dependent on the temperature difference (T) but in a way significantly different from that predicted by Battya et al.[33]. They suggested that the apparent T dependency observed in the experimental results by Sideman and Taitel[15] can be ascribed for the most part to some cause other than the effect of the bubble growth.

Vuong and Sadhal[10,14] (1989) analyzed a partially engulfed drop. In the first part of this study[10], the motion is analyzed in the limit of Stokes flow, and the bubble growth rate has been prescribed arbitrarily. An exact analytical solution for the axisymmetric flow field has been developed in a toroidal coordinate system (coordinate transformation) by combining the solutions separately obtained for a flow field resulting from drop translation and a flow field resulting from the moving boundaries of the drop due to the growth.

In part two of this study[14], the heat transfer problem was solved under the assumption that the liquid-vapor interface and the vapor phase were at the equilibrium temperature corresponding to the hydrostatic pressure. The energy equations, for both the continuous phase and the liquid portion of the dispersed phase with the convective velocity taken from the fluid flow solution, have been numerically solved using finite-difference techniques. The time history of evaporation of a pentane drop immersed in a bath of glycerol

has been provided. The heat transfer coefficient is found to be inversely proportional to the size of the drop and the amount (degree) of superheat.

Shimaoka and Mori[40] (1990) performed experiments with n-pentane drops 2.0-6.5 mm initial diameter evaporating in water under pressures of 0.11-0.49 MPa. The results obtained complemented those obtained by Shimizu and Mori[38] with smaller drops (from 1.4 to 1.7 mm in initial diameter). They observed that the system pressure does not produce a significant effect on the heat transfer characteristics. The instantaneous rise velocity of bubbles correlations were presented in the following form:

$$U = 0.18\, e^{28\,D} \tag{2.16}$$

where D the diameter of bubbles.

Also the heat transfer correlations were presented in the following form:

$$Nu = C\, Pe^{0.5} \tag{2.17}$$

where the constant, C, has a value of 0.234, using in the following ranges of Jacob and Eötvös (Eo) numbers

$$15 \quad Eo \quad 110\; ; \quad 0.4\, Eo^{0.7} \quad Ja \quad 11\, Eo^{0.4}$$

Where $Eo \quad (\rho_c - \rho_{dv})\, g\, D_f^2/\sigma_{cv}$, in which D_f is the final drobble diameter, ρ_{dv} is the saturated-vapor density corresponding to the pressure, in the continuous phase, at the location where the evaporation completed, and σ_{cv} is the interfacial tension between the liquid water and the pentane/water vapor mixture, which is evaluated at saturation temperature corresponding to the pressure in the continuous phase.

Wanchoo et al.[41] (1992) presented a theoretical analysis of the evaporation of a single drobble during its rise in a quiescent column of an immiscible liquid. Governing equations were derived and solved by a

numerical method. In order to solve these equations, the heat transfer and drag coefficients must be known. They used Haberman and Morton[29] relations for the drag coefficients. For the heat transfer coefficients they used the existing relations for the heat transfer coefficients which are the theoretical model of Sideman and Taitel[15], the experimental correlation by Battya et al.[32] and the theoretical model by Raina and Grover[34]. Dimensionless parameters governing the phenomenon were identified and a parametric study was carried out for different non dimensional parameters. The predicted results were compared with experimental results of previous workers. Result of the parametric analysis indicated that (1) the phenomenon is mainly dependent on Peclet and system Jacob numbers; (2) potential flow assumption is a fairly valid assumption and $C_d = 2.6$ can be used for $10^3 < Re < 10^4$.

Celata et al.[42] (1995) carried out an experimental research on direct contact evaporation of liquid droplets of R114 (volatile liquid)flowing upwards in a stagnant water column, with the particular aim of ascertaining the effect of water superheating (difference between water temperature and R114 saturation temperature at system pressure) on the heat transfer process. The experimental data were taken by observing the level variation of the water column after the injection of a known volume of volatile liquid. The level variation, due to the evaporation of the injected droplets, had been correlated to the volatile liquid evaporation in the column using a model which accounts for the actual phenomena such as the local cooling of the continuous medium, due to evaporating drops. They observed that the local cooling of the water column due to the drop evaporation is practically negligible when T > 12-15 K.

Song et al.[43] (1996) established the mathematical model of steady state heat transfer for a moving ellipsoidal drop in an immiscible liquid, and presented results from numerical calculation, that regard the limiting solution

of an unsteady state problem. The relationship of the Nusselt number with the Weber number and the Peclet number was given in the following form

$$Nu = (C + a\,We^b)Pe^m \tag{2.18}$$

where C was taken from analytical solution derived by Sideman and Taitel[15], i.e.

$$C = \left(\frac{3\cos\beta - \cos^3\beta + 2}{\pi}\right)^{0.5}$$

and *a, b* and *m* are fitting coefficients, which were suitable for a relatively large range of *We (*Weber number= $U^2 D/\sigma_c$ *)* and *Pe*. Their theoretical results for the Nusselt number showed a good agreement with experimental data.

Dammel et al.[44] (2003) examined numerically heat transfer from a continuous liquid to a drop of a second immiscible liquid, which rises due to buoyancy and simultaneously evaporates in direct contact to the continuous liquid. They applied finite element method in a pure Lagrangian description to solve the full Navier–Stokes equations. Their calculations were performed for a furan drop and for n-pentane drop evaporating in aqueous glycerol. In the initial stage, when the rising velocity and the vapor fraction of the compound drop are small, heat transfer by conduction was dominant. With increasing time convective heat transfer became more important.

Kendoush[24] (2004) derived the equations for calculating the quasi-steady-state connective evaporation of a rising volatile drop in an immiscible liquid with bubble nucleation inside the drop. He based the solution of the energy equation on a potential flow model and concentric spheres configuration. Also he obtained the heat transfer rate in terms of superheat, degree of non-equilibrium, instantaneous diameters of the bubble and the drop,

properties of the dispersed and continuous phase and the Peclet number, in the following form

$$Nu = 0.921 \frac{T_{2-1}}{(\,T_{3-2})^{1/2}} \left[\left(\frac{k_{dl}\, \rho_{dl}\, Cp_{dl}}{k\, \rho_{dv}\, h_{fg}} \right) \frac{Pe_c}{Ja}\, \zeta \left(\frac{0.5 + \zeta}{1 - \zeta} \right) \right]^{1/2} \tag{2.19}$$

Where T_{2-1} , the temperature difference between drop and bubble (K) and T_{3-2} , the temperature difference between continuous liquid and dispersed liquid.

Mahood[25] (2008) presented a semi–analytical approach to study the transient heat transfer of single volatile drop evaporation in an immiscible liquid with bubble nucleation inside the drop. His solution based on the energy equation included both convection and conduction heat transfer from the continuous liquid to the bubble with the concentric spheres model. He determined the radius of the growing bubble and examined the effect of Pr number, St number, initial radius, initial velocity and ratio of density. He derived the Nu number as a function of the drop velocity in the following form

$$Nu = \frac{2k_{dl}}{k} + 0.044 Pr^{1/3} Re^{0.78} \tag{2.20}$$

Recently, Al-Jaberi[13] 2010, in the first part of his study, investigated experimentally the dynamics and heat transfer process of single n-pentane droplets evaporates in a flowing down distilled water. He presented data for instantaneous growth, rise velocity and instantaneous heat transfer coefficient. Also, he presented an analytical solution, based on the steady state energy equation included both convection and conduction heat transfer from the continuous liquid to the bubble with the concentric spheres model. The following relation for the heat transfer coefficient was obtained,

$$Nu = 0.6308 \frac{T_{2-1}}{(T_{3-2})^{1/2}} \left[\left(\frac{k_{dl}\, \rho_{dl}\, Cp_{dl}}{k\, \rho_{dv}\, h_{fg}} \right) \frac{Pe}{Ja}\, \zeta \left(\frac{\zeta}{1-\zeta} \right) \right]^{1/2} \qquad (2.21)$$

Where T_{2-1} and T_{3-2} , as defined previously in Kendoush[24].

2.4 Evaporation of Multi-Droplets in an Immiscible Liquid (Spray Column Evaporators):

There are limited numbers of experimental, theoretical and numerical investigations dealing with a swarm of droplets undergoing evaporation in an immiscible liquid in the literature.

In 1965 Sideman et al.[45] related experimentally the overall heat transfer coefficient in single and multiparticle systems to the initial drop size of volatile fluids evaporating within immiscible, nonvolatile liquids. Coalescence and turbulence diminish the effects of the initial size, which were limited to the lower part of the exchanger where single-drop characteristics are maintained .

Sideman and Gat[46] (1966) conducted an experiment to investigate the operating characteristics of a spray column utilizing pentane and water. They calculated the volumetric heat-transfer coefficient and average void fraction as a function of the pentane and water superficial velocities, the entrance and exit temperatures of the water and the depth of the water through which the pentane rose.

Suratt and Hart[47] (1977) used isobutane as the dispersed phase and water or simulated geothermal brine as the continuous phase, in a countercurrent flow. They used two columns, one as a pre-heater and the other as an evaporator. Flooding conditions were not reached for the pre-heater or the evaporator. The experimental results of the volumetric heat-transfer coefficient

were similar when using water or simulated geothermal brine in the pre-heater (liquid/liquid system).

Plass et al.[48] (1979) carried out experimental work and found an empirical correlation to evaluate the volumetric heat-transfer coefficient for liquid/liquid countercurrent as a function of hold-up and volumetric flow ratio.

Smith et al.[49] (1982) performed experimental work for a three-phase exchanger where the dispersed phase is injected into a stagnant continuous phase. Specific results were found for cyclopentane injected into a vessel of wafer(stagnant and uniform in temperature). Also they developed an analytical model to calculate the volumetric heat transfer coefficient for direct-contact evaporation. In their model, the thermal resistance of the dispersed phase was assumed to be negligible, and single-droplet velocity was assumed to be of the form

$$U = U_0 \left(\frac{D}{D_0}\right)^{C_1} \tag{2.22}$$

and the fluid dynamics was described by the so-called drift-flux model[50]. Further, the single droplet heat transfer was calculated as

$$Nu = \frac{hD}{k} = C_2 Re^{C_3} Pr^{1/3} \tag{2.23}$$

The values C_1 and C_2 were inferred from experimental data and the value of C_3 is known to be in the range 0.7 to 1.0. They divided the analysis into a preagglomeration and a post-agglomeration stage on the basis of an assumed maximum value for the dispersed phase volume fraction. Also, they used two types of distributor (seven and nineteen of 0.5 mm holes) in their analysis. The obtained analytical results showed good agreement with data obtained from an experimental direct-contact evaporator using cyclopentane and water.

Battya et al.[51] (1983) presented a theoretical analysis of direct contact latent heat transfer between two immiscible liquids in a counter flow spray column. The non- dimensional parameters governing the evaporation process were identified and a study of the effects of the variation of these parameters was made. The longitudinal dispersion in the continuous phase is taken into account in the analysis. The predicted column heights required for complete evaporation compare favorably with the available experimental data. The theoretical model also predicts the rate of evaporation of the dispersed phase along the column.

Tadrist et al.[36] (1987) studied experimentally and theoretically, the vaporization by direct contact of refrigerant R113 and n-pentane dispersed into a column of water flowing countercurrently. They studied vaporization of a multidroplet flowing system using single drop correlation for heat transfer coefficient given in reference[52]. They performed experiments to investigate the influence of the different parameters on the behavior of the direct contact vapor generator. A dimensional analysis based on characteristic transfer times was done. From this point of view correlations established for determining the volumetric heat transfer coefficient and the exchange efficiency. Also, they proposed an analytical model extending the single-drop study to multidroplet systems. The obtained results showed that the volumetric heat transfer coefficient was different for both fluids. The n-pentane water system was having better performance than R113-water system.

Seetharamu and Battya[53] (1989) studied the direct contact evaporation of R113 and n-pentane in a stagnant column of distilled water. The effects of operational parameters such as the column height, the phase temperature difference, the dispersed phase flow rate, and the diameter and number of orifices in the distributor on the volumetric heat transfer coefficient and holdup were investigated. A modified relation, based on the theoretical analysis of

Smith et al.[49], was also developed for predicting the theoretical volumetric heat transfer coefficient. The volumetric heat transfer coefficient was found to be higher at lower part of column heights. The initial drop diameter is found to depend mainly on the orifice velocity, orifice diameter, and the physical properties of the system. Comparison with related works available in the literature showed reasonable agreement.

Core and Mulligan[7] (1990) presented a population balance model to discuss the heat transfer characteristics of direct contact evaporation in a batch reactor. The population balance equation was solved using the Method of Classes by single drop correlation for heat transfer coefficient given by Tochitani et al.[16]. However, they neglected both breakage and coalescence of dispersed droplets. Transient bubble populating characteristics, volumetric heat transfer coefficient, total heat transfer and liquid temperature were predicted, along with the liquid refrigerant holdup.

Mori[54] (1991) analyzed the heat transfer to drops of a volatile liquid sprayed upward in an immiscible liquid flowing down in a vertical column to enable calculation of the volumetric heat transfer coefficient in the column. For this analysis, a model was contrived that assumes no nucleation delay in initially monodispersed drops and the heat transfer to each of the drops, with simultaneous evaporation, could be approximated by an empirical correlation for heat transfer to an isolated drop evaporating in a quiescent, sufficiently extended medium described by Shimizu and Mori[38]. Furthermore, the dispersed phase volume fraction and rise velocity of each drobble were held constant, as average value, during the evaporation. The expression obtained for the volumetric heat transfer coefficient was used to predict its values under some particular column operating conditions, which then compared with relevant experimental data found in the literature.

Ay et al.[55] (1994) developed, a one-dimensional steady state, numerical model of a direct-contact evaporator, which was used to calculate performance information about direct-contact heat transfer between a rising dispersed refrigerant and a counter flow continuous fluid. Results were compared with the existing experimental data. The numerical scheme involves slicing the column of the evaporator into a finite number of horizontal slices and applying continuity, population, and energy balances to each slice. Temperature and holdup ratio distributions through the evaporator were obtained for the operation of a $0.1m$ diameter column, using n-butane as the dispersed refrigerant and distilled water as the continuous fluid. Results were given for a range of values of the initial drop diameter, mass flow rate of the dispersed fluid, and mass flow rate of the continuous fluid.

Song and Steiff[56] (1995) presented a model for drobbles in drobble columns, based on the concept of phase space and the population balance equation. This model allows a consideration of the growth, breakage and coalescence of two-phase drobbles. The model had been used for the simulation of vaporization height in this kind of systems. A correction formula for the single drobble Nusselt number, by the work of [43], and rising velocity of drobbles by Raina et al.[31] with the correction from Marrucci[57] was used in modeling. Detailed information about the variation of distribution density functions with column height is given both with and without consideration of breakage and coalescence of drobbles.

Song et al.[58] (1996) obtained an analytical solution of the model presented by Battya et al.[51] which was solved by numerical method. From their solution the exact relationships between target quantities and influence quantities were given. In their solution the explicit formulae for the column height required for complete evaporation and the temperature of continuous

phase at the end of evaporation were given, which would be very useful for the initial design of spray columns in engineering.

Song et al.[59] (1998) presented a detailed analysis of the influence of several important parameters, such as the breakage of droplets, the temperature difference between the continuous and the dispersed phase, the initial mean diameter of drops from the bottom distributor, and the maximum diameter of stable drobbles on the statistical evaporation height and the density distribution of dispersed droplets in a bubble column. Due to the low number density of particles in the present problem, coalescence has little influence on the evaporation process and was hence assumed negligible. From the energy conservation they derived the growth rate of a drobble, based on a correction formula for the single drobble Nusselt number of[43], and rising velocity of drobbles by[31] with the correction from[57]. Numerical calculations showed that there was an approximately proportional relationship between the evaporation height and the reciprocal of the driving temperature difference.

Song et al.[18] (1999) established a population balance model to predict the volumetric heat transfer coefficient for direct-contact evaporation in a bubble column. The model was based mainly on the energy balance and the population balance. Growth and breakage of droplets were taken into account in the population balance model. In the energy balance, as in their previous works, correlation formula for the single drobble Nusselt number, by[43], and rising velocity of drobbles by[31] with the correction from[57] were used in the modeling. Their results showed that the mean diameter of dispersed drops, just leaving the bottom distributor was a very effective parameter in their model of calculations and, they believed that the same type of sensitivity applies also to other models existing in the literature.

Peng et al.[60] (2001) studied theoretically and experimentally the heat transfer to dispersed droplets in an immiscible continuous phase for the n-pentane–water system. In the theoretical model, the holdup and relative velocity between continuous and dispersed phase assumed to be constant and the heat transfer to each drobble was described by the same heat transfer correlation as that established for single-drop evaporation[43].They divided the exchanger into two zones according to the maximum diameter that the droplet can attain (D_{max}) and obtained the mathematical models for the local and average volumetric heat transfer coefficients for each zone. Their results indicated that the volumetric heat transfer coefficient increased with the increase of the superficial velocity (hence the volume flow rate) of continuous liquid, while the superficial velocity (hence the volume flow rate) of dispersed liquid nearly had no effects on it.

Recently, Al-Jaberi[13] (2010) presented experimental investigation deals with the direct contact evaporation of spray n-pentane drops in flowing column of distilled water. He used three types of distributor (seven, nineteen and thirty six of 0.75 mm holes) in his analysis. Figure 2.4 shows a pentane drops evaporating in a column of distilled water (at a beginning stage of evaporation). The operational parameters investigated in the experimental study are the operating column height, the temperature difference, the dispersed phase flow rate, the continuous phase flow rate, and the diameter and number of orifices in the distributor. The effects of these parameters on average volumetric heat transfer coefficient were investigated. In Addition, he developed an analytical model for calculating volumetric heat transfer coefficients for direct-contact evaporation of multi-drops. Heat transfer was modeled using single drop correlation derived in his theoretical work based on quasi steady state solution of the energy equation, while the holdup and relative velocity between continuous and dispersed phase assumed to be constant.
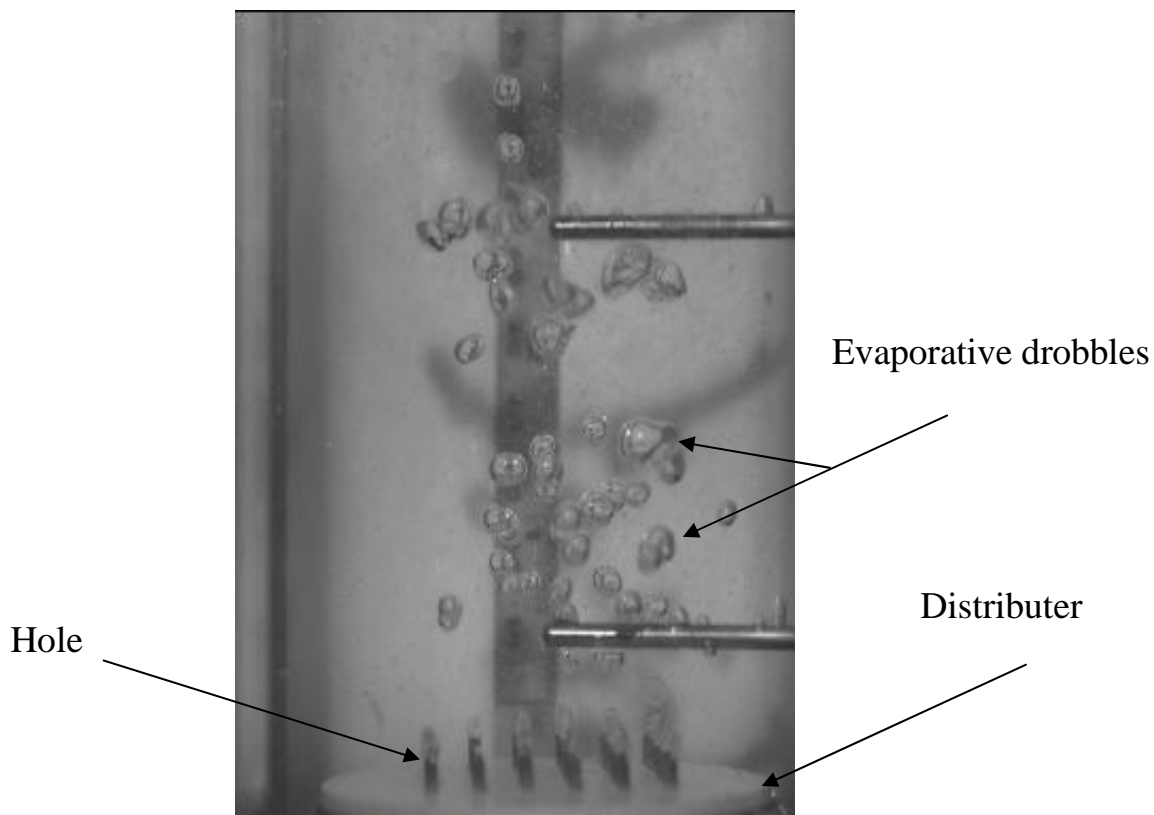
Figure 2.4 shows a pentane drobbles evaporating in a column of distilled water [13].

2.5 Summery

Based on the review of literature the following conclusions can be noted:

1. There are numerous of experimental studies done to investigate the dynamics and heat transfer of single droplets evaporating in an immiscible liquid. Also, there are theoretical studies to investigate this process, most of these studies are based on assuming quasi-steady state for both the dynamics and heat transfer of single droplets evaporation.

2. There are experimental works done to investigate the evaporation of multi drops in column of an immiscible liquid. In addition, there are limited theoretical studies on this field. The most of the available theoretical studies are based on using experimental correlations of heat transfer coefficient for single drobbles.

3. To the author knowledge, in spite of a large number of experimental investigations, a comprehensive theoretical analysis of direct contact evaporation of drobbles in immiscible liquids is found to be lacking in the literature. There is no theoretical model studying the complete evaporation process ($0 \quad \beta \quad \pi$) taking in to account the unsteady state heat transfer, alongside the growth and translation of evaporating drobble.

4. In addition, there is no universal theoretical model to study the evaporation of multidrobbles based on using theoretical model for heat transfer and the motion of single drobbles, instead applying an experimental correlations as depicted by nearly all the previous studies.

Therefore, the purpose of this research is the attempt to solve, to some extent, these problems.

Chapter Three

THEORETICAL ANALYSIS

Chapter Three

Theoretical Analysis

3.1 Introduction:

Consider droplets of liquid are injected into a column of another immiscible liquid. One liquid, called dispersed phase, while the other liquid, called continuous phase. If the continuous phase has a temperature higher than the boiling point of the dispersed phase, the drops will evaporate and hence extract heat from the continuous phase. The continuous phase is immiscible with either of phases, vapor and unevaporated liquid, of the dispersed phase. As the dispersed droplets complete their evaporation, the vapor exists through the free surface of the continuous liquid and subsequently withdrawn from the head part of column. In the course of evaporation the droplet forms a vapor-liquid two-phase bubble; this droplet has been named "Drobble". As mention in the previous chapters, different configurations of a drobble are possible. Figure 3.1 shows the drobbles column and the most common configuration of drobble.
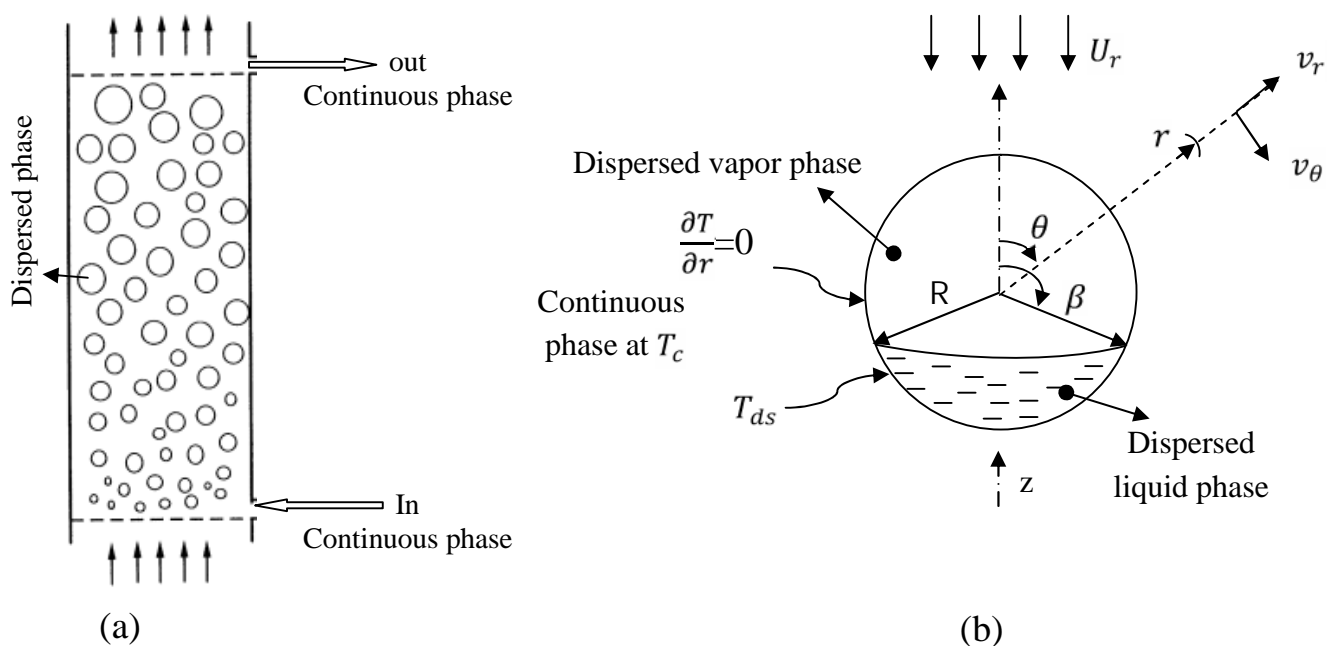

Figure 3.1 Evaporating drobbles (a) Drobbles column (b) Single drobble in a spherical coordinate

This configuration is employed in the present study in order to develop a theoretical model to study the unsteady state evaporation of the growing drobbles in an immiscible liquid. The main problem in modeling of such systems is that of drobble-drobble interactions. The present model adapted the cell models[61,62], which replace the difficult of many-drobble problem by a simple and conceptually more attractive one involving only one drobble.

The cellular model consists in dividing the drobble assemblage into a number of identical cells, each cell occupying one drobble. Thus, boundary value problem is reduced to consideration of a single drobble and its enveloping boundary. Within the framework of the cell model, inter-drobble hydrodynamic interaction are approximated by postulating that each drobble to be surrounded by a hypothetical envelope of continuous fluid of radius R_{cell} as shown in Figure 3.2. The size of the envelope is chosen such that the volume fraction of dispersed phase of each cell is equal to the overall mean volume fraction of dispersed phase[63].

The volume fraction of the dispersed phase or holdup, denoted by the symbol (ε), either of these terms relates the volume of the dispersed phase (droplet or bubble) to the total volume[1], thus the radius of cell, R_{cell}, can be related to the mean volume fraction of the dispersed phase in the swarm as follow:

$$R_{cell} = R\,\varepsilon^{-1/3} \tag{3.1}$$

where ε is the volume fraction of the dispersed phase. Therefore, one can simulate the swarms of various holdups including the limiting case of a single drobble by setting R_{cell} , i. e., ε 0. Conversely, one can readily calculate the value of R_{cell} for known values of the dispersed phase volume fraction and the drobble size.
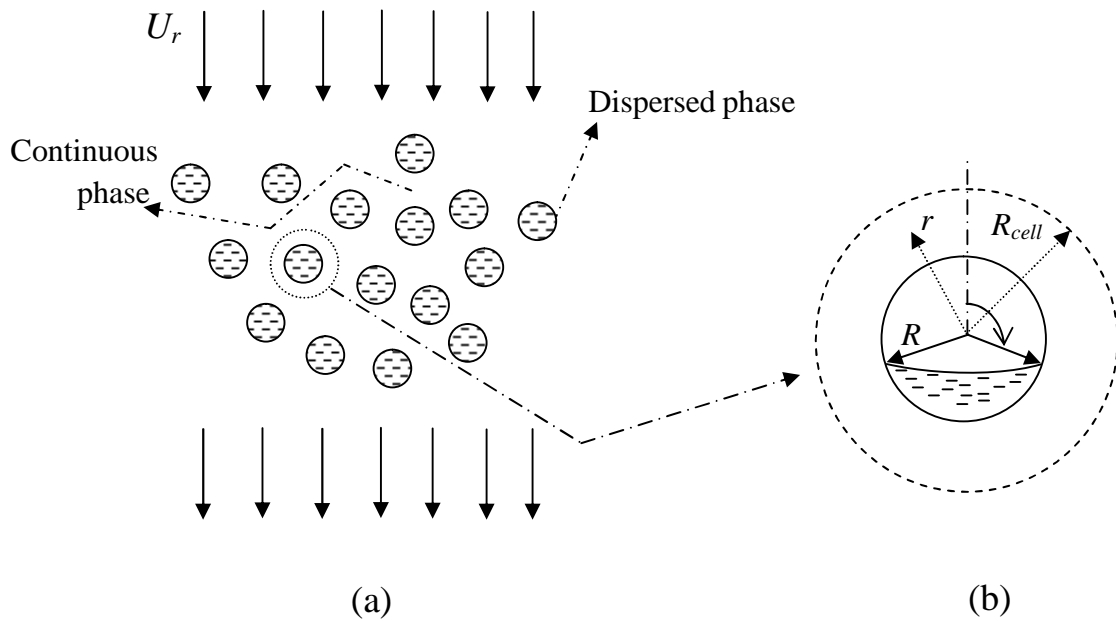
Figure 3.2(a) Schematic representation of flow and (b) cell model idealization.

3.2 Governing Equations:

3.2.1 The Potential Flow Field:

To drive the velocity components of the flow (v_r, v_θ) in r and directions, the following assumptions are employed to simplify the actual physical phenomenon:

1. The fluids are Newtonian.
2. The flows are laminar and two dimension in r and   directions.
3. The physical properties (density and viscosity) are constant.
4. The surface tension is supposed to be large enough to keep the drobbles spherical in shape against any deforming effect of viscous forces. The unvaporized liquid and the vapor inside the drobbles are symmetrical about the vertical axis as shown in Figure 3.1(b).

5. The growing drobble is assumed to be rising in a vertical path with an instantaneous relative velocity U_r. Alternatively, it can be imagined as being at rest, and the continuous medium moving against it with the same velocity.

6. The flow is irrotational and inviscid outside the reference drobble without internal circulation inside it. The hypothesis of irrotational flow is justified by the fact that the vorticity transfer into the cell by the wakes of the upper drobble may be neglected, since that wake is formed at the rear of each two phase bubble at a very early stage of evaporation ($\zeta < 0.01$)[64]. The hypothesis of inviscid flow is justified since the viscous effect is small when the Reynolds number exceeds two or three hundred[65].

The velocity of the flow can be written as the gradient of some scalar function (stream lines function); i.e.

$$v = {}'\varphi \tag{3.2}$$

Where φ is conventionally termed a "velocity potential"[66]. From this designation, irrotational motions derive the name "potential flow".

The velocity component (v_r, v_θ) can be defined in the following general relation as

$$v_\theta = -\frac{1}{r}\frac{\partial\varphi}{\partial\theta} \tag{3.3 a}$$

$$v_r = -\frac{\partial\varphi}{\partial r} \tag{3.3 b}$$

According to the above assumptions for incompressible potential flow it can be shown that φ satisfies the Laplace equation (from continuity equation):-

$$\nabla^2 \varphi = 0 \qquad\qquad (3.4)$$

Where

$$\nabla^2 = \frac{1}{r^2} \frac{\partial}{\partial r}\left(r^2 \frac{\partial}{\partial r}\right) + \frac{1}{r^2 \sin\theta} \frac{\partial}{\partial\theta}\left(\sin\theta \frac{\partial}{\partial\theta}\right)$$

Equation (3.4) can be solved for expanding and translating boundary motion separately and superposition of two solutions gives the solution for the simultaneous motions[28]

$$\varphi = \varphi_1 + \varphi_2 \qquad\qquad (3.5)$$

Where

φ_1: represent the expanding solution term.

φ_2: represent the translating solution term.

Substituting equation (3.5) into equation (3.4), two equations can be obtained one for the expanding motion as

$$\frac{1}{r^2} \frac{\partial}{\partial r}\left(r^2 \frac{\partial\varphi_1}{\partial r}\right) + \frac{1}{r^2 \sin\theta} \frac{\partial}{\partial\theta}\left(\sin\theta \frac{\partial\varphi_1}{\partial\theta}\right) = 0 \qquad\qquad (3.6\ a)$$

and the other for translating motion as

$$\frac{1}{r^2} \frac{\partial}{\partial r}\left(r^2 \frac{\partial\varphi_2}{\partial r}\right) + \frac{1}{r^2 \sin\theta} \frac{\partial}{\partial\theta}\left(\sin\theta \frac{\partial\varphi_2}{\partial\theta}\right) = 0 \qquad\qquad (3.6\ b)$$

The boundary conditions for the expanding boundary[20] are:-

$$v_\theta = -\frac{1}{r} \frac{\partial\varphi_1}{\partial\theta} = 0 \qquad at \qquad 0 \quad \theta \quad 2\pi \ and \ R \quad r \quad R_{cell} \qquad (3.7\ a)$$

$$v_r = -\frac{\partial\varphi_1}{\partial r} = \frac{dR}{dt} \qquad at \qquad 0 \quad \theta \quad 2\pi \ and \ r = R \qquad (3.7\ b)$$

Using these boundary conditions, equation (3.6 a) can be reduce to

$$\frac{1}{r^2} \frac{\partial}{\partial r} \left(r^2 \frac{\partial \varphi_1}{\partial r} \right) = 0 \tag{3.8}$$

Since, $\dfrac{\partial \varphi_1}{\partial \theta} = 0$

Integrating equation (3.8) becomes

$$\varphi_1 = -\frac{C_1}{r} + C \tag{3.9}$$

Applying boundary conditions at *(r=R)* lead to

$$C_1 = -R^2 \frac{dR}{dt}$$

or

$$C_1 = 0 \ (impossible)$$

And hence, the solution for an expanding spherical boundary is:

$$\varphi_1(r, t) = \frac{R^2}{r} \frac{dR}{dt} + C \tag{3.10}$$

where, *C*, arbitrary constant.

For a translating spherical boundary, the boundary conditions are:

$$v_\theta = -\frac{1}{r} \frac{\partial \varphi_2}{\partial \theta} = U_r \sin \theta \quad at \ 0 \quad \theta \quad 2\pi \quad and \quad r = R_{cell} \tag{3.11 a}$$

$$v_r = -\frac{\partial \varphi_2}{\partial r} = -U_r \cos \theta \quad at \ 0 \quad \theta \quad 2\pi \quad and \quad r = R_{cell} \tag{3.11 b}$$

$$v_r \quad 0 \quad\quad\quad at \quad 0 \quad \theta \quad 2\pi \quad and \quad r = R \tag{3.11 c}$$

For the translation motion equation (3.6 b), the general solution of this equation is given by Lamb, as cited by kendosh[24] as follows

$$\varphi_2 = \left(Ar + \frac{B}{r^2} \right) U_r \cos \theta \qquad\qquad (3.12)$$

Applying the boundary conditions equation (3.11) in to the above equation yields

$$A - \frac{2B}{R_{cell}^3} = 1. \qquad\qquad at\ r = R_{cell} \qquad\qquad (3.13)$$

And

$$A - \frac{2B}{R^3} = 0. \qquad\qquad at\ r = R \qquad\qquad (3.14)$$

Solving these two equations by substitution, the values of A and B can be obtain as

$$A = \frac{R_{cell}^3}{(R_{cell}^3 - R^3)} \qquad\qquad (3.15)$$

$$B = \frac{R^3\, R_{cell}^3}{2\,(R_{cell}^3 - R^3)} \qquad\qquad (3.16)$$

It shpuld be mentioned here that A and B are time dependent, since the radius R is time dependent variable.

Applying the relations (3.15) and (3.16) into the general solution equation (3.12) becomes

$$\varphi_2 = \left(\frac{R_{cell}^3}{(R_{cell}^3 - R^3)}\, r + \frac{R^3\, R_{cell}^3}{2\,(R_{cell}^3 - R^3)}\, \frac{1}{r^2} \right) U_r \cos \theta \qquad (3.17)$$

Finally, superposition of the expanding solution equation (3.10) and the translating solution (3.17) gives

$$\varphi(r,\theta,t) = \frac{1}{1 - \left(R/R_{cell}\right)^3}\left(r + \frac{1}{2}\frac{R^3}{r^2}\right) U_r \cos\theta + \frac{R^2}{r}\frac{dR}{dt} + C \qquad (3.18)$$

The radial and tangential velocity components in the liquid medium can be determined using equation (3.3 a, b) and by utilizing equation (3.18) to give

$$v_r = -\frac{U_r}{(1-\varepsilon)}\left(1 - \frac{R^3}{r^3}\right)\cos\theta + \frac{R^2}{r^2}\frac{dR}{dt} \qquad (3.19a)$$

$$v_\theta = \frac{U_r}{(1-\varepsilon)}\left(1 + \frac{R^3}{2r^3}\right)\sin\theta \qquad (3.19b)$$

where

$$\varepsilon = \left(\frac{R}{R_{cell}}\right)^3$$

As ε 0 the above equations reduces to that obtained by sideman and Taitel[15] and other researchers[33, 39] for the velocity components around a single drobble. From equation (3.19) it becomes clear; that the components of the flow velocity around the drobble are affected as a result of the drobble interacting with every other drobble around it in the flow field. The means of interaction are coming through the volume fraction (holdup) parameter.

3.2.2 Equation of Motion of the Growing Drobble:

Assume a spherical drobble growing and accelerating along the vertical path in an immiscible liquid, the unsteady motion of the growing drobble is subjected to the following forces:

i.   Buoyancy force, F_B due to density difference.

ii. Drag force, F_D, on the surface of the drobble.

iii.   The impulse due to virtual mass (added mass) of the drobble.

The equation of motion can thus be written as follows

$$\frac{d}{dt}[(m_{00} + \bar{m})U] = F_B - F_D \qquad (3.20)$$

Where

m_{00}: Mass of growing drobble.

For constant mass drobble

$$m_{00} = \frac{4}{3}\pi R^3 \rho_{av} \qquad (3.21a)$$

where

$$\rho_{av} = \rho_{dl}\left(\frac{R_0}{R}\right)^3 \qquad (3.21b)$$

And

R_0: Initial radius of drobble.

For bubbles, the added mass term $\bar{m}$ is greater than the other components of the hydrodynamic force; these bubbles (spheres) accelerate as if their masses were equal to the mass of the fluid occupying half of their volume[11], hence added mass is

$$\bar{m} = \frac{1}{2}\frac{4}{3}\pi R^3 \rho_c \qquad (3.21c)$$

$$F_B = \frac{4}{3}\pi R^3 g(\rho_c - \rho_{av}) \qquad (3.21d)$$

The drag force over the surface of the growing drobble is given[67] as follows:

$$F_D = \frac{1}{2} \pi R^2 \rho_c U^2 C_d \qquad (3.21e)$$

Substituting equation (3.21 a, b, c, d and e) into equation (3.20), performing the differentiation and rearranging yield the following equation

$$\frac{dU}{dt} = \frac{1}{\frac{4}{3}\pi R^3 \left(\rho_{av} + \frac{\rho_c}{2}\right)} \left[\frac{4}{3}\pi R^3 g(\rho_c - \rho_{av}) - \frac{\pi \rho_c R^2 U^2}{2} C_d - 2\pi \rho_c R^2 U \frac{dR}{dt}\right]$$

$$(3.22)$$

This is a nonlinear ordinary differential equation of motion of the growing drobble. Where C_d in equation (3.22) is the drag coefficient of a drobble rising in an immiscible liquid. In order to calculate the instantaneous velocity, the drag coefficient must be determined. In spite of the lack of data on drag coefficients for a drobble moving in another immiscible liquid, the correlation obtained by Haberman and Morton[29] for air bubble moving in water may reasonably be used in the case of a drobble when the weight vaporization ratio is greater than 1%, since in this case the corresponding volumetric vapor ratio is about unity (volume of vapor/ total volume)[36].

$$C_d = 2.6 \qquad for \quad 10^3 \quad Re \quad 10^4 \qquad (3.23a)$$

The same relation is used in the theoretical analysis of direct contact evaporation of a drobble by Mokhtarzadeh and El-Shirbini[28], Battya et al.[32], Tadrist et al.[36], Wanchoo et al.[41] and other researchers. Also for low Reynolds number the drag coefficient was taken as[68]

$$C_d = \frac{14.9}{Re^{0.78}} \qquad for \quad 1 \quad Re < 10^3 \qquad (3.23b)$$

However, since the hydrodynamic effects of liquid surrounding each drobble are not negligible, then the drobble-drobble interaction can affect the motion of individual drobble during evaporation process. Therefore the relative

velocity between the drobbles and continuous phase need to be represented by a swarm model, which was obtained by Marrucci[57], who showed that the effect of the dispersed phase holdup could be expressed by

$$U_r = U \frac{(1 - \varepsilon)^2}{1 - \varepsilon^{5/3}}$$
(3.24)

where U is the instantaneous single drobble velocity and ε dispersed phase holdup.

This correlation was also employed by[7, 18] etc. in their population balance models.

3.2.3 Equation of Conservation of Mass:

Consider the volume of vapor phase V_v, and the liquid phase V_l (volume of spherical cup as shown in figure 3.3) and its total volume V, are related to each other and to the initial drop volume V_0, then

$$V = V_l + V_v$$
(3.25)

The mass balance for a constant drobble mass is

$$\rho_{dl} V_0 = \rho_{dl} V_l + \rho_{dv} V_v$$
(3.26)

From this equation we can obtain relation for liquid volume V_l in drobble as

$$V_l = V_0 \left(1 - \frac{\rho_{dv}}{\rho_{dl}} \frac{V_v}{V_0} \right)$$

And hence

$$V_l = V_0 (1 - \zeta)$$

Substituting this relation into equation (3.25) and divided the result by V_0 yields

$$\frac{V}{V_0} = \left(\frac{R}{R_0}\right)^3 = 1 + \zeta\left(\frac{\rho_{dl}}{\rho_{dv}} - 1\right) \tag{3.27}$$

Where ζ (the weight vaporization ratio or the mass fraction of vapor in drobble) is defined as

$$\zeta = \frac{\rho_{dv} V_v}{\rho_{dl} V_0} \tag{3.28}$$

And by simplifying this equation, the relation for vapor volume in drobble V_v can be obtain as

$$V_v = \frac{\rho_{dl}}{(\rho_{dl} - \rho_{dv})} (V - V_0)$$

$$= \frac{\rho_{dl}}{(\rho_{dl} - \rho_{dv})} \frac{4\pi}{3} (R^3 - R_0^3) \tag{3.29}$$

Equation (3.26) can be written with the geometric relation using the model shown in figure 3.3 as

$$\frac{4}{3}\pi R_0^3 \rho_{dl} = \frac{\pi}{3}(3RH^2 - H^3)\rho_{dl} + \left|\frac{4}{3}\pi R^3 - \frac{\pi}{3}(3RH^2 - H^3)\right|\rho_{dv} \tag{3.30}$$

This equation can be re arranged as

$$H^2(3R - H) = \frac{4\left(\frac{\rho_{dl}}{\rho_{dv}} R_0^3 - R^3\right)}{\frac{\rho_{dl}}{\rho_{dv}} - 1} \tag{3.31}$$

It can be rearranged in terms of the weight vaporization ratio (ζ) as

$$\zeta = \frac{\rho_{dv} \left|\frac{4}{3}\pi R^3 - \frac{\pi}{3}(3RH^2 - H^3)\right|}{\rho_{dl}\left(\frac{4}{3}\pi R_0^3\right)} \tag{3.32}$$

where

$$H = R(1 + \cos\beta) \tag{3.33}$$

Note that both , H and β are time dependent. The combination of equations (3.27), (3.31) and (3.33) gives

$$3\cos\beta - \cos^3\beta + 2 = \frac{4(1-\zeta)}{1 + \zeta(\frac{\rho_{dl}}{\rho_{dv}} - 1)} \tag{3.34}$$
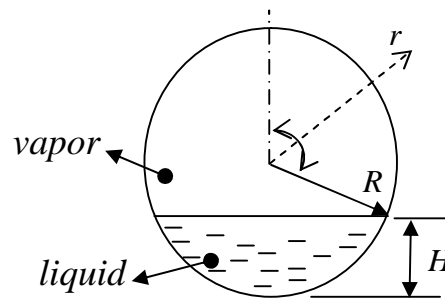

Figure 3.3 Theoretical model of an evaporating drobble.

3.2.4 Energy Equation:

The liquid drops are injected into another hotter immiscible liquid with a higher boiling point. There is sufficient superheat to allow heterogeneous nucleation of the liquid drops. The vapor then grows, and at same time the compound drop thus formed (see figure 3.1(b)).

The heat transfer is described by the time dependent energy equation which includes conduction and convection. Unlike most of the previous studies by other authors[15, 22, 26] etc., the transient term(in the energy equation) is included in this analysis since the present analysis handle the unsteady state evaporation process. In addition, unlike most of the previous studies by other authors[33, 39] etc., the opening angle (2) and the non-dimensional bubble growth rates ($\frac{R}{\alpha}\frac{dR}{dt}$) are taken to be changed instantaneously during evaporation process.

The additional following assumptions are used to simplify the mathematical model of the problem:

1. The drobble is assumed to be a sphere in which the vapor phase is bounded at the upper part by the opening angle (2), between angle 0 and , and the liquid phase at the lower part is bounded by the angle 2(-), between angle   and , where   is time dependent variable which increase due to the vaporization process progress.

2. There is no heat transfer across the continuous liquid and the dispersed vapor interface, Heat transfer is assumed to take place at the liquid-liquid interface and the thermal resistance of the dispersed liquid phase is neglected.

3. The interface between the continuous phase and the unvaporized liquid is maintained uniformly at a certain temperature (T_{sat}), and uniform temperature of continuous liquid T_c at infinity (undisturbed water temperature).

4. No heat transfer is assumed at the boundary between cells.

5. The radiation inside and outside drobble is neglected.

The energy equation is solved for the continuous liquid phase with the convective velocity taken from the fluid flow solution equation (3.19 a, b). As a result the heat transfer problem can be solved numerically since an analytical solution does not appear to be possible. The governing equation for the temperature field is as following;

$$\frac{\partial T}{\partial t} + v_r \frac{\partial T}{\partial r} + \frac{v_\theta}{r} \frac{\partial T}{\partial \theta} = \alpha \left[\frac{1}{r^2} \frac{\partial}{\partial r} \left(r^2 \frac{\partial T}{\partial r} \right) + \frac{1}{r^2 sin\theta} \frac{\partial}{\partial \theta} \left(sin\theta \frac{\partial T}{\partial \theta} \right) \right| \qquad (3.35)$$

The boundary conditions are:

- axis of symmetry of drobble

$$\frac{\partial T}{\partial \theta} = 0 \; ; \quad at \quad R \quad r \quad R_{cell} \quad and \quad \theta = 0, \pi \qquad\qquad (3.36\ a)$$

-surface of drobble

$$T = T_c \; ; \quad at \quad R \quad r \quad R_{cell} \quad\quad and \quad 0 \quad \theta \quad \beta \qquad\qquad (3.36\ b)$$

$$T = T_{ds} \; ; \quad at \quad r = R \quad\quad\quad and \quad \beta \quad \theta \quad \pi \qquad\qquad (3.36\ c)$$

-cell boundary

$$\frac{\partial T}{\partial r} = 0 \; ; \quad at \quad r = R_{cell} \quad and \quad 0 \quad \theta \quad \pi \qquad\qquad (3.36\ d)$$

The initial conditions are:-

$$at \quad t = 0 \; ; \quad U = U_0 \; ; \quad R = R_0 \; ; \quad \frac{dR}{dt} = 0 \qquad\qquad (3.37\ a)$$

$$\begin{matrix} T = T_c \\ T = T_{ds} \end{matrix} \quad when \quad \begin{matrix} r > R_0 \\ r = R_0 \end{matrix} \quad and \quad 0 \quad \theta \quad \pi \qquad\qquad (3.37b)$$

where R_0 denotes the initial droplet radius, and that is, the radius of a liquid drop to be changed into a two-phase bubble after the instant of $t = 0$. This condition can be used to obtain a steady temperature profile around a drobble (or drop) at the instant of $t=0$. It is obtained as the solution for steady heat transfer to a bubble of constant radius R_0 and used as initial condition in our model.

Boundary condition (3.36 b) is derived from the fact that at the upper part of the drobble (vapor phase), constitutes an adiabatic insulating plane. Thus, at θ β the temperature of the continuous liquid is T_c.

The evaporation is completed when all the liquid phase contained in drobble is converted to vapor phase and hence the radius of drobble at the end of evaporation process R_f can be written as

$$R_f = R_0 \left(\frac{\rho_{dl}}{\rho_{dv}} \right)^{\frac{1}{3}} \qquad\qquad (3.38)$$

3.2.5 The Growth Rate of Growing Drobble:

After solving the energy equation (3.35), the entire temperature field for the continuous phase fluid and the heat transfer rate to the drop can be obtained. This energy is used to evaporate the drop from liquid phase to vapor phase, resulting in growth of the drobble. The growth of a drobble is predicted based on the energy balance on the drobble

$$\frac{d}{dt}\left(h_{fgd}\, \rho_{dv} V_v \right) = 4\pi R^2 h\; T \qquad\qquad (3.39)$$

Where V_v denotes the vapor-phase volume which can be obtained using equation (3.29).

The average outside heat transfer coefficient h related to the total surface area of drobble is calculated as[22]

$$h = \frac{1}{4\pi R^2} \int_{\beta}^{\pi} h_\theta\, 2\pi R^2 sin\theta\; d\theta \qquad\qquad (3.40)$$

where the local heat transfer coefficient is

$$h_\theta = \frac{q_\theta^{\;''}}{T} \qquad\qquad (3.41)$$

and the local heat flux $q_\theta^{\;''}$ through the continuous phase is given by,

$$q_\theta{}'' = k \left. \frac{\partial T}{\partial r}\right|_{r=R}$$
(3.42)

Where T is the driving temperature difference between the continuous and dispersed liquid phases (degree of superheat) $(T_c - T_{ds})$

Differentiations equation (3.39) after substitute equation (3.29), and after rearrangement the resulted equation becomes

$$\frac{dR}{dt} = \frac{\alpha}{2R}\left(1 - \frac{\rho_{dv}}{\rho_{dl}}\right)\left(\rho_c C_{pc} \frac{\Delta T}{\rho_{dv} h_{fgd}}\right)\left(\frac{2Rh}{k}\right)$$
(3.43)

From this equation the increment in drobble radius in each time step can be found.

3.3 Method of Solution:

For the purpose of dimensionless formulation, we use the following transformations of the variables[32,39]

$$U^+ = \frac{U}{U_0}; \quad B = \frac{R}{R_0}; \quad \tau = \frac{\alpha t}{R_0^2}; \quad Re = \frac{2\rho_c U R}{\mu_c}; \quad Re_0 = \frac{2\rho_c U_0 R_0}{\mu_c}$$

$$Pe = \frac{2UR}{\alpha}; \quad Pe = \frac{2R_0 U}{\alpha}; \quad Pe_0 = \frac{2U_0 R_0}{\alpha}$$

$$Fr_o = \frac{U_0^2}{2R_0 g}; \quad Nu = \frac{2hR}{k}; \quad St = \frac{C_{pc}\, T}{h_{fgd}}$$

$$DRC = \frac{\rho_{dl}}{\rho_c}; \quad DRD = \frac{\rho_{dv}}{\rho_{dl}}; \quad Ja = \rho_c C_{pc}\frac{T}{\rho_{dv} h_{fgd}} = \frac{St}{(DRD\,.\,DRC)}$$
(3.48)

$$T = T_c - T_{ds}\,; \quad G = \frac{\rho_{av}}{\rho_c} = \frac{DRC}{B^3}; \quad E = \frac{(1 - \varepsilon)}{(1 - \varepsilon^{5/3})}$$

$$= \frac{T - T_c}{T_{ds} - T_c} \; ; \qquad y = \frac{r - R}{R} \; ; \qquad \mu = -\cos\theta$$

The transformation of $(r, \ )$ coordinates to (y, μ) coordinates which is shown in figure 3.4 is used in the energy equation in order to transform the geometry into a suitably spaced rectangular grid so that the finite-difference method can be easily applied [33].

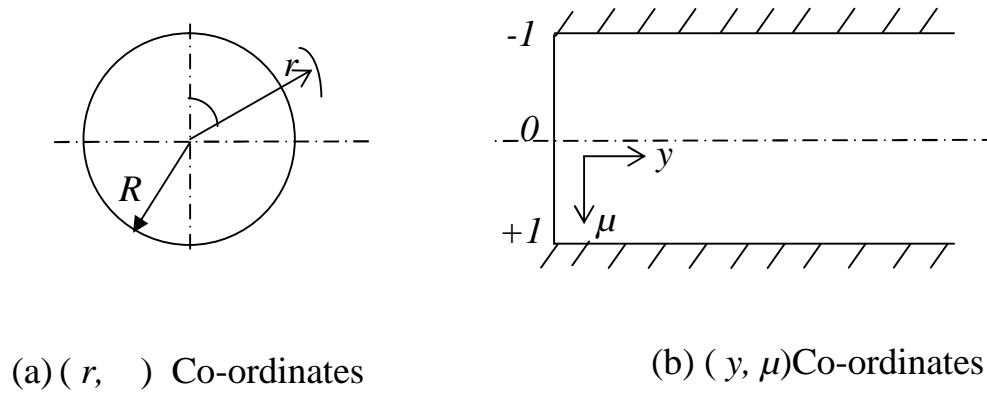(a) (r,) Co-ordinates   (b) (y, μ)Co-ordinates

Figure 3.4 Transformation of coordinates

Equations (3.22), (3.27), (3.34), (3.35), (3.43) and the boundary and initial conditions; equations (3.36), (3.37), and the condition for complete evaporation equation (3.38) can be non-dimensionalized using the above transformations, the resulting dimensionless equations are:-

$$\frac{dU^+}{d\tau} = \frac{Pe_0}{4Fr_0} \frac{1}{(G + 0.5)} \left| (1 - G) - \left(\frac{1}{B}\right) \left[0.75C_d Fr_0 U^{+2} + 6U^+ \frac{Fr_0}{Pe_0} \frac{dB}{d\tau} \right] \right|$$

(3.49)

$$B^3 = 1 + \zeta \left(\frac{1}{DRD} - 1 \right)$$

(3.50)

$$3\cos\beta - \cos\beta^3 + 2 = \frac{4(1 - \zeta)}{1 + \zeta(\frac{1}{DRD} - 1)}$$

(3.51)

$$\frac{\partial}{\partial\tau} + \left[\frac{Pe\ E}{2}\left(1 - \frac{1}{(1+y)^3}\right)\mu + \frac{1}{(1+y)^2}\frac{dB}{d\tau} - \frac{2}{(1+y)B}\right]\frac{1}{B}\frac{\partial\Phi}{\partial y}$$

$$+ \left[\frac{Pe\ E}{2}\left(1 + \frac{1}{2(1+y)^3}\right)\frac{(1-\mu^2)}{(1+y)} + \frac{2\mu}{(1+y)^2 B}\right]\frac{1}{B}\frac{\partial}{\partial\mu}$$

$$- \frac{1}{B^2}\frac{\partial^2}{\partial y^2} - \frac{(1-\mu^2)}{B^2(1+y)^2}\frac{\partial^2}{\partial\mu^2} = 0 \qquad\qquad (3.52)$$

$$\frac{dB}{d\tau} = \frac{(1 - DRD)}{2B}\ Ja\ Nu \qquad\qquad (3.53)$$

Where,

$$Nu = \frac{h\ D}{k} = -\ \int_{-cos\beta}^{+1}\left.\frac{\partial\Phi}{\partial y}\right|_{y=0}\ d\mu \qquad\qquad (3.54)$$

The initial and boundary conditions become:

$$\tau = 0\ ;\quad U^+ = 1\ ;\quad B = 1\ ;\quad \frac{dB}{d\tau} = 0 \qquad\qquad (3.55\ a)$$

$$\begin{aligned}&= 0\\&= 1\end{aligned}\quad when \quad \begin{aligned}y &> 0\\ y &= 0\end{aligned}\quad and \quad -1\quad \mu\quad +1 \qquad (3.55\ b)$$

$$\frac{\partial}{\partial\mu} = 0\ ;\quad at \quad y_{cell}\quad y\quad 0\quad and \quad \mu = -1, 1 \qquad (3.56\ a)$$

$$= 0\ ;\quad at \quad y_{cell}\quad y\quad 0\quad and \quad -1\quad \mu\quad -\cos\beta \qquad (3.56\ b)$$

$$= 1\ ;\quad at \quad y = 0\quad and \quad -\cos\beta\quad \mu\quad +1 \qquad (3.56\ c)$$

$$\frac{\partial}{\partial y} = 0\ ;\quad at \quad y = y_{cell}\quad and \quad -1\quad \mu\quad +1 \qquad (3.56\ d)$$

The complete evaporation condition becomes

$$B = DRD^{-1/3} \qquad\qquad (3.57)$$

The equations (3.49, 3.50, 3.51, and 3.53) are solved simultaneously by using the variable step Runge-Kutta method for the quantities $U, \zeta, \quad and \ R$. The heat transfer coefficient, employed in this solution can be obtained by solving equation (3.52) numerically using finite difference scheme and utilizing equation (3.54). The solution methods will be described in the following sections.

3.3.1 The Instantaneous Rising Velocity of the Growing Drobble:

It is calculated by solving equation (3.49) by Runge-Kutta Algorithm[69] using the initial condition as:

$$U^+(\tau = 0) = 1; \quad B(\tau = 0) = 1 ; \quad \frac{dB(\tau = 0)}{d\tau} = 0;$$

$$Ku1 = d\tau \, Fu\left(U^{+i}, B^i, \frac{dB^i}{d\tau}, Fr_0, DRC, Pe_0\right)$$

$$Ku2 = d\tau \, Fu\left(U^{+i} + Ku1/2, B^i, \frac{dB^i}{d\tau}, Fr_0, DRC, Pe_0\right)$$

$$Ku3 = d\tau \, Fu\left(U^{+i} + Ku2/2, B^i, \frac{dB^i}{d\tau}, Fr_0, DRC, Pe_0\right)$$

$$Ku4 = d\tau \, Fu\left(U^{+i} + Ku3, B^i, \frac{dB^i}{d\tau}, Fr_0, DRC, Pe_0\right)$$

$$U^{+i+1} = U^{+i} + \frac{Ku1 + 2(Ku2 + Ku3) + Ku4}{6} \tag{3.59}$$

Where

$$Fu\left(U^{+i}, B^i, \frac{dB^i}{d\tau}, Fr_0, DRC, Pe_0\right) = \frac{dU^+}{d\tau}$$

3.3.2 The Evaporation Ratio and the Half Opening Angle:

For any value of dimensionless radius B^i in equation (3.50), the corresponding value of ζ^i can be obtained as

$$\zeta^i = \frac{1}{\left(\frac{1}{DRD} - 1\right)}\left((B^i)^3 - 1\right) \tag{3.60}$$

Then by solving the nonlinear equation (3.51) numerically by the successive substitutions method [70] for the half opening angle β which can be written as

$$\beta^i = \cos^{-1}\left(\frac{1}{3}\left(\frac{4(1 - \zeta^i)}{1 + \zeta^i\left(\frac{1}{DRD} - 1\right)} + \cos(\beta^i)^3 - 2\right)\right) \tag{3.61}$$

The corresponding value of the half opening angle (β) can be obtained, which is necessary in the next section for solving the energy equation.

3.3.3 The Heat Transfer Rate:

Equation (3.52) represents the time dependent energy equation written in (y, μ) coordinates with heat conduction and convection in the y and μ directions. The geometry of the drobble is changing continuously as it grows during the evaporation process, and the solution points of the problem in each time step is depending on the solution points of the previous step, therefore, uniform discretization step of (y and μ), but different number of node in y direction, is used for all the time domain in order to handle this problem. Equation (3.52) can be solved numerically by finite difference methods and can be written as:-

$$\frac{\partial}{\partial \tau} + a_1\frac{\partial}{\partial y} + a_2\frac{\partial}{\partial \mu} + a_3\frac{\partial^2}{\partial y^2} + a_4\frac{\partial^2}{\partial \mu^2} = 0 \tag{3.62}$$

Where

$$a_1 = \frac{1}{B}\left[\frac{Pe\ E}{2}\left(1 - \frac{1}{(1+y)^3}\right)\mu + \frac{1}{(1+y)^2}\frac{dB}{d\tau} - \frac{2}{B(1+y)}\right]$$

$$a_2 = \frac{1}{B}\left[\frac{Pe\ E}{2}\left(1 + \frac{1}{2(1+y)^3}\right)\frac{(1-\mu^2)}{(1+y)} + \frac{2\mu}{(1+y)^2 B}\right]$$

$$a_3 = \frac{-1}{B^2}; \quad a_4 = \frac{-1}{B^2}\frac{(1-\mu^2)}{(1+y)^2}$$

Applying the first order explicit time differencing to equation (3.62), one can obtain

$$^{i+1} = {}^{i} - \tau\left[a_1\frac{\partial\ ^{i}}{\partial y} + a_2\frac{\partial\ ^{i}}{\partial\mu} + a_3\frac{\partial^2\ ^{i}}{\partial y^2} + a_4\frac{\partial^2\ ^{i}}{\partial\mu^2}\right] \qquad (3.63)$$

Where ^{i} denotes the dimensionless temperature at the current time step, $^{i+1}$ denotes the temperature at the next time step and τ denotes the time interval.

The above equation describes the method to advance the solution for one time step. In order to solve equation (3.63), one also needs to approximate the spatial derivatives $\frac{\partial\Phi}{\partial y}, \frac{\partial\Phi}{\partial\mu}, \frac{\partial^2\Phi}{\partial y^2}$ and $\frac{\partial^2\Phi}{\partial\mu^2}$ by finite differences. The diffusion terms associated with the second order spatial derivatives are approximated by central difference as follows:

$$\frac{\partial^2}{\partial y^2} = \left(\frac{\Psi_{j+1,k} + {}_{j-1,k} - 2\ _{j,k}}{y^2}\right)$$

$$\frac{\partial^2}{\partial\mu^2} = \left(\frac{\Psi_{j,k+1} + {}_{j,k-1} - 2\ _{i,k}}{\mu^2}\right)$$

and the convective terms associated with the first order spatial derivatives are approximated by first-order upwind scheme[71] (see appendix A) as follows

$$a_1 \frac{\partial}{\partial y} = a_1^+ \left(\frac{\Psi_{j,k} - \Psi_{j-1,k}}{y} \right) + a_1^- \left(\frac{\Psi_{j+1,k} - \Psi_{j,k}}{\wedge y} \right)$$

$$a_2 \frac{\partial}{\partial \mu} = a_2^+ \left(\frac{\Psi_{j,k} - \Psi_{j,k-1}}{\mu} \right) + a_2^- \left(\frac{\Psi_{j,k+1} - \Psi_{j,k}}{\wedge \mu} \right)$$

Where

$$a_1^+ = \max(a_1, 0); \quad a_1^- = \min(a_1, 0)$$

$$a_2^+ = \max(a_2, 0); \quad a_2^- = \min(a_2, 0)$$

The second order upwind differencing for the convective fluxes could be used to improve the accuracy. However the reason for using the first order upwind differencing here is to simplify the programming effort and to reduce the computer time. Besides, we are using a fine grid in our computation and the accuracy lost in using the first order approximation will be minimized.

Applying the central difference approximation for diffusion terms and the upwind differencing approximation for convective terms, one can obtain

$$
\begin{aligned}
\Phi_{j,k}^{i+1} = \Phi_{j,k}^i - \tau \Big[a_1^+ \left(\frac{\Phi_{j,k}^i - \Phi_{j-1,k}^i}{y} \right) + a_1^- \left(\frac{\Phi_{j+1,k}^i - \Phi_{j,k}^i}{y} \right) \\
+ a_2^+ \left(\frac{\Phi_{j,k}^i - \Phi_{j,k-1}^i}{\mu} \right) + a_2^- \left(\frac{\Phi_{j,k+1}^i - \Phi_{j,k}^i}{\wedge \mu} \right) \\
+ a_3 \left(\frac{\Phi_{j+1,k}^i + \Phi_{j-1,k}^i - 2\Phi_{j,k}^i}{y^2} \right) \\
+ a_4 \left(\frac{\Phi_{j,k+1}^i + \Phi_{j,k-1}^i - 2\Phi_{j,k}^i}{\mu^2} \right) \Big]
\end{aligned}
\qquad (3.64)
$$

The explicit equation (3.64) requires a four–point scheme for each point (*j, k*) in the y, μ directions as shown in figure 3.5.
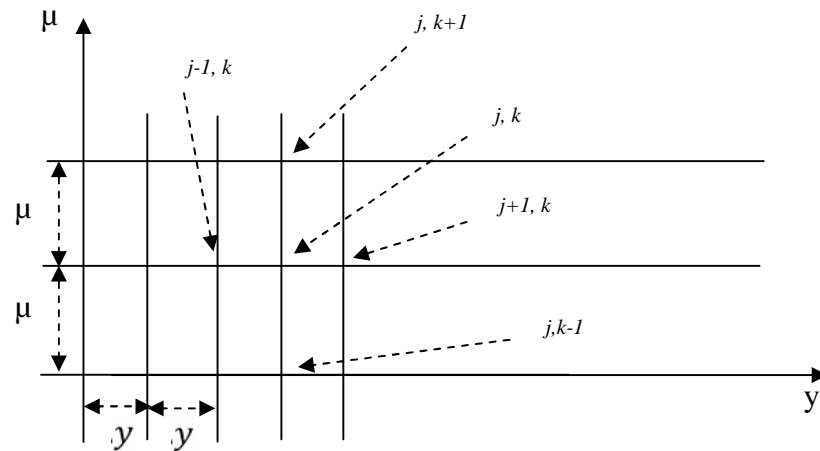
Figure 3.5 General grid layout for numerical solution for a time step.

The numerical solutions were done in the domain defined by $(0 \leq y \leq y_{cell})$ and $(-1 \leq \mu \leq 1)$, and calculated in a mesh with the discretization steps $y = 1/100 \; and \; \mu = 1/100$. Numerical trials were made on grids with the discretization steps $y = 1/50, 1/100, 1/125, 1/150,$ and $\mu = 1/50, 1/100, 1/125, 1/150, 1/250$. The solutions obtained using the grid with $y = 1/100$ and $\mu = 1/100$ were found to be mesh-independent. For this reason, the heat transfer results presented here were computed on the base of mesh with $y = 1/100$ and $\mu = 1/100$. The time step was variable and changed from the start of the computation to the final stage. The upwind scheme is stable if the following Courant-Friedrichs-Lewy condition (CFL) is satisfied [72], which is

$$|a \cdot \tau| \leq 1 \tag{3.65}$$

Hence

$$\tau = C_1 \frac{1}{a} \tag{3.66}$$

Where

$$a = \left(\frac{a_1^+}{\Delta y} - \frac{a_1^-}{y} + \frac{a_2^+}{\mu} - \frac{a_2^-}{\mu} - \frac{2a_3}{y^2} - \frac{2a_4}{\mu^2} \right)$$

The constant (C_1) in equation (3.66) was determined by 'trial and error' of different values (0.01-1.2) ,after more trails and taking the best value in order to insure the optimum accepted convergences be less than or equal (1.0) when β varing from 0 to π.

The temperature gradient at the drobble surface is evaluated using the temperatures at the drobble surface and at the nearest node outside the surface with the aid of the second-order upwind scheme that is:

$$\frac{\partial \Phi}{\partial y}\bigg|_{y=0} \simeq \frac{1}{2 \, y}\big|-3 \,{}_{j=1,k} + 4 \,{}_{j+1,k} - \,{}_{j+2,k}\big| \tag{3.67}$$

This equation can be applied in the Nusselt relation, equation (3.54), and by the integrating numerically; using trapezoidal rule one can obtained the instantaneous average value of Nusselt number which is necessary in the growth rate equation.

3.3.4 The Growth Rate and the Instantaneous Radius of Drobble:

Substituting the Nusselt number obtain from previous section into equation (3.53) and solving this equation by Runge-Kutta Algorithm the growth rate and hence the new radius of the grown drobble can be obtained as

$$B(\tau = 0) = 1$$

$$Kb1 = d\tau \, Fb(B^i, DRD, Jac, Nu^i)$$

$$Kb2 = d\tau \, Fb(B^i + Kb1/2, DRD, Jac, Nu^i)$$

$$Kb3 = d\tau \, Fb(B^i + Kb2/2, DRD, Jac, Nu^i)$$

$$Kb4 = d\tau\, Fb(B^i + Kb3, DRD, Jac, Nu^i)$$

$$B^{i+1} = B^i + \frac{Kb1 + 2(Kb2 + Kb3) + Kb4}{6} \tag{3.68}$$

and

$$\frac{dB^{i+1}}{d\tau} = Fb\left(B^{i+1}, DRD, Jac, Nu^i\right) \tag{3.69}$$

where

$$Fb\left(B^i, DRD, Jac, Nu^i\right) = \frac{dB}{d\tau}$$

3.4 The Volumetric Heat Transfer Coefficient:

For the design and the layout of the heat exchangers, models are needed to describe the influence of the different parameter on the evaporation of multidroplets, where the drobbles interaction cannot be neglected. Because of motion of the interfaces between the phases, the heat transfer area changes with time and can hardly be determined. Therefore, it is better to describe the process in terms of volumetric heat-transfer coefficient. The volumetric heat-transfer coefficient and other important characteristic quantities, such as the height for complete evaporation, were calculated by applying single drops empirical correlations, which are modified and extended for the case of an evaporating multidrobbles. While the experimental studies have yielded valuable data and experience concerning the industrial application of direct-contact evaporation, there is lack of theoretical model (comprehensive) for volumetric heat transfer coefficients. There is a growing demand for an analytical model for situations when empirical correlations do not exist. The purpose of this part of the present work is to develop such a model.

In addition to the assumptions mentioned in the previous sections, the following assumptions are employed to simplify the actual physical phenomena:

1. The fundamental assumption in the present model is that multi-droplets direct-contact evaporation can be described using specific heat-transfer rate of individual droplets inside cell of liquid, derived in previous section.

2. The dispersed phase injected in the form of saturated liquid drops of a uniform size, is resulting in an immediate start of evaporation.

3. No significant axial temperature gradient along the column and the temperature of the continuous liquid is spatially uniform and quasi-steady with respect to the evaporation time of drobbles.

4. The fragmentation and coalescence do not occur thus, the number density of drobbles remain constant as the two-phase drobble rising and their diameters increase.

The model is intended to obtain the relationship between the rate of evaporation of drobbles and their displacement during rising (hence, the time), so that the local volumetric heat-transfer coefficient may be calculated as a function of this displacement with the following equation[60]

$$h_{v,z} = A_d N_d h_d \tag{3.70}$$

And the average volumetric heat-transfer coefficient can be written as[49] (see figure 3.6)

$$h_{mv}(z) = \frac{1}{z} \int_{z0}^{z} A_d(z) N_d h_d(z) dz \tag{3.71}$$

Where, Z, is the axial coordinate, A_d, the drobble surface area, N_d, the droplet number density, and h_d is the droplet heat-transfer coefficient (denoted h in

previous section). All these parameters depend on the time of the evaporating drobbles. Therefore, the subsequent calculations can be simplified if these quantities are expressed in terms of *D*, which is defined as instantaneous equivalent spherical diameter. Hence, equation (3.71) becomes

$$h_{mv}(D) = \frac{1}{z} \int_{D0}^{D} A_d(D) N_d h_d(D) \frac{dz}{dD} dD \qquad (3.72)$$
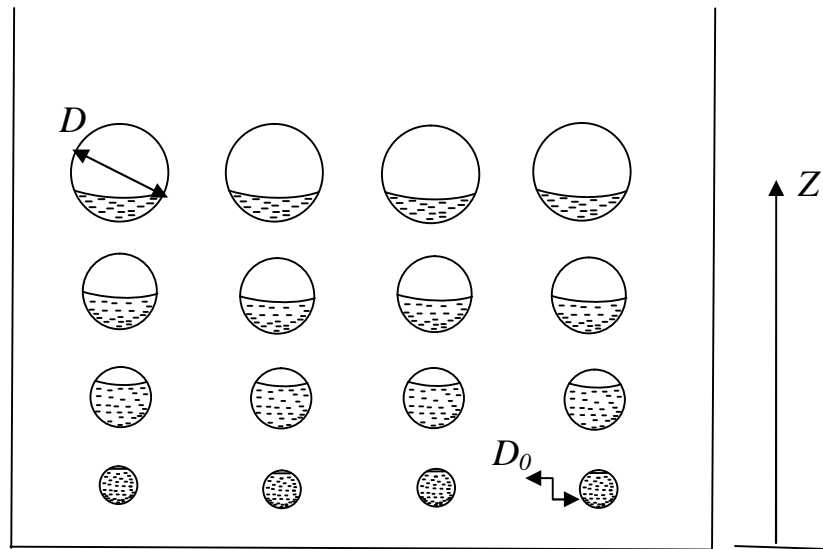

Figure 3.6 Illustration of drobbles size dependence on height.

Also, the diameter (*D*) can be expressed in term of time; so this equation can be rewritten in term of time.

During evaporation process, the droplets do not depart from sphericity so that the surface area can be approximated by:

$$A_d(D) = \pi D^2 \qquad (3.73)$$

The single drobble heat-transfer coefficient can be calculated theoretically using the model derived in the previous part of this work ,and this can be considered a new attempt in this field, since most of the available works

in this field is based on assumed experimental models for the single drobble heat transfer coefficient [7, 18, 49] etc..

Seetharamu and Battya[53] observed that there is no significant axial temperature gradient along the column. This was observed by Smith et al.[49] and may be attributed to the presence of turbulence during the evaporation process. Hence, it is assumed that the temperature of the continuous liquid is spatially uniform and quasi-steady with respect to the evaporation time of an individual drobble.

According to the assumption that there is no coalescence and fragmentation phenomena between the drobbles, this was also assumed by Peng et al.[60] and other researchers, which may be attributed to the weak effects of these phenomena during the drobbles evaporating. Thus, the number density of droplets is assumed to be constant that is ($N_d = N_{d0}$) as the drobbles rising and their diameters increase.

The initial droplet number density N_{d0} can be calculated by using[60]:

$$N_{d0} = \frac{U_d}{(1/6) \, \pi \, D_0^3 \, U_0} \tag{3.74}$$

$$U_d = \frac{\dot{V}_d}{A} \tag{3.75}$$

Where $\dot{V}_d$ denote the volumetric flow rate of the dispersed phase; U_0 is the initial velocity of the dispersed phase (drobbles) and A is the cross section area of the column. Because the mass of the dispersed phase entering the distributor is equal to that leaving the distributor, U_0 can be calculated by using

$$U_0 = \frac{4 \, \dot{V}_d}{\pi \, N_h \, d_h^2} \tag{3.76}$$

Substituting equations (3.75) and (3.76) in to equation (3.74) yield

$$N_d = \frac{6 \, N_h \, d_h^2}{4 \, D_0^3 \, A} \tag{3.77}$$

During the evaporation process, the subsequent calculations is to define a dispersed phase volume fraction (holdup) by[49]:

$$\varepsilon(D) = \frac{\pi}{6} \, D^3 \, N_d \tag{3.78}$$

The diameter of the cell, D_{cell}, can be related to the volume fraction of the dispersed phase in the cell as mentioned previously in equation (3.1) as follow:

$$D_{cell} = D \, \varepsilon^{-1/3} \tag{3.79}$$

Where D ,ε denote the instantaneous diameter and holdup, respectively.

The mass balance can be utilized for a differential volume of the column of height dZ (as shown in the simple sketch, figure 3.7). Thus, the net increment of mass of vapor per unit time in the differential element

$$d\dot{m} = \dot{m}_{out} - \dot{m}_{in} = \rho_{dv} \, A \, N_d d(U_r \, V_v) \tag{3.80}$$

where U_r the relative velocity between the drobbles and continuous phase (as defined previously in equation (3.24)) which is

$$U_r = U \, \frac{(1 - \varepsilon)^2}{(1 - \varepsilon^{5/3})}$$

The volume of dispersed vapor phase per drobble (as mention previously, equation (3.29)) is given by

$$V_v = \frac{\rho_{dl}}{(\rho_{dl} - \rho_{dv})} \frac{\pi}{6} \, (D^3 - D_0^3)$$

Substituting the above equation into equation (3.80) yields

$$d\dot{m} = \frac{\pi}{6} \, C_{m1} \, A \, N_d \, d\big(U_r \, (D^3 - D_0^3)\big) \tag{3.81}$$

67

where

$$C_{m1} = \frac{\rho_{dl}\,\rho_{dv}}{(\rho_{dl} - \rho_{dv})}$$

So the rate of heat transfer from the continuous phase to the dispersed phase is given by

$$dQ = d\dot{m}\,h_{fg} = \frac{\pi}{6}\,C_{m1}\,h_{fgd}A\,N_d d\big(U_r\,(D^3 - D_0^3)\big) \tag{3.82}$$
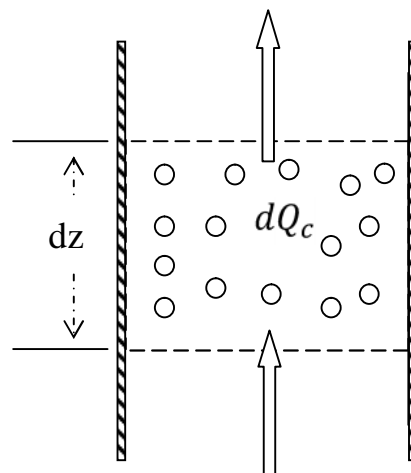
In addition, according to the Newton law of cooling, the rate of heat transfer, dQ_c can be written as

$$dQ_c = h_d\,\pi D^2 N_d\;T\,A\,dz \tag{3.83}$$

Equating equation (3.83) to equation (3.82), the following relation can be obtained;

$$\frac{d\big(U_r\,(D^3 - D_0^3)\big)}{dz} = \frac{6\,h_d D^2\;T}{h_{fg}\,C_{m1}} \tag{3.84}$$

Mass of vapor leaving per unit time,
$\dot{m}_{out} = \rho_v\,A\,N_d U_r\,V_v + \rho_v\,A\,N_d d(U_r\,V_v)$

Mass of vapor entering per unit time,
$\dot{m}_{in} = \rho_v\,A\,N_d U_r\,V_v$

Figure 3.7 Mass balances in a differential element.

68

By differentiating and utilizing chain rule,

$$\frac{dU_r}{dD} = \frac{dU_r}{dt} \frac{1}{dD/dt}$$

$$\frac{dz}{dD} = \frac{dz}{dt} \frac{1}{dD/dt}$$

and since Z and U_r are time dependent then the left side of equation (3.84) becomes

$$\frac{d(U_r\,(D^3 - D_0^3))}{dz} = \frac{1}{dz/dt}\left(3D^2 U_r \frac{dD}{dt} + (D^3 - D_0^3)\frac{dU_r}{dt}\right) \qquad (3.85)$$

Combining equation (3.84) with equation (3.85), the following equation can be obtained:

$$\frac{dz}{dt} = \frac{C_{m1}\,h_{fg}}{6\,h_d D^2\,T}\left(3D^2 U_r \frac{dD}{dt} + (D^3 - D_0^3)\frac{dU_r}{dt}\right) \qquad (3.86)$$

Integrating equation (3.86) between *Z=0, at t=0 and   Z=Z, at t= t* gives

$$Z(t) = \frac{C_{m1}\,h_{fg}}{6\,T}\int_0^t \frac{1}{h_d\,D^2}\left(3D^2 U_r \frac{dD}{dt} + (D^3 - D_0^3)\frac{dU_r}{dt}\right)dt \qquad (3.87)$$

It can be noted here that the derivative ($\frac{dU_r}{dt}$), which is necessary to be determined in the previous equation, is calculated numerically using three point formula method as

$$\frac{dU_r^i}{dt} = \frac{U_r^{i+1} - U_r^{i-1}}{2\,t} \qquad\qquad 1 < i < nt$$

and the extrapolation for boundary points as

$$\frac{dU_r^{i=1}}{dt} = 2\frac{dU_r^{i=2}}{dt} - \frac{dU_r^{i=3}}{dt}$$

and

$$\frac{dU_r^{i=nt}}{dt} = 2\frac{dU_r^{i=nt-1}}{dt} - \frac{dU_r^{i=nt-2}}{dt}$$

From equation (3.87) the local position of drobbles can be calculated for each time of the evaporation process.

The average volumetric heat transfer coefficient from the location of drobble formation to the height Z, which is defined by equation (3.71), is related to the time as

$$h_{mv}(t) = \frac{1}{z(t)} \int_0^{z(t)} A_d(t) N_d h_d(t) dz(t) \tag{3.88}$$

With the substitution of equation (3.73), equation (3.86) and equation (3.87) into equation (3.88), followed by a rearrangement, the average volumetric heat transfer coefficient is obtained as:

$$h_{mv}(t) = \frac{\int_0^t \left(\pi N_d \left(3D^2 U_r \frac{dD}{dt} + (D^3 - D_0^3)\frac{dU_r}{dt} \right) \right) dt}{\int_0^t \left(\frac{1}{h_d(t)\,D^2} \left(3D^2 U_r \frac{dD}{dt} + (D^3 - D_0^3)\frac{dU_r}{dt} \right) \right) dt} \tag{3.89}$$

By solving equation (3.89) numerically (using trapezoidal rule for the integration) the average volumetric heat transfer coefficient is obtained for each time; and hence for each Z.

70

3.5 The Calculation Procedure:

The following iterative procedure is adopted:

i. Assuming an initial configuration with given initial values of R_0, U_0 and β.

ii. With known geometry, a grid is generated and the temperature field is solved (equation 3.64).

iii. The Nusselt number is calculated from equation (3.54) using equation (3.67).

iv. The new radius and growth rate are obtained from equations (3.68) and (3.69), respectively.

v. The rising velocity of the growing drobble is calculated from equation (3.59).

vi. The evaporation ratio and the half opening angle are calculated from equations (3.60) and (3.61), respectively.

vii. Return back to step (ii) and iterate until the the drobble has almost evaporated.

viii. The local position of drobbles is calculated from equation (3.87) for each time of the evaporation process.

ix. The average volumetric heat transfer coefficient is calculated by solving equation (3.89) numerically for each time; and hence for each Z.

This procedure gives the complete evaporation of drobbles.

Chapter Four

RESULTS AND DISCUSSION

Chapter Four

Results and Discussion

4.1 Introduction:

In order to investigate the direct contact evaporation process of droplets in an immiscible liquid, the governing equations are solved for the certain important characteristics, relating to this process. In the present discussion two cases are considered the first when the interactions between drobbles may be insignificant such case represents the single drobble evaporation, and the second case is the multi-drobbles evaporation process, where the interactions between drobbles is a significant parameter. For the first case (the evaporation of single drobble) the relative velocity and evaporative drobbles position, the radius and average density ratio, the vaporizing angle (half opening angle), and the specific heat transfer coefficient of a growing drobbles are investigated. For the second case (evaporation of the multi-drobbles) the dispersed phase holdup, the relative velocity and evaporative drobbles position, the average volumetric heat transfer coefficient, and the total time and height for complete evaporation are evaluated. Since the evaluation of these characteristics are essential for designing and constructing direct contact evaporation equipments.

The n-pentane/distilled water system is chosen for calculations in this study since firstly, this pair of fluid system is satisfying the assumption and most common configuration as mentioned previously which employed in this study and secondly, this pair of fluid system was described experimentally for single and multi-droplets evaporation by many authors and it can be compared with the results of present models.

The physical properties of fluids forming the drobbles and the continuous medium must be specified in order to perform the calculation, so

72

the results presented were obtained with physical properties (using EES (Engineering Equation Solver) software program[73]) relevant to n-pentane drobbles evaporating in a water under the appropriate temperatures and the atmospheric pressure .Separate presentation of the results and the discussions for each studied case i.e. single and multi-drobbles evaporation is followed. In additions a comparison between the present theoretical work and the published theoretical and experimental works of other researchers are also performed.

4.2 The Direct Contact Evaporation When Interactions between Drobbles Insignificant (Single Drobble Evaporation):

For spheres and most other types of immersed objects, it is accepted that one may apply the theory of a single sphere inside a flowing mixture of monodisperse spheres, if the average distance between the centers of the spheres is greater than 6 R, that is, if the outer surfaces of the spheres are separated by a distance of at least two diameters[11], hence, $R_{cell}=3R_f$ is assumed in this section, in order to obtain the single drobble evaporation results.

Before starting in obtaining the results of this part, the accuracy of the numerical scheme that used in the solution is verified by comparing the results of the present work with the analytical solutions of the steady state evaporation by Sideman and Taitel[15]. The two physical systems become similar when the unsteady term in the energy equation (3.52) of the present analysis is neglected. The numerical solution of the resulting energy equation was carried out using computer program as shown in the flow chart (appendix B).

The comparison is shown in figure 4.1 for the temperature profiles which is established for the location $\beta = 0^0$ and $\theta = 90^0$ for different values of Peclet number (1000, 5000, 10000). Also, figure 4.2 shows the comparison of

73

the value of $Nu/Pe^{0.5}$, the good agreement obtained is an indication of the accuracy of the present numerical scheme. Based on these results this numerical scheme can be used to investigate the evaporation process of growing drobbles.

The procedure of solution outlined in the previous chapter (section 3.3.5) is used to solve the mathematical model for the the evaporation of drobbles and the calculations were done using a computer programs as shown in the flow chart (Appendix C).

In order to illustrate the influence of the several physical parameters on the evaporation process under consideration, a parametric analysis is carried out. These parameters are the initial droplets diameter, the degree of superheat (driving temperature difference) and the initial velocity of droplets.

The values of these parameters were chosen according to the more common case of the evaporation process, which exist in the literature and also it is selected to suit the experimental evidence and observations by the other authors.

The ranges of these parameters used in this analysis are:-

- The initial droplet diameter D_0 : 1.5 D_0 $3\ mm$.
- The degree of superheat $T = (T_c - T_{ds})$: 2. T $16\ K$.
- The initial droplet velocity U_0: 0.15 U_0 $0.25\ m/s$.

The influences of each one of these parameters on the evaporation process results such as the relative velocity and the position of the evaporating drobbles, the radius and average density, the vaporizing angle (half opening angle) and the heat transfer coefficient of a growing drobbles are presented and discussed in the following sections.

4.2.1 Instantaneous Relative Velocity and the Evaporative Drobbles Position:

The evaluation of the instantaneous relative velocity of drobble U_r is obtained numerically form equation (3.59) and utilizing equation (3.24). The variation of the velocity with the time is shown in figures 4.3 to 4.5 for different selected parameters (D_0, T, U_0).

The general trend in these figures is slightly fluctuation of the velocity at the early stage of evaporation, then fall to minimum value, and after short time it is again increasing to reach its maximum value. The earliest fluctuation of the velocity may be due to abruptly exposed of the droplet to a high temperature continuous liquid, and that affect on the heat transfer and the growth of droplet at this stage consequently the droplet velocity but this effect vanished after a short time. In the next stage, the velocity drop to its minimum value due to higher growth rate of drobble (due to heat transfer rate) which causes increasing the resisting force against the motion of drobble (see equation (3.22)) and since in this stage, the average density of drobble is relatively high (see figures 4.12-4.14) the buoyancy force (that tend to lift drobble) is small, and the drag force being the dominate force which tend to decelerate the drobble velocity. After a short time the velocity start to rise till it reaches the maximum value, this is due to the continuous evaporation process and hence the buoyancy force becomes larger than the other forces due to increase the volume of vapor phase in drobble.

The effect of initial diameter on the variation of instantaneous relative velocity of the drobble with the time is depicted in figure 4.3. The relative velocity is found to be increase with the initial droplet diameter increment (while the other parameters are kept constants), and that increases in the velocity is found to be accompanied by increasing of the final time for

complete evaporation (this is also obtained by Ay. et al.[55]). This may be due to, the increase in the initial diameter means more initial mass of the droplet and hence it needs more heat to complete its evaporation, and hence the process become longer for larger initial diameter, and since the growth of vapor phase is continuous, the buoyancy force become larger which increases the relative velocity.

The heat transfer due to large degree of superheat T leads to rapid evaporation process and consequently, shorter time for complete evaporation as shown is figure 4.4. As T increases, the vapor generation becomes faster which leads to decrease the average density of drobble (see figure 4.13) and consequently, large difference between the continuous and drobble densities ($\rho_c - \rho_{av}$) is obtained. The increasing in both volume of drobble (due to increase vapor generation) and the densities difference, lead to increase the buoyancy force which try to lift the drobble quickly and increases U_r.

No significant influence of the initial velocity of droplet on the rising velocity of evaporating drobble was observed at any time of evaporation except at the early stage of evaporation process (nearly 3% evaporation), as shown in figure 4.5. This behavior of velocity is also confirmed theoretical by the results of [28]. This is because there is no important effect of the initial droplets velocity on the rising velocity in most the evaporation stages where the buoyancy force becomes the dominated force in these stages.

The solution of equation (3.87), which gives the instantaneous position of the evaporating drobble with the time are illustrated in figures 4.6 to 4.8 for different selected parameter(D_0, T, U_0). The general obvious trend from these figures is increasing of the drobble height with the time since the drobble is rising continuously during the evaporation process.

The effect of initial diameter on the instantaneous position of the evaporating drobbles with the time is shown in figure 4.6. The height for complete evaporation is found to be larger when the initial droplet diameter is larger. This is because the initial mass for the large droplet is greater than that for small droplet and hence it needs a longer time for complete evaporation.

Figure 4.7 shows the effect of the degree of superheat on the height of evaporative drobbles position. The instantaneous position increases with the time for various value of the degree of superheat. As degree of superheat increase the final position (for complete evaporation) decreases since the evaporation process become more rapid.

No significant influence of the initial droplets velocity on evaporative drobbles position at any time of evaporation is observed in figure 4.8. This is due to the reason mentioned previously in discussion of figure 4.5.

4.2.2 The Instantaneous Radius and Average Density of Drobble:

Evaluation of the instantaneous radius of the evaporative drobble is done by equation (3.68). The variation of the radius with the time is shown in figures 4.9 to 4.11 for different selected evaporation parameters $(D_0,\ T, U_0)$. The general behavior observed in these figures is increment of the radius with the time. This is due to increasing the size of vapor-phase which is generated due to continuous evaporation process.

The effect of the initial diameter on the instantaneous radius of drobble is shown in figure 4.9. From this figure it is observed that the growing of the smaller drop is faster than the larger one. This may be due to that the small droplet has small amount of dispersed liquid and so it completes evaporation quickly.

Figure 4.10 shows the effect of the degree of superheat on the instantaneous radius of drobble. As one would expect the longer evaporation time is needed for the smaller degree of superheat (the heat driven force) when the other controlling parameters are kept constant. This may be attributed to that, increasing the degree of superheat leads to increase the heat transfer rate to the drobble and hence the evaporation process becomes faster, so that the time required to complete evaporation of drobble will be smaller.

The influence of initial velocity of droplet on the instantaneous radius is shown in figure 4.11. This figure indicates that the effect of the initial velocity of droplet on the radius of drobble is insignificant. This may be due to the fact that the initial droplets velocity acts only in the early stage of evaporation, as evaporation proceeds its effect vanished on the heat transfer, rising velocity and vapor growth rate.

The solution of equation (3.21b), which gives the variation of average density of drobble with the time are illustrated in figures 4.12 to 4.14 for different selected parameters (D_0, T and U_0). From these figures, it is obvious that the average density ratio of drobble decreases with the time due to continuous increasing in the volume of drobbles as evaporation process continuous.

Figure 4.12 shows the behavior of the average density ratio with the time for different initial diameters. The average density ratio increases (for fixed time in the range where the evaporation process take place for different values of D_0) with increasing initial diameter due to increase the volume of drobble and it concern mass. Figure 4.13 shows the behavior of the average density ratio with the time for different degree of superheat, which is decreasing with increasing the amount of superheat for fixed time. This is due to faster increase of the vapor generation with increasing the degree of superheat. The effect of

the initial velocity on the average density ratio of drobble is insignificant as shown in figure 4.14; this may be due to the absence of the effect of the initial droplets velocity on the drobble radius as mentioned before, since the average density is proportional to the cubic radius of drobble.

4.2.3 The Half-Opening Angle of the Drobble:

The half-opening angle β of vaporization is calculated numerically using equation (3.61). The variations of the half-opining angle with the time are indicated in figures 4.15 to 4.17 for different selected parameters (D_0, T and U_0). From these figures similar behavior can be observed for the different cases of these parameters, in which the half opening angle β is about 90^0 at 1 % of the total time of evaporation, increases up to about 135^0 in 3-10 % of the total time. Increasing of angle above the range is quite moderate till it reaches the maximum value at the end of evaporation.

Figure 4.15 shows the effect of initial diameter of droplet on the half-opening angle of vaporization, while the other parameters are kept constants. The variation of the half-opening angle of vaporization with the time is found to be rapid for the small drop than the large one. Figure 4.16 shows the effect of the degree of superheat on the the half-opening angle of vaporization. From this figure it is obvious that the increasing in the degree of superheat makes the process more rapid due to increase the heat absorbed from the continuous liquid. Also, there is no significant effect of the changes the initial droplets velocity on the the half-opening angle of vaporization as shown in figure 4.17.

4.2.4 The Heat Transfer Coefficient:

The theoretical predication of the instantaneous heat transfer coefficient is obtained by solving equation (3.54). The variation of the instantaneous heat transfer coefficient against the evaporation ratio is shown in figures 4.18 to 4.20 for different selected parameters (D_0, T and U_0).

The general trend, which is clear in these figures, is the decrease of the heat transfer coefficient with increasing the vaporization ratio. This can be explained as follows, when the drop first emerges from the orifice into a higher temperature continuous liquid, the initial temperature distribution has a discontinuity at the liquid-liquid interface, where, at least in the physical model[44], the temperature change abruptly from the far field temperature T_c to the saturation temperature of dispersed phase T_{ds} and that lead to a very large temperature gradient in this region. Therefore, the rate of heat flow is very high at the beginning. A short time later, a thin thermal boundary layer outside the drobble begins to form due to transient effect and the energy is transferred from the continuous liquid to the drobble. The influence of the decreasing in the heat flux, due to decrease the temperature gradient (see equation (3.42), as the evaporation process proceeds can be interpreted the decreasing in the average heat transfer coefficients.

The effect of the initial diameter on the heat transfer coefficient is shown in figure 4.18. This figure shows the behavior of the heat transfer coefficient for three droplets of 1.5, 2, and 3 mm initial diameter with a superheat temperature of 8 K and initial velocity of drobbles 0.2 m/s. As shown in this figure the average heat transfer coefficient for the small drobble is higher than for the large drop, which is in agreement with the theoretical works done by Vong and Sadhal[10] and Ay et al.[55]. This was also verified by Sideman et al.[45]. The reason may be attributed to the lower thermal resistance

accompanied the smaller thickness of conduction boundary layer for smaller initial diameter droplet, which promotes the heat transfer to the drobble.

The effect of the degree of superheat on the heat transfer coefficient against the vaporization ratio is shown in figure 4.19. In this figure, the results are given for the three superheat temperature with initial drop diameter 2 mm and initial droplets velocity 0.2 m/s. For a lower superheat temperature a higher value of the heat transfer coefficient was obtained. This is because, at any given time, a lower superheat temperature results in a lower growth rate of drobble which makes the thermal boundary layer become thin, but the temperature gradient at the drobble surface becomes larger resulting in an increasing in the heat transfer coefficient. This behavior was also verified by the other researchers (Shimizu & Mori[39], Vuong & Sadhal[10]). From this figure, it can be seen that the three curves reaching nearly the same value of heat transfer coefficient at the end of evaporation process since the three droplets have same mass, for same D_0, and hence it have the same thermal resistance at the end of evaporation process.

The effect of the initial droplet velocity on the variation of heat transfer coefficient versus vaporization ratio is shown in figure 4.20. It is obvious from this figure that the effect of initial droplet velocity on the heat transfer coefficient is insignificant. This result was also confirmed by Ay et al.[55]. They indicated that the initial dispersed fluid diameter has the strongest effect on the heat transfer coefficient, while the mass flow rate (and hence the initial velocity) of dispersed phase exerts little influence. This behavior can be explained as; the initial velocity have small effect on the rise velocity of the drobble (only at the early stages of evaporation, see figure 4.5), and on the radius of growing drobble (see figure 4.11). Therefore, its effect is not apparent on the heat transfer coefficient.

4.3 Comparison the Present Results for Single Droplet with that of Other Investigator's:

In order to prove the validity of the present model, the results obtained are compared with the theoretical and experimental results of other researchers as follows:

i.   **The Half-Opening Angle:**

The half-opening angle β predicated from the present model are compared with the measured half opening angle of Tochitani et al.[16], when single pentane drop of 1.4*mm* diameter evaporates along a constant temperature glycerol column. The column was maintained at superheat temperature $(T_c - T_{ds})$ of 3.1 K. The data for the fluid properties was taken from[16]. Figure 4.21 shows the half-opening angle versus the vaporization ratio. The present analysis gave a good agreement with the experimental data and also gave a very good agreement with the theoretical results of[16]. Since both the present model and [16] assumed the drop to be of spherical shape with the vapor phase occupying the upper portion and the dispersed liquid phase assumed to be staying at the bottom portion, while in their experiment they noted that the profile of the unevaporated liquid of the drop jutted out from the spherical boundary of the vapor with continuous phase. In other words, the drop is far from being of a spherical shape, this resulted in small discrepancy between the present and their theoretical results compared with the experimental results.

ii.   **The Instantaneous Rise Velocity and Diameter of Growing Drobble:**

For butane-water system the instantaneous velocity versus instantaneous dimensionless radius predicated from the present model is compared with the experimental data of Mokhtarzadeh and El-Shirbini[35] for conditions

($D_0 = 3.6 - 4.2 \, mm$ and $T = 1.9 - 4.6 \, K$) as shown in figure 4.22 .The theoretical results obtained from the present model is based on the evaporation parameters ($D_0 = 4. \, mm, \quad T = 3 \, K$ and $U_0 = 0.167 \, m/s$). This figure shows a good agreement between the present predicated results compared with the experimental one.

The present theoretical result is compared with the experimental result of Sideman and Taitel[15] for pentane droplet injected in water column, for the same parameters ($D_0 = 3.2 \, mm, \quad T = 8 \, K$ and $U_0 = 0.167 \, m/s$). Figure 4.23, shows the comparison of the velocity and diameter of growing drobble for both studies. As demonstrated in this figure, there is a good agreement between the present results and experimental one, expect in the early stages of the process for the velocity curve, in which there is a difference about 25% which is vanished gradually.

Also, the predicated velocity is compared with the experimental results of Al-Jaberi[13] for initial droplet diameter ($D_0 = 3 - 3.65 \, mm$) and degree of superheat ($T = 1.52 - 9.75 \, K$) as shown in figure 4.24. The results of the present model are represented for two cases of controlling parameter ($D_0 = 3.2, 3.65 \, mm ; \quad T = 6.45, 1.6 \, K$ and $U_0 = 167 \, mm/s$). From this figure a good agreement between the results is obtained, expect in the early stages of the process in which there is a difference about 20% which is vanished gradually.

iii.   The Heat Transfer Coefficient:

The heat transfer coefficient predicted in the present model is compared with theoretical model of Sideman and Isenberg[26] and with the experimental results of Sideman and Taitel[15] as shown in figure 4.25. The input parameter were obtained from the experimental data where ($D_0 = 3.2 \, mm, \quad T =$

8 K and $U_0 = 0.167\ m/s$). It is obvious from this figure, that the comparison with [26] shows reasonable agreement. Concerning the comparison with the experimental results shown in this figure, it is obvious that there is a significant difference between both results, start from about 20% of vaporization ratio and increases as the vaporization ratio increase. This may be attributed to the fact that the change from spherical shape can occur in the early stages of evaporation process or in later stages, depending on the initial size of droplets. The spherical assumption can be applied to droplet of relatively small size (e.g. less than 1.2 mm initial diameter) from about 1-100% of' evaporation and for droplets of relatively large size (about 3-5 mm initial diameter), from about 1-10% evaporation [28], hence, the drobble deformation and oscillation during the experiments yield larger heat transfer coefficient than predicted by the spherical model as evaporation proceed.

The heat transfer coefficient obtained from the present model is compared again with both the theoretical model of Tochitani et al.[22] and the theoretical model of Raina and Grover[30], using the evaporation parameter ($D_0 = 3.2\ mm,\quad T = 8\ K$ and $U_0 = 0.167\ m/s$). Figure 4.26 shows compareison between the heat transfer coefficients for the three studies. From this figure similar trend is observed, however the heat transfer coefficient of the present model is slightly smaller, which may be due to the fact that their models [22, 30] did not take into consideration the effect of transient term in the energy equation during the evaporation process.

In general the comparison between the results of this model and the result of the others models shows a good agreement, which gives validity of the present theoretical model.

4.4 The Direct Contact Evaporation of Multi-Drobbles in an Immiscible Liquid:

In this section, the results of solving the mathematical model of multi-drobbles evaporation are presented. The calculations are carried out by numerical method using a computer program as shown in the flow chart (appendix D). It should be mentioned that the heat transfer coefficient of the single drobble inside a spherical cell of continuous liquid is employed, which is explained in chapter three, to obtain the volumetric heat transfer coefficient.

In order to present a wide scope for the multi-drobbles evaporation, the influences of more parameters, likely to be affective on this process, are studied. These parameters are the initial diameter of drobble, the degree of superheat, the column diameter, the holes diameters, the number of holes and the dispersed phase flow rate. The values of these parameters were chosen according to the more common cases of the multi-drobble evaporation process which exist in the literature. The ranges of these parameters are taken as:

- The degree of superheat T varies from 4 to 16 K.
- Initial diameter of drobbles D_0 varies from 1.5 to 3 mm.
- The column diameter d_c varies from 90 to 150 mm.
- The holes diameter d_h varies from 0.5 to 1 mm.
- The number of holes N_h varies from 7 to 36.
- The dispersed phase flow rates $\dot{V}_d$ vary from 10 to 20 L/hr.

The influences on the evaporation characteristics by each one of these parameters, while the other parameters are kept constant, will be illustrated in the flowing section.

4.4.1 The Instantaneous Dispersed Phase Volume Fraction (Holdup):

The instantaneous dispersed phase holdup ( ) is calculated in the present theoretical model using equation (3.78). The variation of the dispersed phase holdup with the time is shown in figures 4.27 to 4.30 for different selected parameters. The general trend, which is shown in these figures, is the increment of the dispersed phase holdup (start from very small value) with the time. This is due to the growing size of drobbles, as a result of continuous evaporation process.

Figure 4.27 shows the effect of the initial diameter (D_0) on the dispersed phase holdup. Higher dispersed phase holdups are achieved at lower values of the initial diameter of drobbles after a short time of evaporation, due to the increasing in the number density of drobbles accompanied the smaller drobbles and the faster growing of small drobbles than the large drobbles. Also, it is noted that the three curves reach nearly same value of holdup at the end of the evaporation process since the increasing D_0 leads to increase the final radius (see figure 4.9), and also it leads to decrease the number density of drobbles (see equation (3.77)), and hence, these inversely effects of (D_0) make the three curves reachs nearly same value of the dispersed phase holdup.

The influence of the column diameter (d_c) on the dispersed phase holdup is shown in figure 4.28. As d_c decreases, higher dispersed phase holdup is obtained. This may be due to, the decrement of d_c leads to increase the number density of drobbles (according to equation 3.77), and hence increase the dispersed phase holdup.

The effect the holes diameter (d_h) and the number of holes (N_h) on the variation of dispersed phase holdup with the time is shown in figures 4.29 and 4.30, respectively, where the other controlling parameters are kept constant. Increasing d_h and N_h leads to higher values of dispersed phase holdup. The

86

reason of the increment obtained in dispersed phase holdup may be due to that the increasing in these factors d_h and N_h leads to increase the number density of drobbles, and hence increase the dispersed phase holdup (according to equation 3.77). It is worth to mention that the effect of d_h is found to be higher than the effect of N_h , as a result of the different degree of dependences of the number density on these parameter.

4.4.2 The Instantaneous Relative Velocity and the Evaporative Drobbles Position:

Evaluation of the instantaneous relative velocity (U_r) and instantaneous evaporative drobbles position (Z(t)) is done by solving equation (3.24) and equation (3.87), respectively. The variation of the instantaneous relative velocity and instantaneous height of the evaporative drobbles with the time is shown in figures (4.31 to 4.35) and figures (4.36 to 4.39), respectively, for different selected parameters.

The effect of the initial diameter (D_0) on the the instantaneous relative velocity is shown in figure 4.31. In the early stage, the behavior of the velocity curves is rather similar to that for single drobble (where the velocity decreases till it reaches minimum value, and this behavior can be noticed in all the velocity figures later). In the next stages, as D_0 increases, the evaporation process required more time to be completed. At fixed time the increasing of D_0 leads to increase U_r due to increase volume of drobble and, in turn, increases buoyancy force of drobbles and also, the decreasing of the holdup as D_0 increase (see figure 4.27) makes the drobbles more fast (the interaction between drobbles decrease). Figure 4.36 shows the effect of D_0 on $Z(t)$, as it is evident from this figure, for fixed time the increment in D_0 leads to higher Z,

due to the higher accompanied relative velocity. Also, the increment in $Z(t)$ with D_0 can be attributed to increase mass of dispersed phase as D_0 increases.

Figures 4.32 and 4.37 show the effect the column diameter (d_c) on the variation of U_r and $Z(t)$ with time, respectively, where the other parameters are constant. As it is obvious from these figures, no significant effect of d_c on U_r and $Z(t)$ is noted at the early stage of evaporation process (from 0 to 0.25 t_f). This may be due to that, the variation of holdup is small in this stage and therefore have no effect on U_r and consequently on Z. As the evaporation process proceeds the holdup decreases with increases d_c (see figure 4.28) and lead to small increase in relative velocity, figure 4.32, and hence small increases in $Z(t)$, figure 4.37.

The effect the holes diameter (d_h) on the variation of U_r and $Z(t)$ with the time is shown in figures 4.33 and 4.38, respectively. From these figures it can be observed that, increasing the value of d_h has no considerable effect on U_r and $Z(t)$ at the early stage of evaporation process (less than 0.125 t_f). This is due to, the value of holdup is small in this region (see figure 4.29) and the behavior becomes rather similar to that of the single drobbles case, and in the after stages, the increasing of d_h leads to decrease in U_r and consequently in $Z(t)$. This is due to increase of the dispersed phase holdup as d_h increases.

The variation of the number of holes (N_h) has similar effect to that of (d_h) with the time on U_r and $Z(t)$. Figures 4.34 and 4.39, show the effect of (N_h) on U_r and $Z(t)$ with the time, respectively. From these figures it can be noted that, at the early stage of evaporation (less than 0.125 t_f) there is no considerable effect of N_h but with progress of evaporation stages, the increasing of N_h leads to decrease in U_r and consequently, $Z(t)$. This is due to the same reason mentioned for the previous parameter (d_h).

Negligible effect of the variation of the dispersed phase flow rates ($\dot{V}_d$) on U_r with the time as shown in figure 4.35 and consequently *Z(t)*, while the other parameters (D_0, d_c, d_h, and N_h) are kept constant. This is may be due to that, the dispersed phase flow rates ($\dot{V}_d$) is appeared in the numerator and denominator of the number density of drobbles (equation (3.74)). Therefore, its effect is disappear on the number density of drobble and hence on the dispersed phase holdup (see equations (3.77) and (3.78)), consequently, it has no effect on U_r and *Z(t)*. Also, the dispersed phase flow rates have negligible effect not only on U_r and *Z(t)* but also on all the other evaporation characteristics, so that these effects are not presented and only figure 4.35 is given.

It is worth to mention, that the effect of $\dot{V}_d$ on the evaporation characteristics which may be observed in the experimental results may be due to its experimental influence on the initial diameter of drobbles, which represent the dominate factor in the evaporation process as specified by the present and other works in this field.

4.4.3 The Volumetric Heat Transfer Coefficient:

In this section the results will be presented for the variation of the average volumetric heat transfer coefficient (h_{mv}) with time and the variation of the average volumetric heat transfer coefficient for complete evaporation (h_{mvf}) with the degree of superheat. The evaluation of the average volumetric heat transfer coefficient is done by the solution of equation (3.89).

The variation of the average volumetric heat transfer coefficient with the time is shown in figures 4.40 to 4.43 for different selected parameter. The general trend in these figures is the increasing h_{mv} with the time. This may be due to increasing the total surface area of drobbles as evaporation process

proceeds that leads to increasing the heat transfer from the continuous phase to the drobbles.

The effect of the initial diameter of drobble (D_0) on the variation of h_{mv} with the time is shown in figure 4.40, while the other parameters are kept constant. From this figure it can be seen that the decreasing of h_{mv} as D_0 increases. This may be due to, the decreasing in the initial size of drobble means increasing in the total surface area of drobbles, per unit volume, that exposed to the heat transfer, that leads to increase the heat rate and hence increases h_{mv}. In addition to that, this behavior may be due to the decrement in the specific heat transfer coefficient for a single drobble with increasing the initial diameter as mention before in figure 4.18.

The influence of the column diameter (d_c) on the variation of h_{mv} with the time is shown in figure 4.41, where the other evaporation parameters are kept constant. From this figure one can see that, as the value of d_c increases, a decrease in h_{mv} is obtained. This is may be attributed to, the increasing in the column diameter reduce the number density of drobbles in the column (according to equation 3.77). The reduction in number density of drobbles leads to decrease the average volumetric heat transfer coefficient, due to decrease the rate of heat absorbed from the continuous phase which required for evaporating the drobbles.

The effect of the holes diameter (d_h) and number (N_h) on the variation of h_{mv} with time is shown in figure 4.42 and 4.43, respectively. As evident from these figures, increasing the value of d_h and N_h leads to increase in h_{mv}. This is may be due to, the increasing of these parameters d_h and N_h leads to increase the initial velocity of drobbles (according to equation 3.76) and consequently increase the number density of drobbles (according to equation 3.77). This increment in number density of drobbles leads to increase the

average volumetric heat transfer coefficient. Also from these figure it can be noted that d_h have more effect on h_{mv} than N_h , since the number density of drobbles is directly proportional to the square of hole diameter, and it is directly proportional to the number of holes.

Concerning the variations of the average volumetric heat transfer coefficient for complete evaporation h_{mvf}, with the the degree of superheat (ΔT), figures 4.44 to 4.47 show these variations for different selected parameter. The general trend in these figures is the reduction of the average volumetric heat transfer coefficient for complete evaporation (h_{mvf}) with ΔT. This is because of the, h_{mvf}, which defined as ($\bar{Q}/(V.\Delta T)$) is inversely related to both ΔT and V, where $\bar{Q}$ represent the average heat rates, V denotes the optimal volume based on height for complete evaporation. The increasing in ΔT leads to decrease ($\frac{\bar{Q}}{\Delta T}$), but this increasing in ΔT leads to decrease the other parameter V, since the parameter V is proportional to the height of complete evaporation, which is decreasing as ΔT increases due to rapid evaporation process as shown in figures 4.52- 4.55. Careful analysis of these figures indicated that h_{mvf} should decrease as ΔT increases.

The effect of initial drobble diameter (D_0) on h_{mvf} is shown in figure 4.44, where the other controlling parameters (d_c, d_h, N_h and $\dot{V}_d$) are kept constant. From this figure it can be seen that h_{mvf} is increasing with decreasing of D_0 for a fixed value of the degree of superheat ΔT. This may be due to increasing the heat rate ($\bar{Q}$) as D_0 decrease since the surface area, per unit volume, exposed to heat transfer become larger.

The effect the column diameter (d_c) on the variation of h_{mvf} with ΔT is shown in figure 4.45. As the value of d_c increases, decrease of the volumetric heat transfer coefficient for a fixed ΔT is obtained. The reason may be due to,

increasing d_c leads to decreasing the number density of drobbles that in turn reduce the rate of heat absorbed from continuous phase to evaporate the drobbles.

The variation of h_{mvf} with ΔT for different values of d_h and N_h is shown in figures 4.46 and 4.47, respectively. Increasing the value of d_h and N_h leads to increase in h_{mvf}, at a fixed value of ΔT. This is because of the increasing of these parameters d_h and N_h leads to increase the number density of drobbles, and hence increase the rate of heat absorbed from continuous phase to evaporate the drobbles.

4.4.4 The Total Time and Height for Complete the Evaporation:

The variation of the time (t_f) and height (Z_f) for complete evaporation with ΔT is shown in figures (4.48 to 4.51) and figures (4.52 to 4.55), respectively, for different selected parameters. The general trend in figures 4.48 to 4.51, is reduction of t_f with increasing ΔT. Also, the general trend in figures 4.52 to 4.55, is reduction of Z_f with increasing ΔT. The reduction in t_f and Z_f with ΔT may be due to, the increasing in the degree of superheat ΔT lead to rapid evaporation process of dispersed phase and then the time for complete evaporation is reduced, in turn, reduced the height required for complete evaporation of all drobbles.

The effect of the initial diameter of drobble (D_0) on the variation of t_f and Z_f with ΔT is shown in figure 4.48 and 4.52, respectively. Increasing the value of D_0 leads to increase in t_f and Z_f, at a fixed ΔT value. This is related to that; the larger drobbles required more energy for complete evaporation in the column, with lower average volumetric heat transfer coefficient as shown in

figure 4.44 so that the process requires more time and hence larger height for complete evaporation.

Figure 4.49 and 4.53 are drawn to show the effect the column diameter (d_c) on the variation of t_f and Z_f with T, respectively. As it is obvious from figure 4.49, no significant effect of d_c on t_f is observed. The reason may be attributed to that, the increasing of the column diameter reduce the number density of drobbles in the column (according to equation 3.77) .This reduction of the number density of drobbles leads to increment in the relative velocity (as noted previously in figure 4.33) and also increment in the height of drobble (as noted previously in figure 4.37). The increasing in both relative velocity and height of drobble as d_c increase can be interprets the negligible effect of d_c on t_f since the time is related to the ratio of these characteristics ($t \quad (\frac{Z}{U_r})$). Also, the increasing in the relative velocity of drobbles leads to increase the height required for complete evaporation, as d_c increase, as shown in figure 4.53.

The effect the holes diameter (d_h) on the variation of t_f and Z_f with T , is shown in figures 4.50 and 4.54, respectively. From figure 4.50 it is noticed that, increasing the value of d_h lead to small increasing in t_f , and from figure 4.54 it is noticed that, the increasing in d_h lead to marked decrement in Z_f.The reason may be due to increases in the number density of drobbles, accompanied by increasing d_h (according to equation 3.77), which leads to increase the dispersed phase holdup (see figure 4.29) that leads to decreases the relative velocity of drobbles (see figure 4.33) and consequently, decreasing in the height for complete evaporation as shown in figure 4.54. The decreasing in both relative velocity and height of drobble as d_h increase can be interprets the small effect of d_h on t_f as shown in figure 4.50.

The effect of number of holes (N_h) on the variation of t_f and Z_f with T is shown in figure 4.51 and 4.55, respectively. From these figures it is noted that, increasing the value of N_h has small effect on t_f , as shown in figure 4.51, and leads to decrease in Z_f, as shown in figure 4.55. This is due to the the the fact that, the increasing in the N_h lead to increase the number density of drobbles, and hence the dispersed phase holdup (see figure 4.30) and that leads to decrease the relative velocity of drobbles (see figure 4.34) and consequently, decreasing in the height for complete evaporation as shown in figure 4.55. The decreasing in both relative velocity and height of drobble as N_h increase can be interprets the small effect of N_h on t_f as shown in figure 4.51.

Figures 4.56 to 4.59 are drawn to show the variation of the height for complete evaporation (Z_f) with the total time (t_f), for different selected parameters. The general trend in these figures is increasing of Z_f with increasing of t_f. Figure 4.56 shows effect the initial diameter of droplets (D_0), figure 4.57 shows the effect the column diameter (d_c), figure 4.58 shows the effect the holes diameter (d_h) and figure 4.59 shows the effect of holes number (N_h) on these characteristics. The reasons of these behaviors as mentioned in previous sections.

4.5 Comparison the Present Results with the Other Experimental and Theoretical Results:

In order to prove the validity of the present model, the obtained results are compared with the results of Seetheramu and Battya[53], Mori [54] and Smith et al.[49].

Seethearmu and battya[53] used n-pentane or R113 as the dispersed phase to be sprayed into stagnant column of distilled water. They carried their experiment using n-pentane sprayed through thirty six 0.5 mm diameter holes at dispersed phase mass flow rate of 1 g/sec (5.9 L/hr). Their results and the theoretical results of Mori[54]are plotted in figure 4.60. The physical properties of n-pentane are evaluated at pentane saturation temperature $(T_{ds} = 36^0 C)$ corresponding to the atmospheric pressure. The properties of water coupled with n-pentane are evaluated at a temperature higher than T_{ds} by $5^0 C$ that used by Mori[54] .

The initial diameter D_0 of the drobbles formed at the orifices was difficult to determine. Sideman et al.[45] have reported that attempts to determine the initial drop diameter in their system accurately but these were unsuccessful due to the presence of partially evaporated drops and entrained vapor bubbles in the bottom part of the column. Smith et al.[49], who have conducted similar experiments, also did not attempt to determine the initial drop diameters. Because of the uncertainty in the initial drop diameters, the theoretical volumetric heat transfer coefficients are calculated assuming different initial drop diameters and a comparison is made with the experimentally determined volumetric heat transfer coefficients[53]. In this work several different initial drop diameters were assumed in order to compare the present results with the results of the other authors. From this figure the agreement with both experimental[53] and theoretical results[54] are good.

Figure 4.61 shows the comparison between the result of the present theoretical model and that of the experimental one of Smith et al.[49],where the height required for complete evaporation versus the degree of superheat is compared. Experimental data obtained under condition that cyclopentane was sprayed through seven of 0.5 mm holes diameter at dispersed phase flow rate of $6.31*10^{-6}m^3$/s (22.71 L/hr). Because of the uncertainly in the initial drobble diameter values, Smith et al.[49] performed their calculation over a range of initial drop diameter (1, 1.5 and 2 mm) and hence in the present work the calculation with initial drop diameter of 1.5 mm was taken. The agreement between the predication and experimental results is acceptable.

Generally, the agreement between the present model predictions and the other author's experimental and theoretical results proves the validity of the present model.
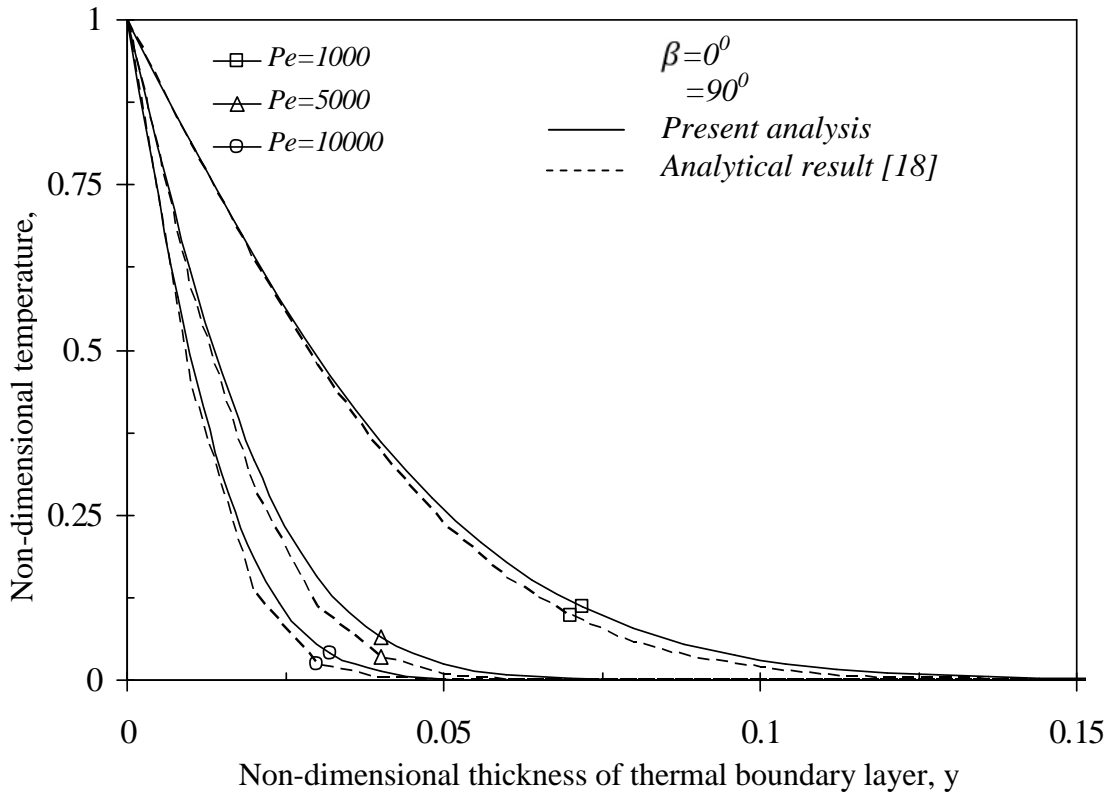
Figure 4.1 Comparison between the present predictions and other analytical results.
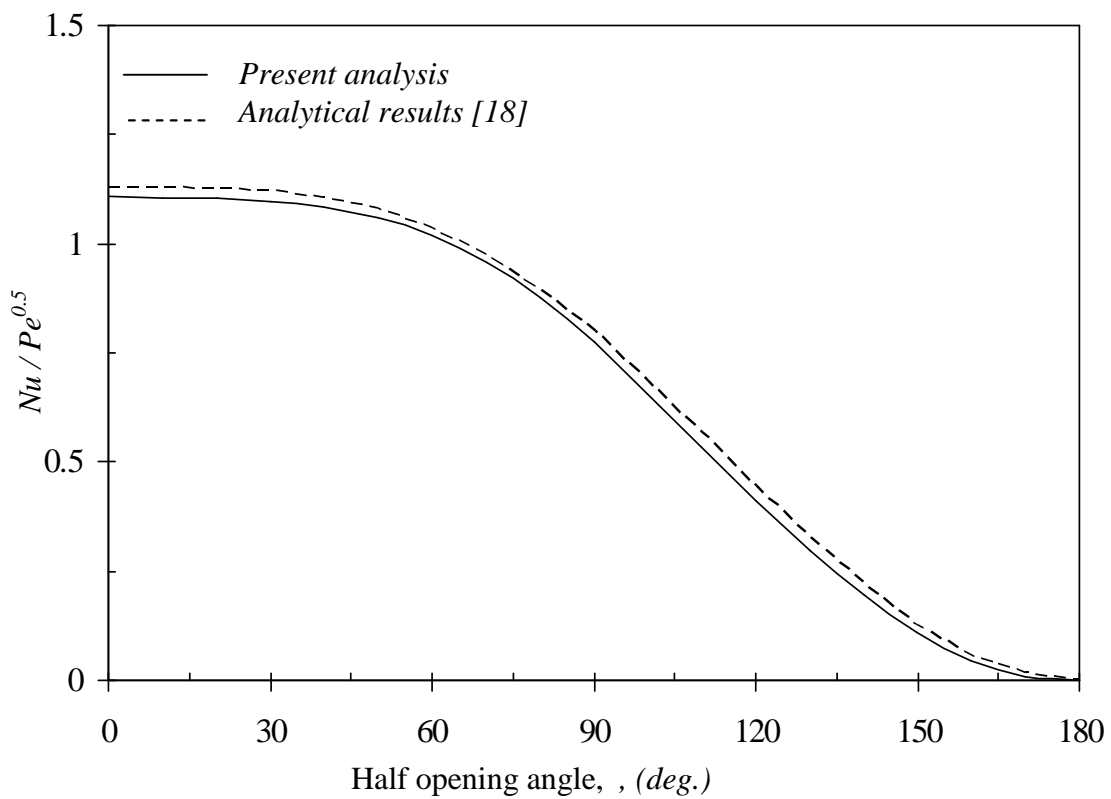
Figure 4.2 Comparison between the present predictions and other analytical results.
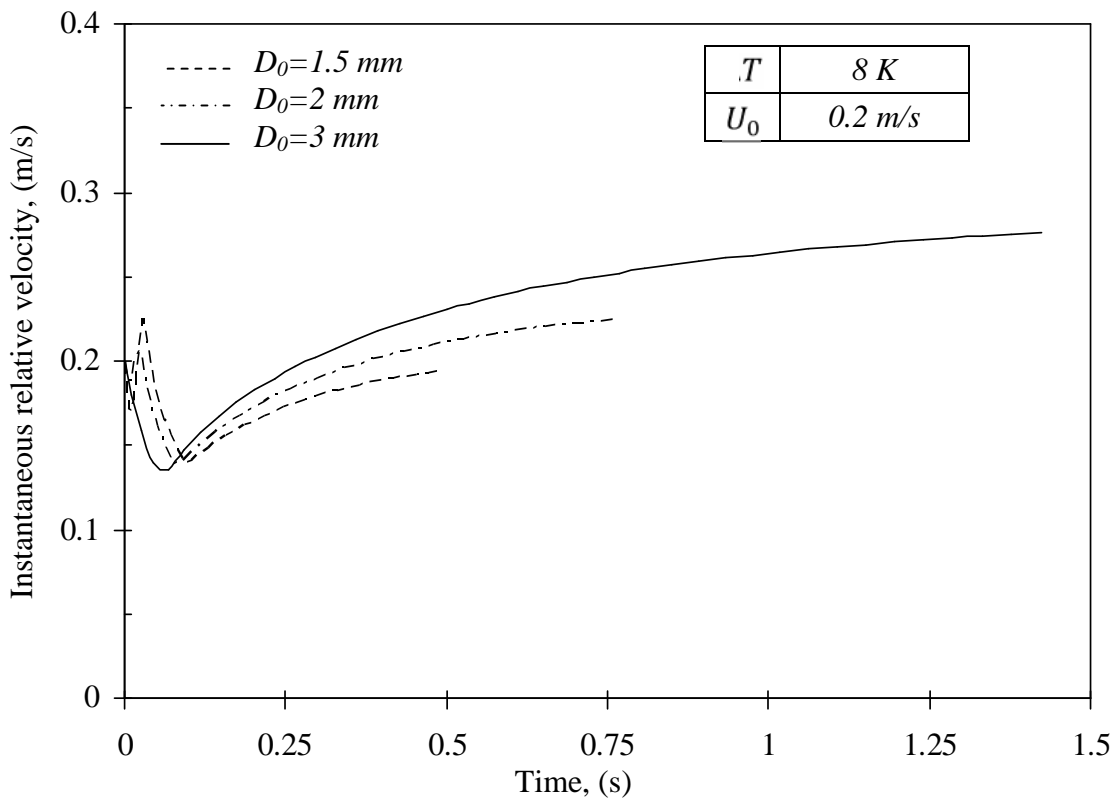
Figure 4.3 Effect of initial diameter on the instantaneous relative velocity of drobble versus time.
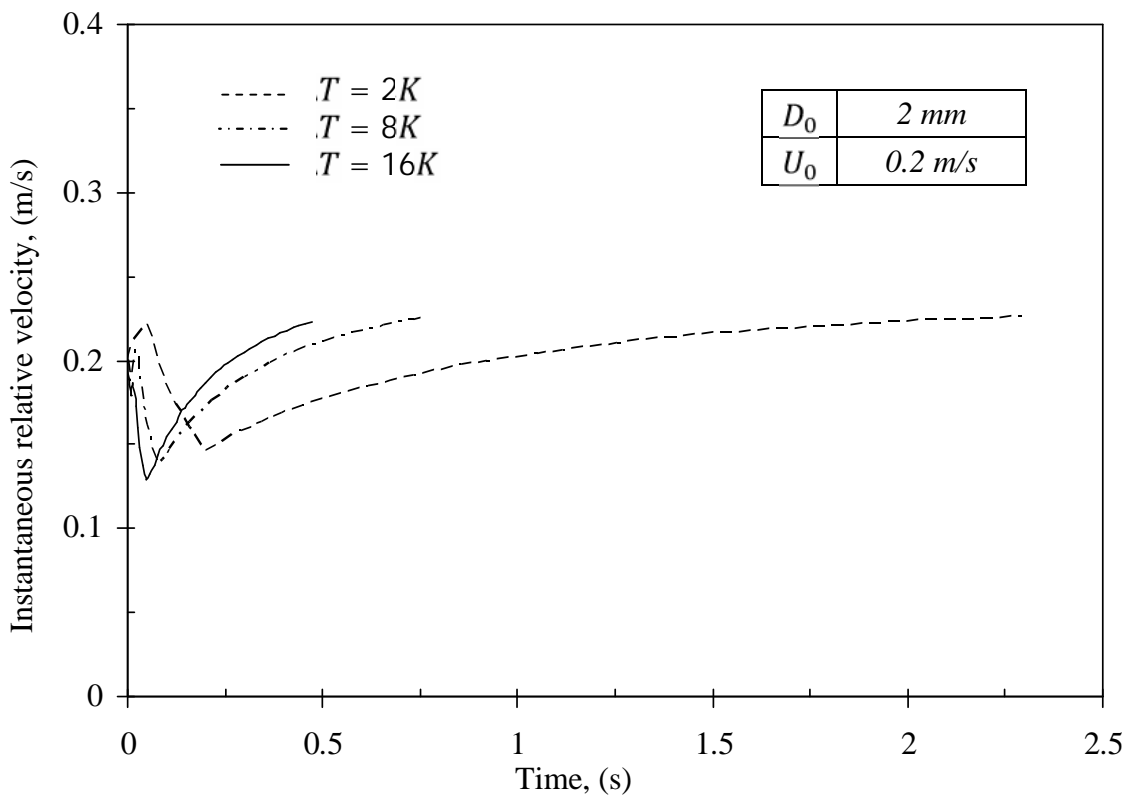
Figure 4.4 Effect of the degree of superheat on the instantaneous relative velocity of drobble versus time.
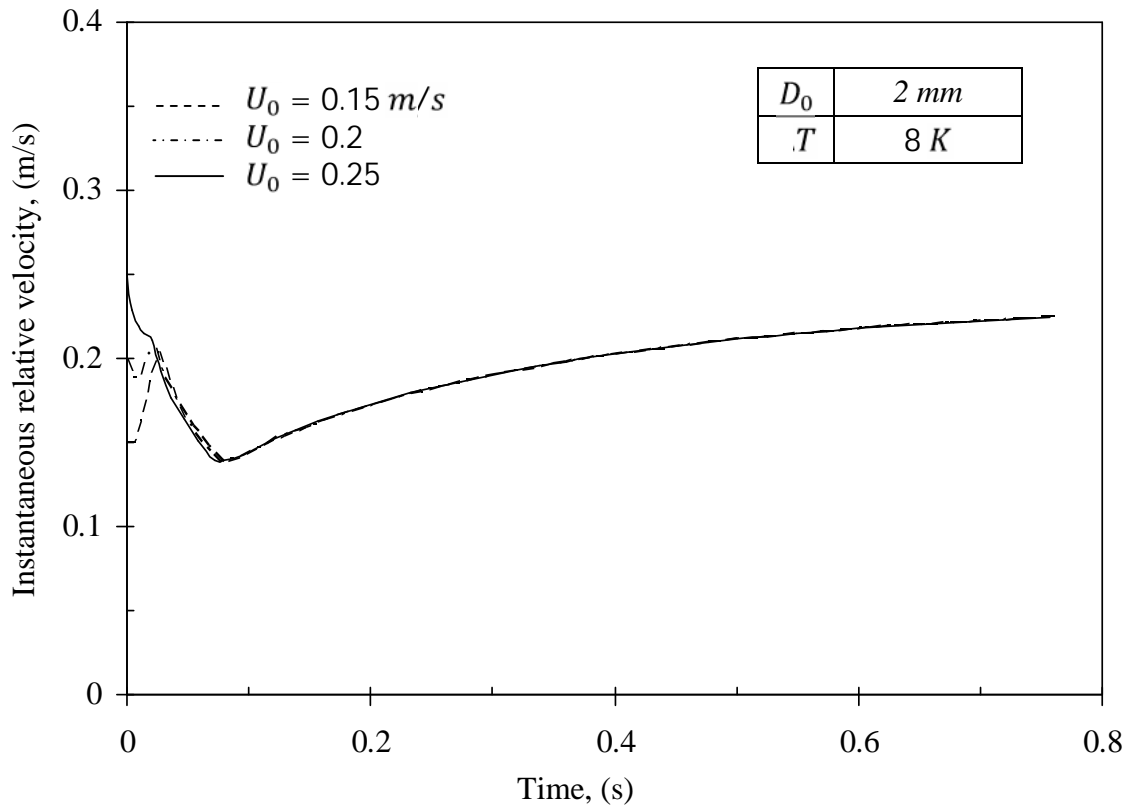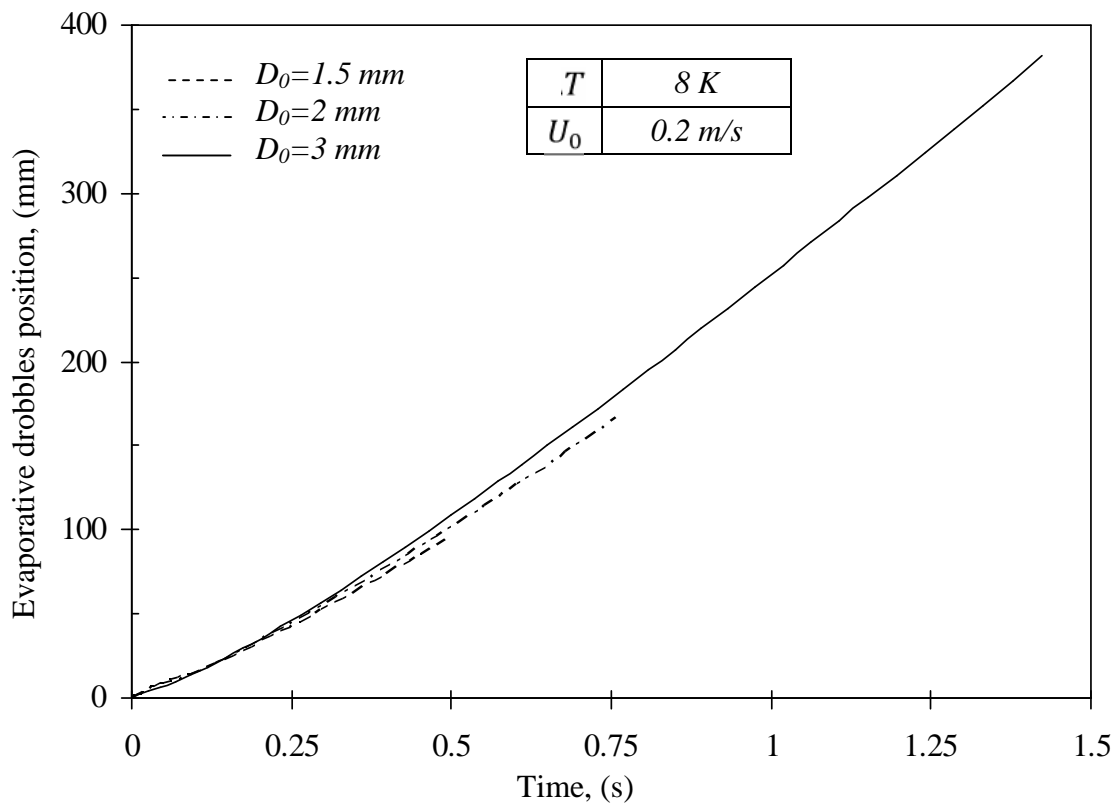
Figure 4.5 Effect of the initial velocity on the instantaneous relative velocity of drobble versus time.

Figure 4.6 Effect of initial diameter on the evaporative drobbles position versus time.
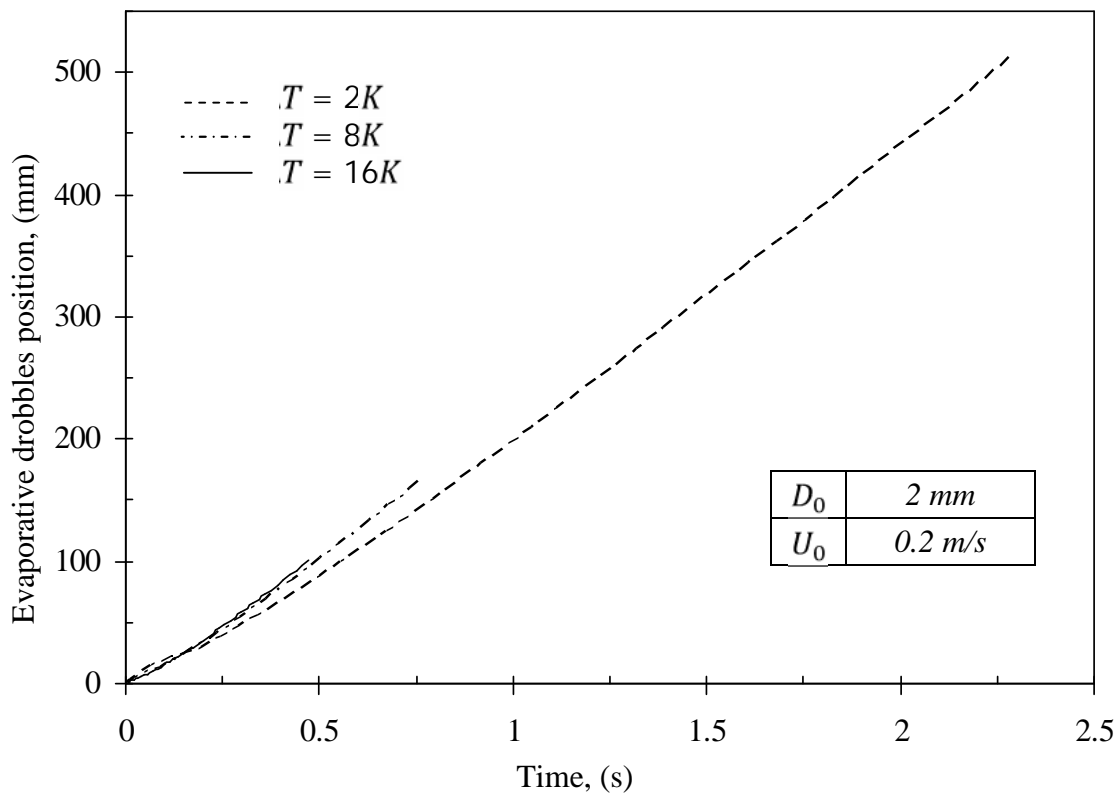
Figure 4.7 Effect of the degree of superheat on the evaporative drobbles position versus time.
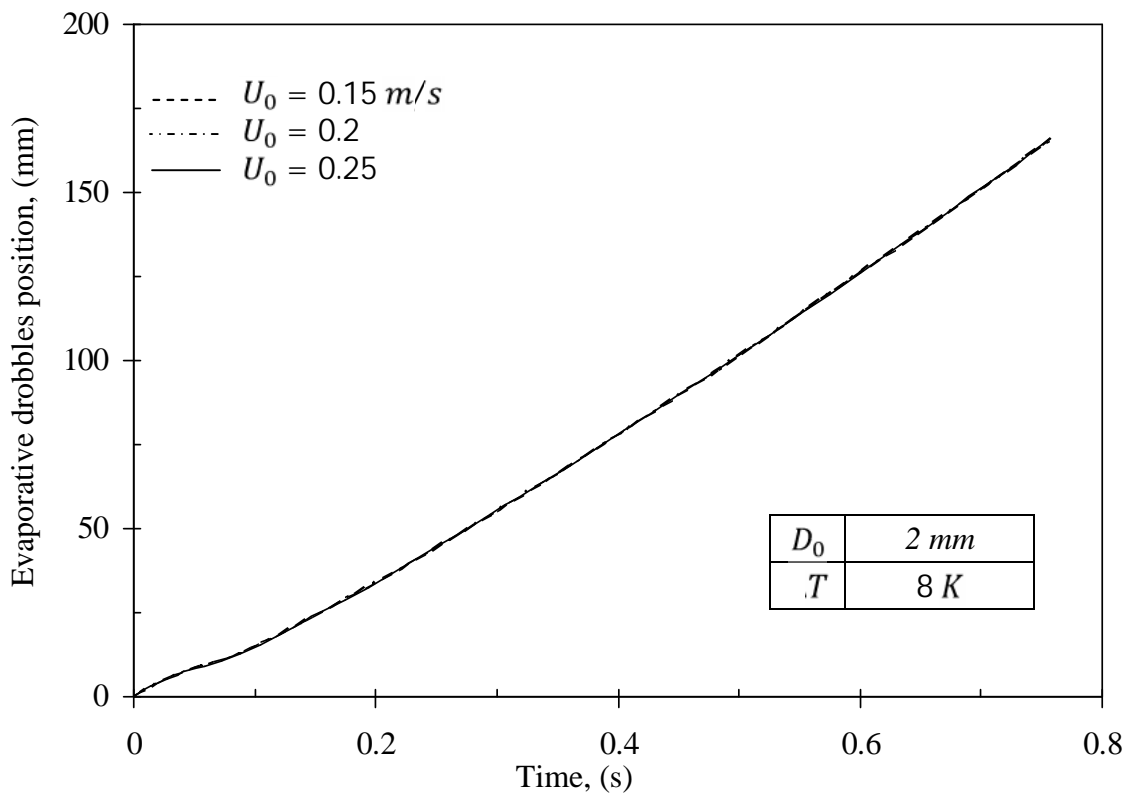
Figure 4.8 Effect of the initial velocity on the evaporative drobbles position versus evaporation time.
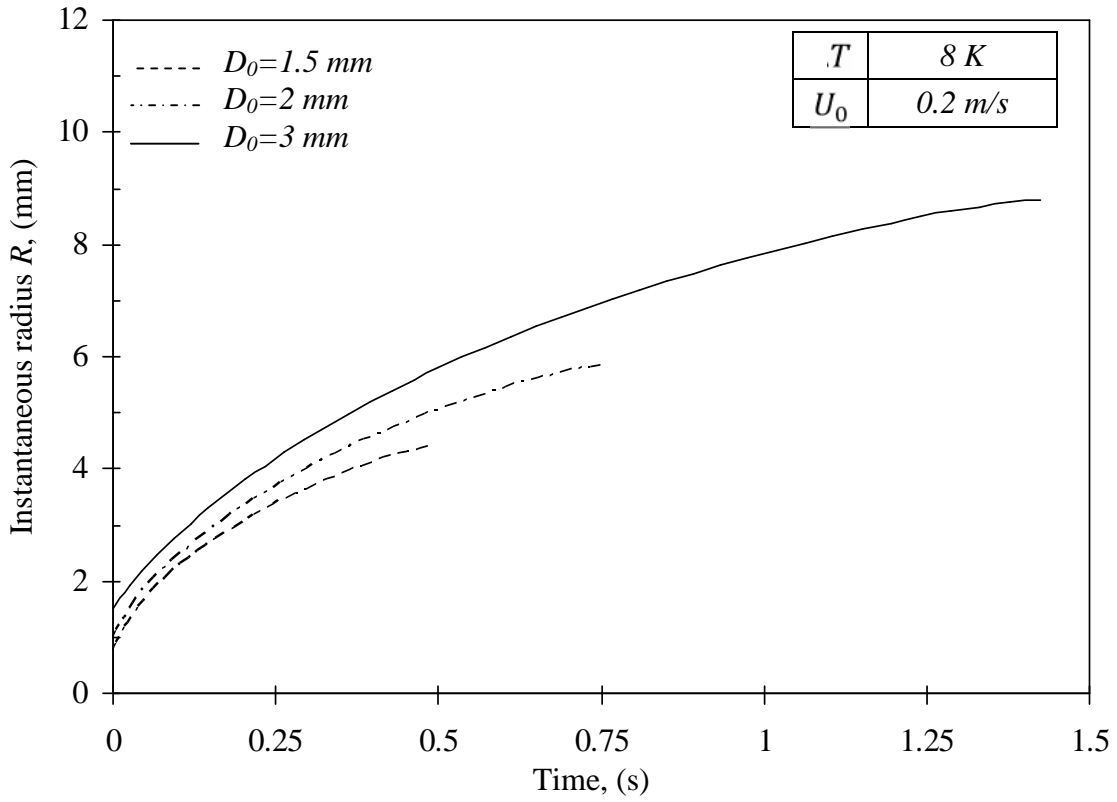
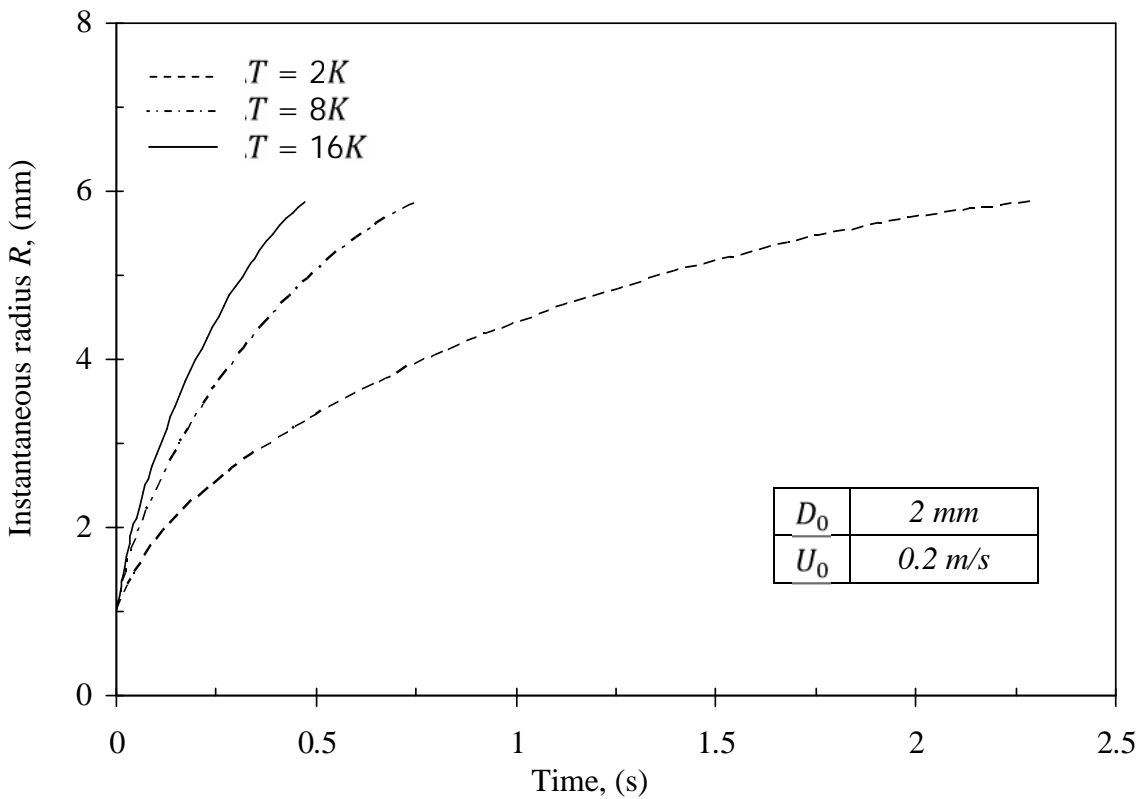Figure 4.9 Effect of initial diameter on the instantaneous radius versus time.

Figure 4.10 Effect of the degree of superheat on the instantaneous radius versus time.
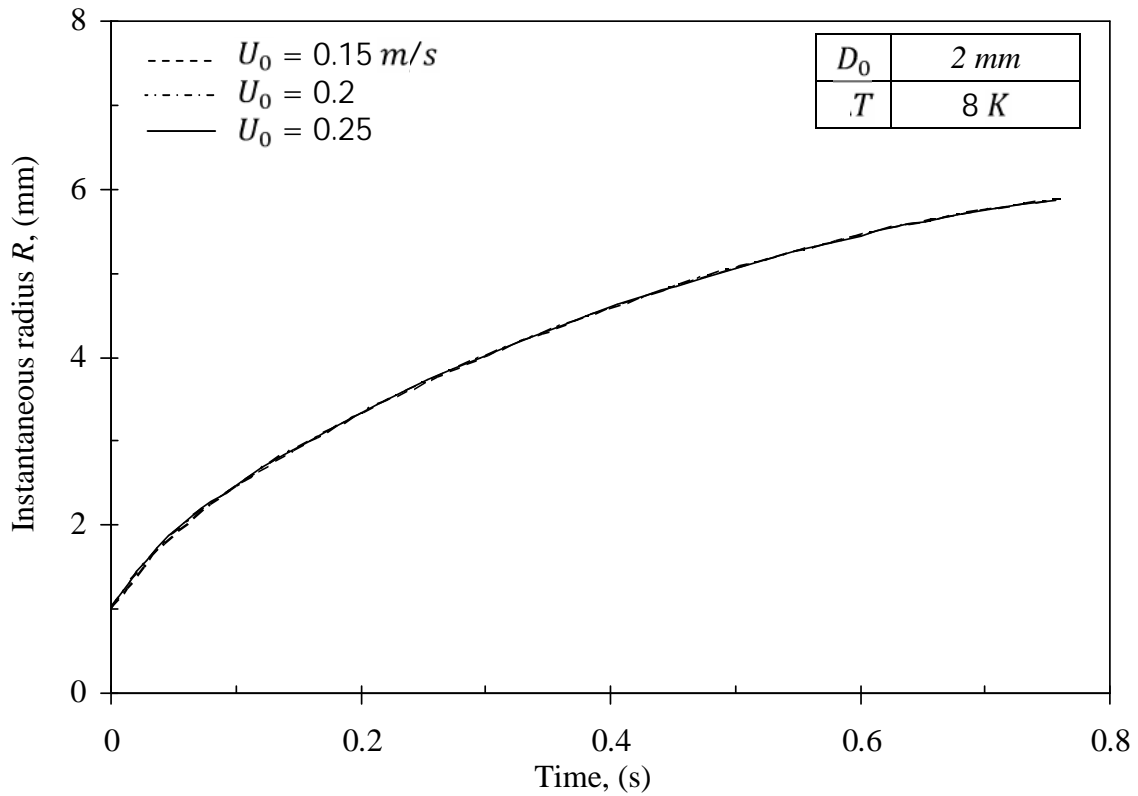
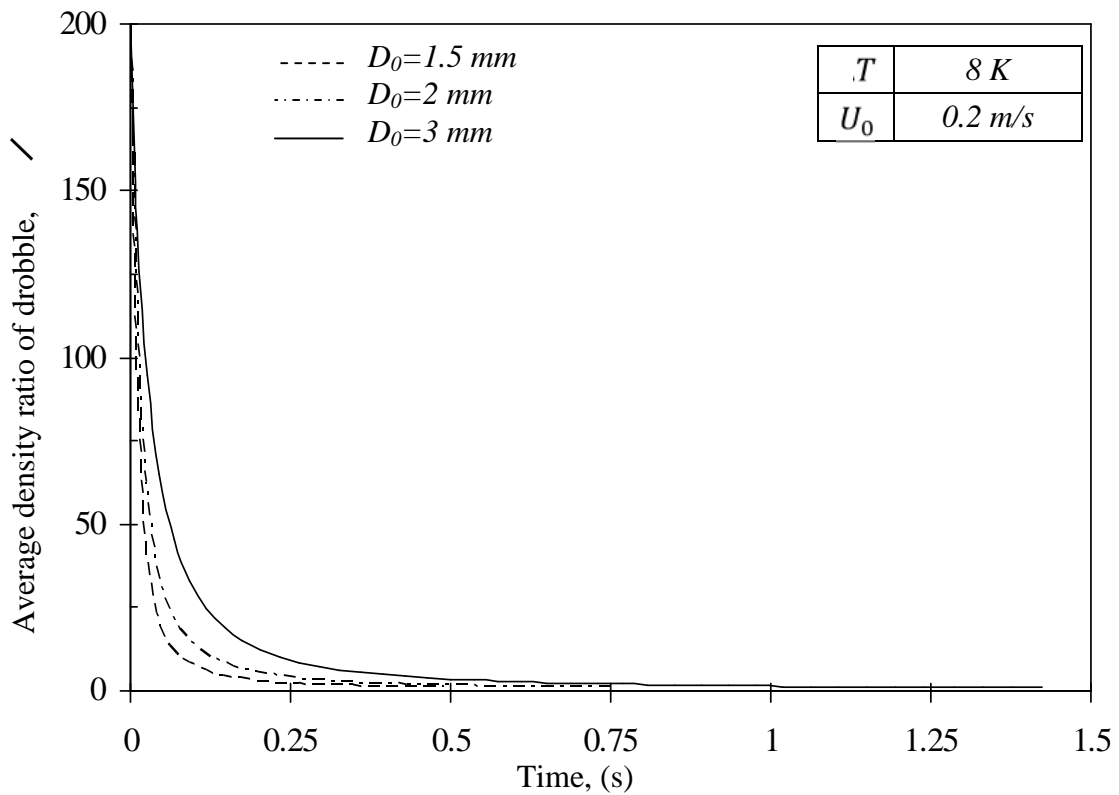Figure 4.11 Effect of the initial velocity on the instantaneous radius versus time.

Figure 4.12 Effect of initial diameter on the average density ratio of drobble versus time.
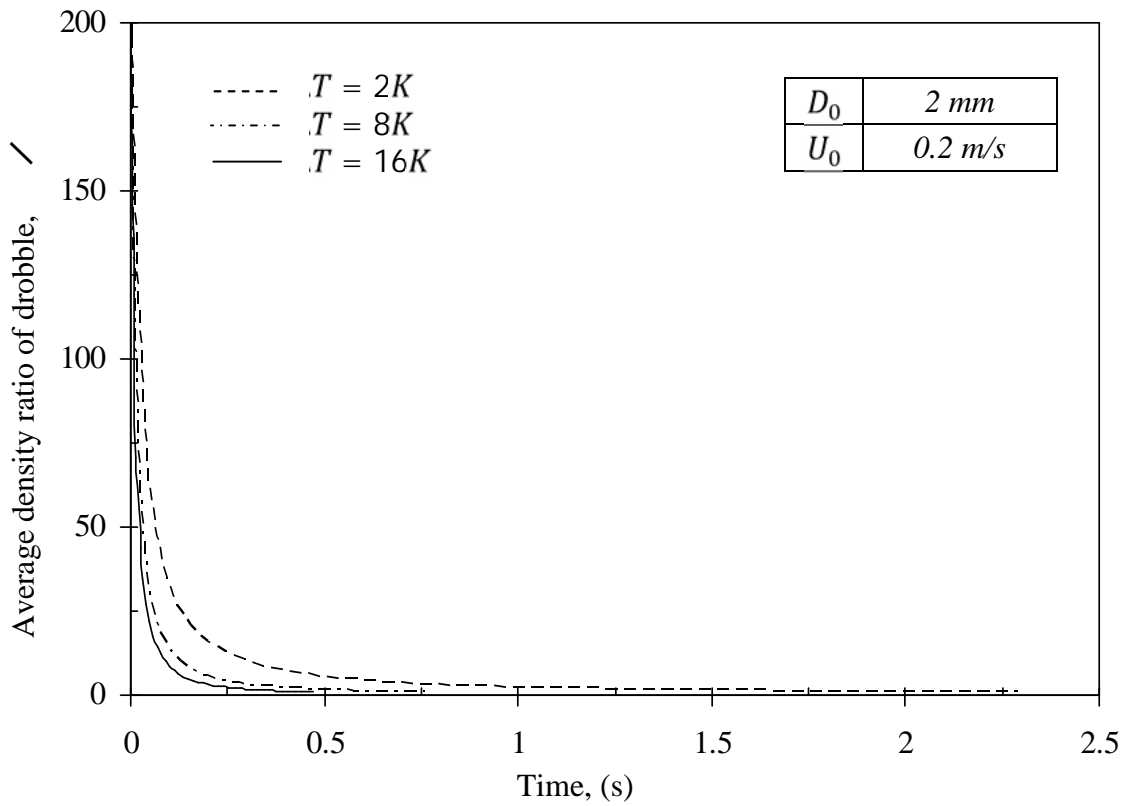
Figure 4.13 Effect of the degree of superheat on the average density ratio of drobble versus time.
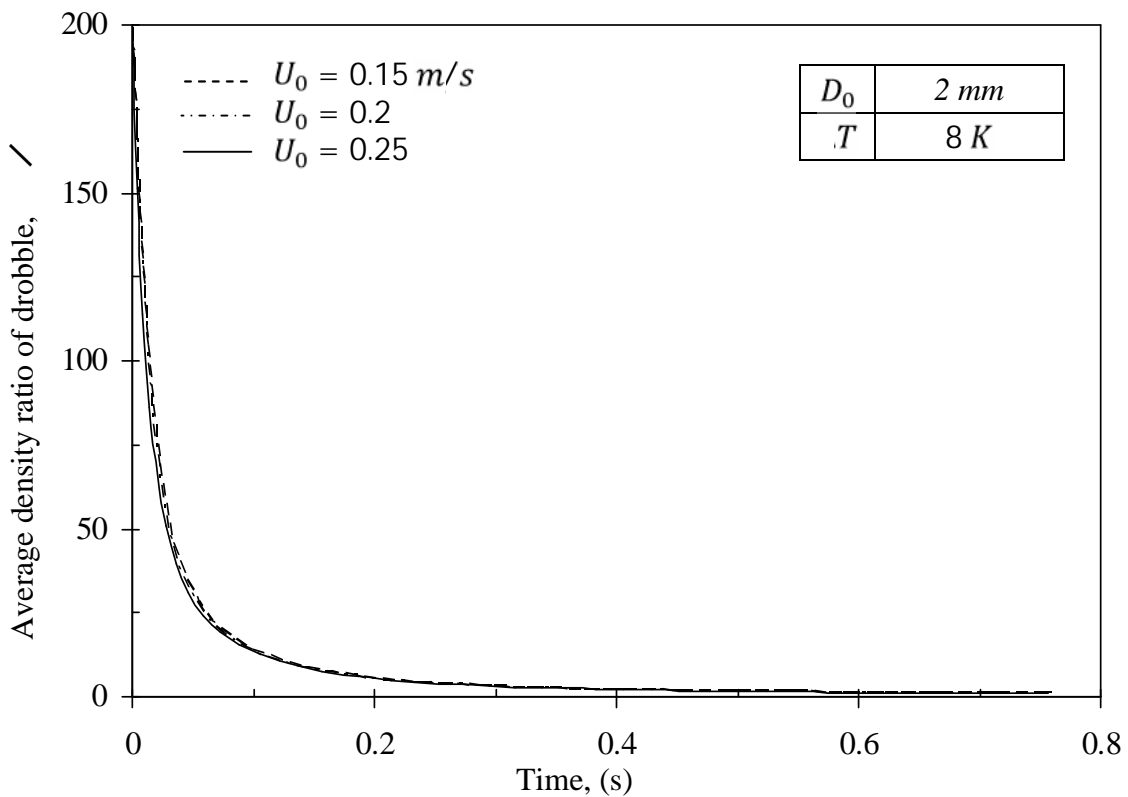

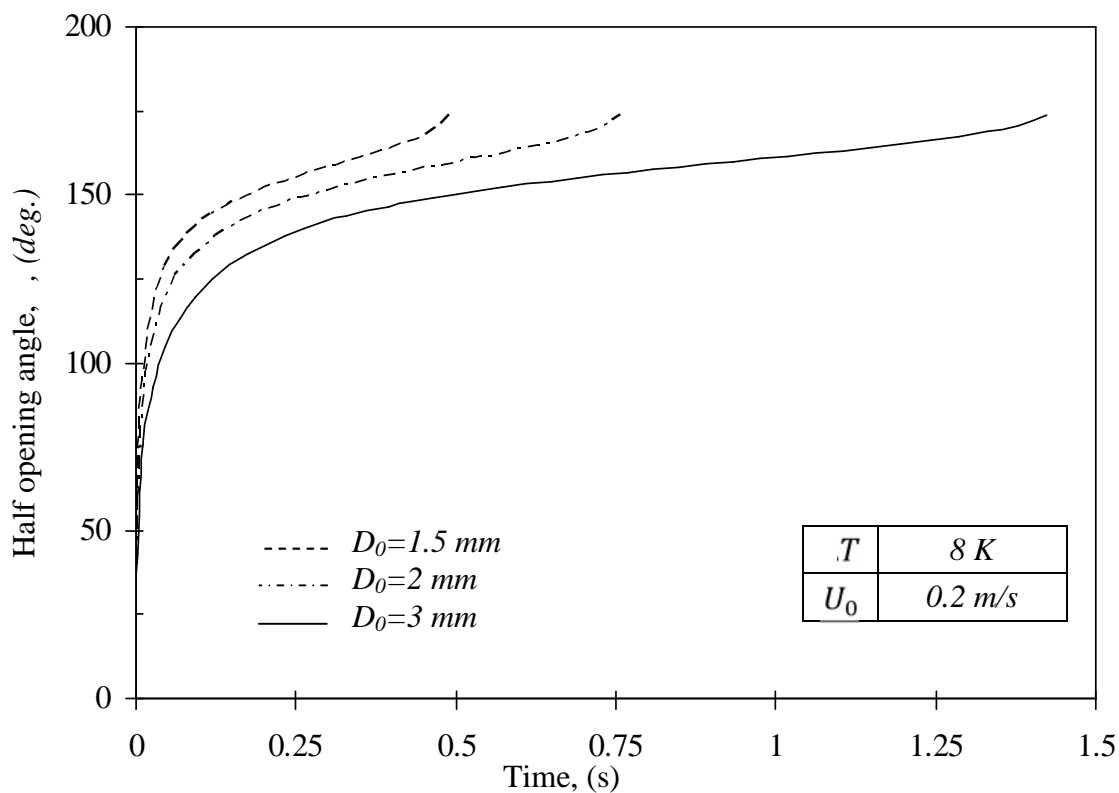Figure 4.14 Effect of the initial velocity on the average density ratio of drobble versus time.

Figure 4.15 Effect of initial diameter on the half opening angle versus time.
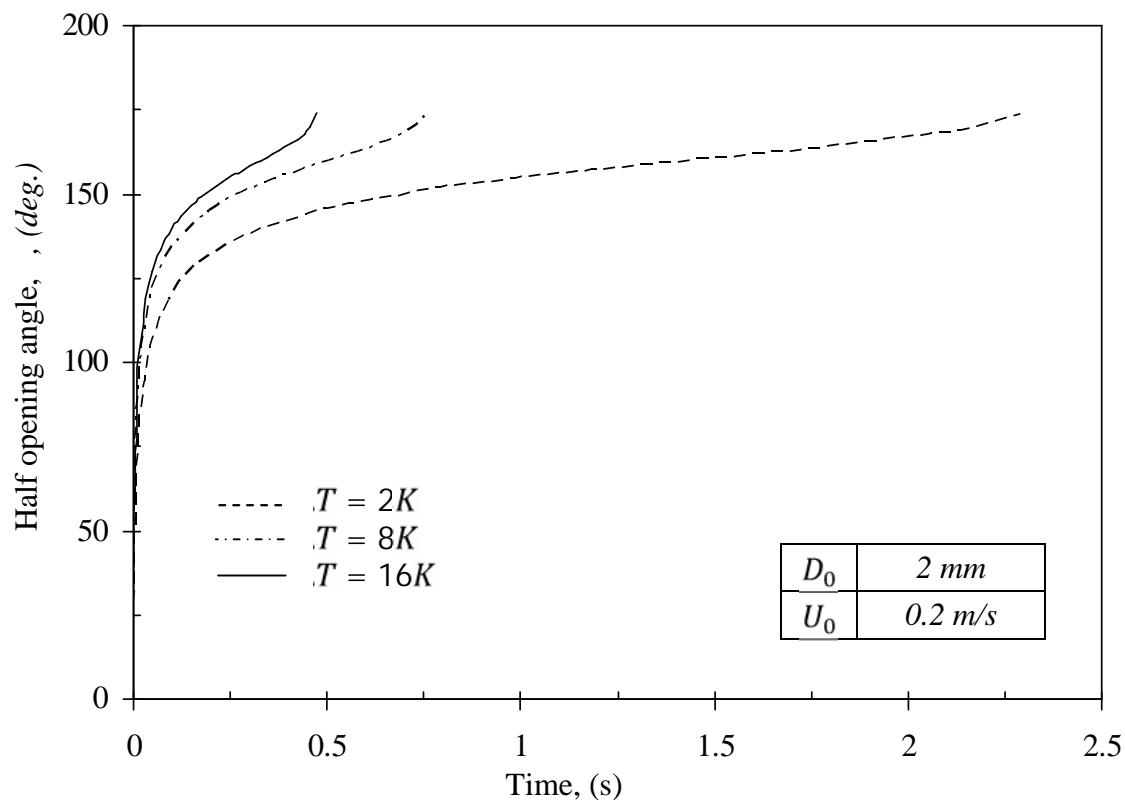
Figure 4.16 Effect of the degree of superheat on the half opening angle versus time.
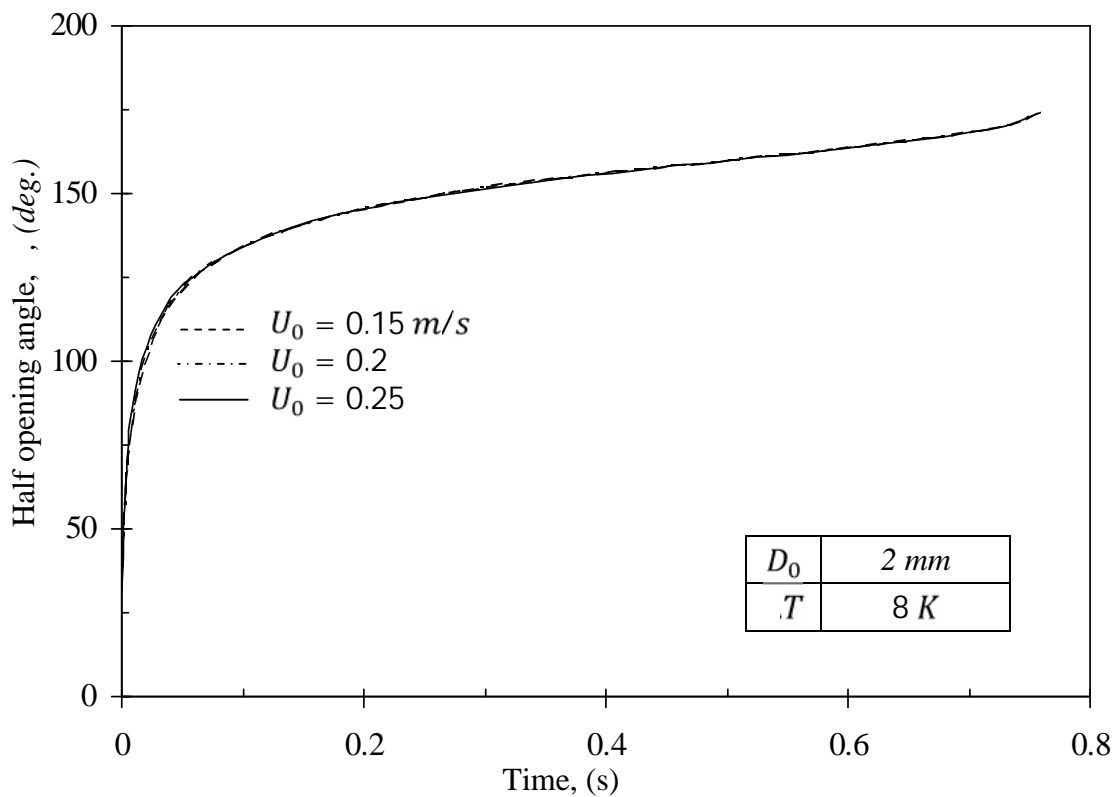
Figure 4.17 Effect of the initial velocity on the half opening angle versus time.
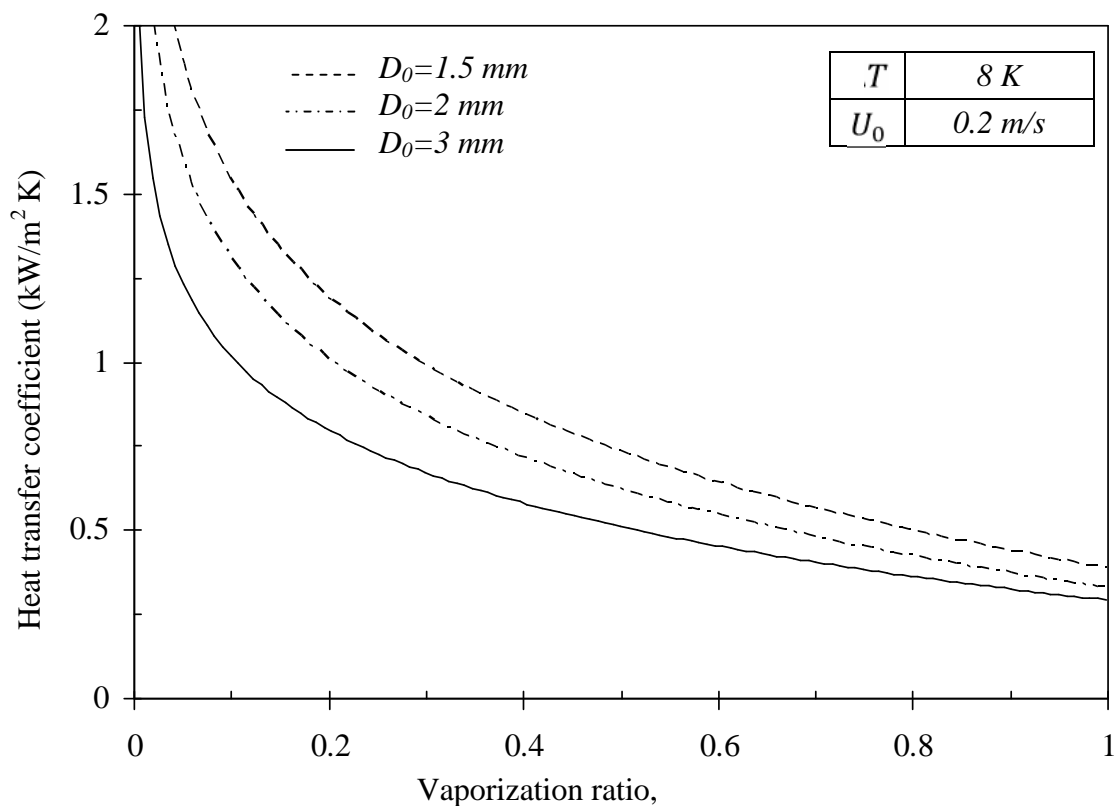
Figure 4.18 Effect of initial diameter on the heat transfer coefficient versus vaporization ratio.
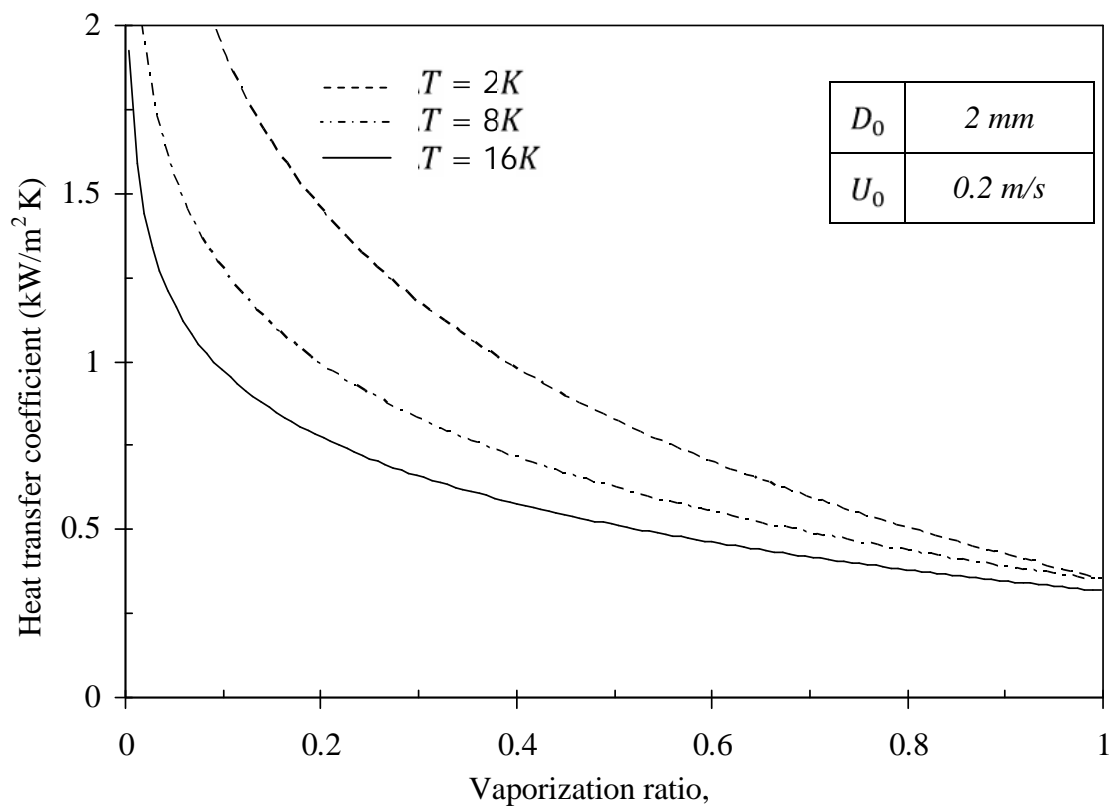
Figure 4.19 Effect of the degree of superheat on the heat transfer coefficient versus vaporization ratio.
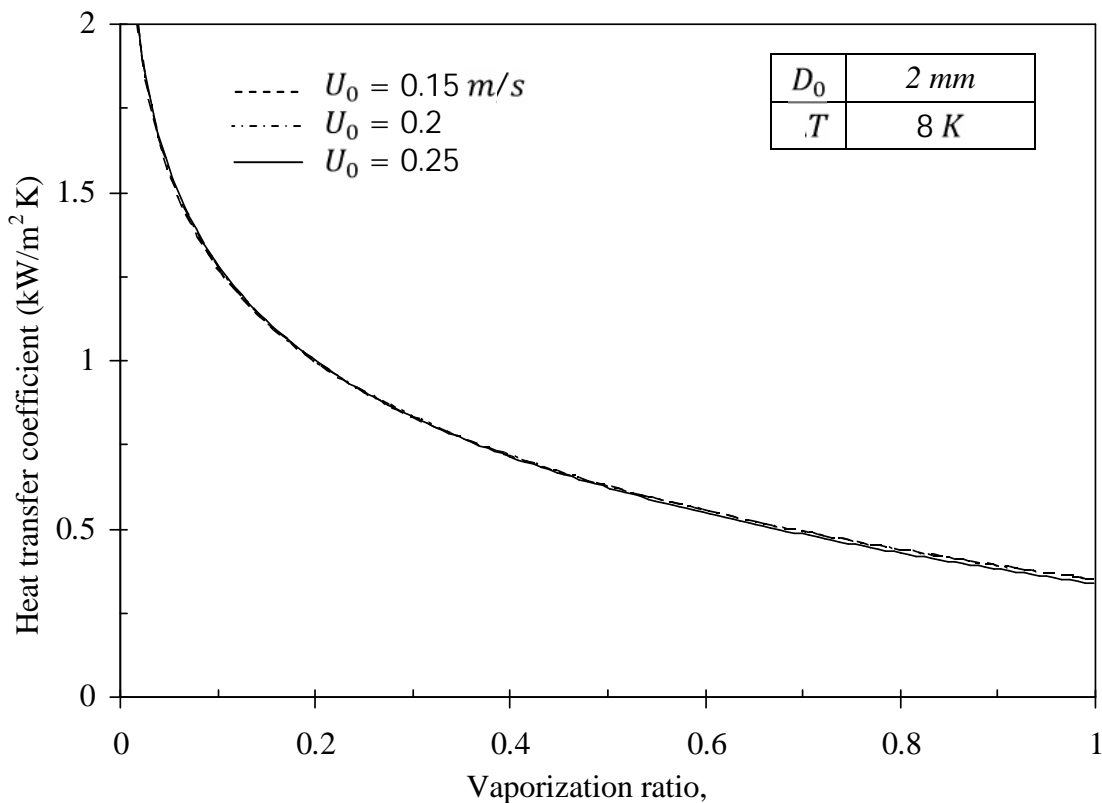
Figure 4.20 Effect of the initial velocity on the heat transfer coefficient versus vaporization ratio.
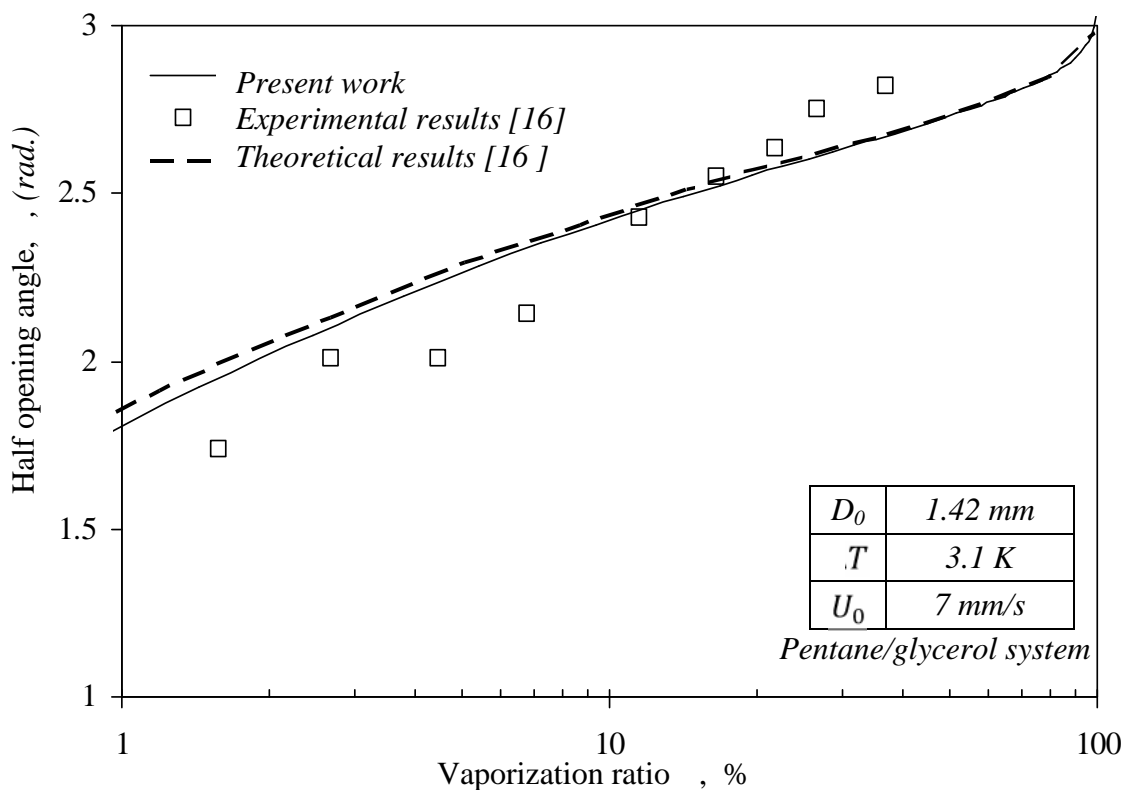
Figure 4.21 Comparison between the present predictions and other theoretical and experimental results.
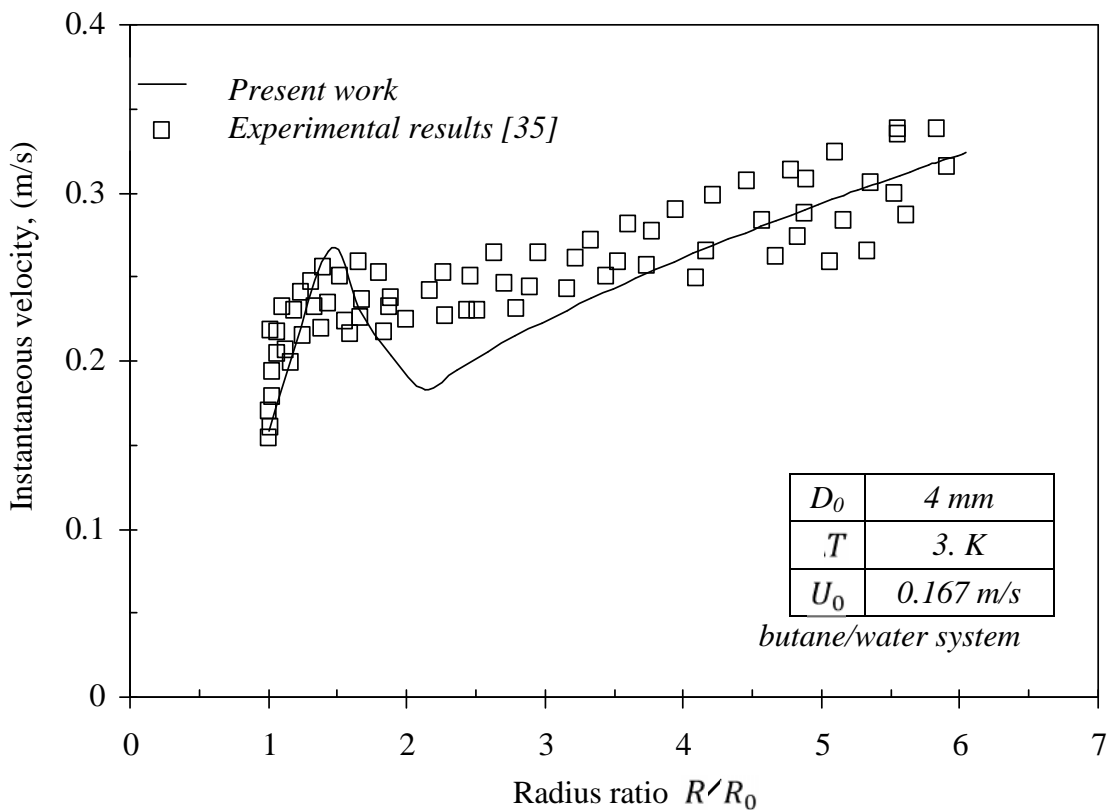
Figure 4.22 Comparison between the present predictions and other experimental results.
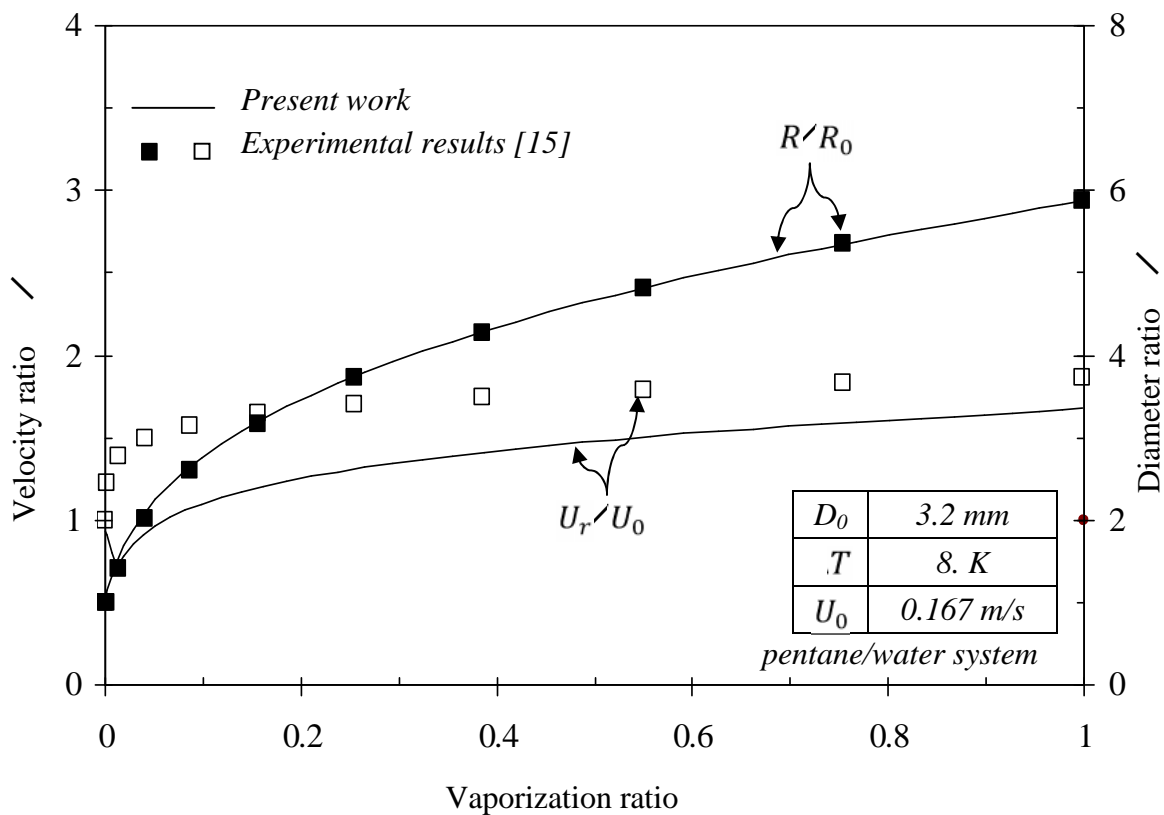
Figure 4.23 Comparison between the present predictions and other experimental results.
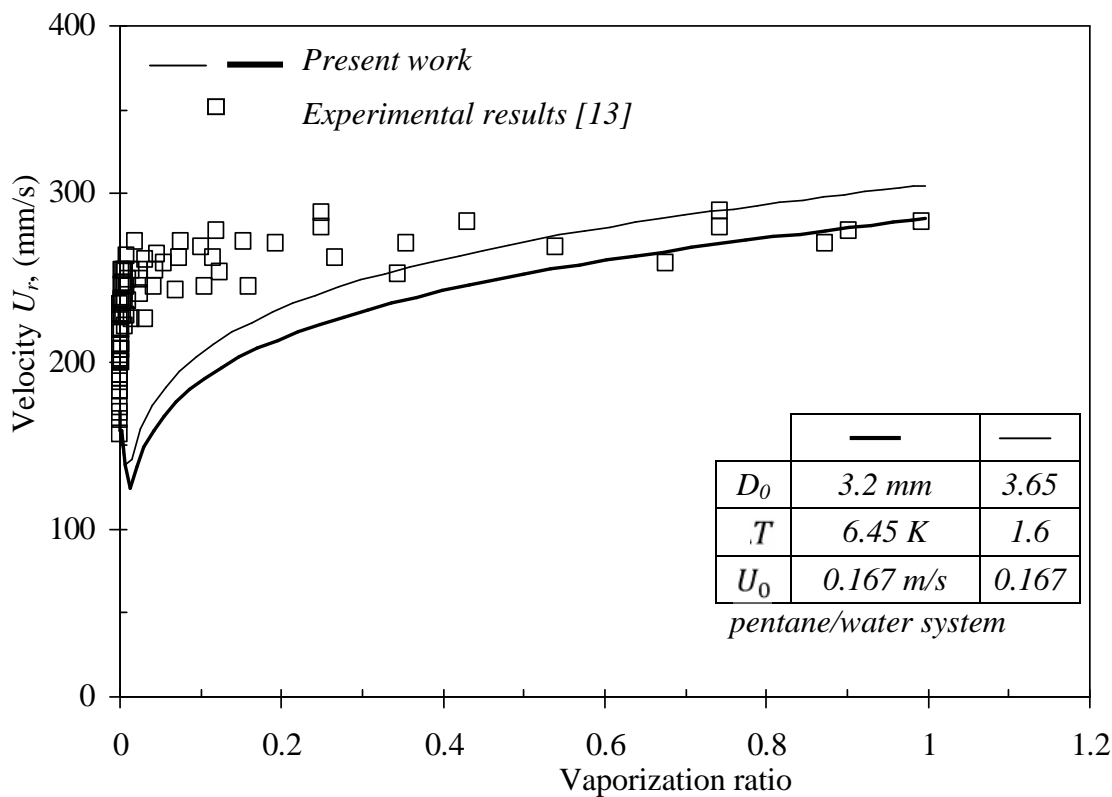
Figure 4.24 Comparison between the present predictions and other experimental results.

108
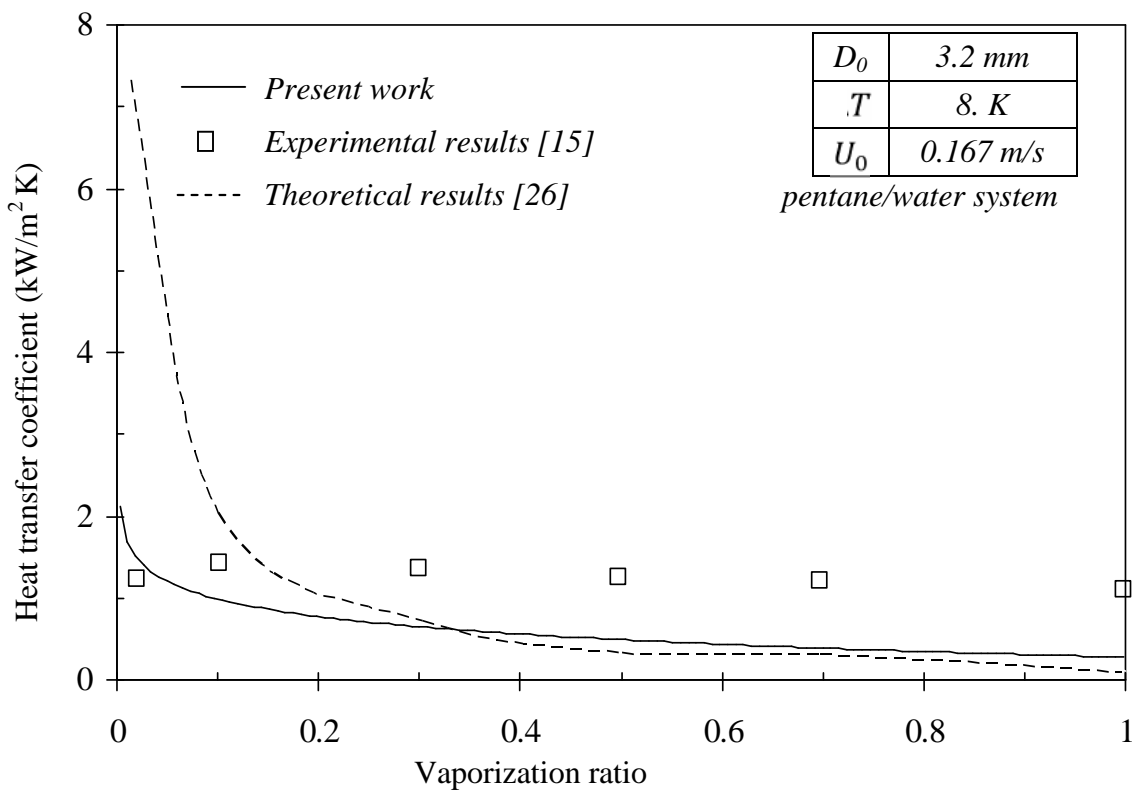
Figure 4.25 Comparison between the present predictions and other theoretical and experimental results.
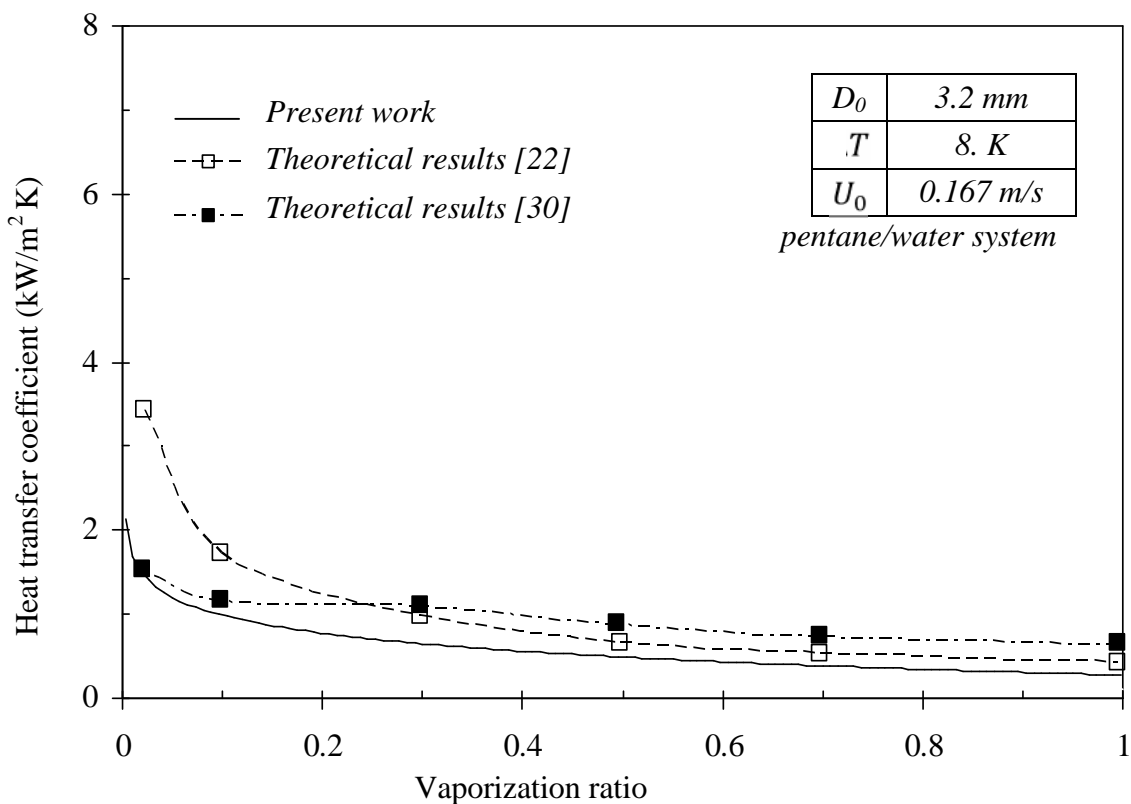
Figure 4.26 Comparison between the present predictions and other theoretical and experimental results.
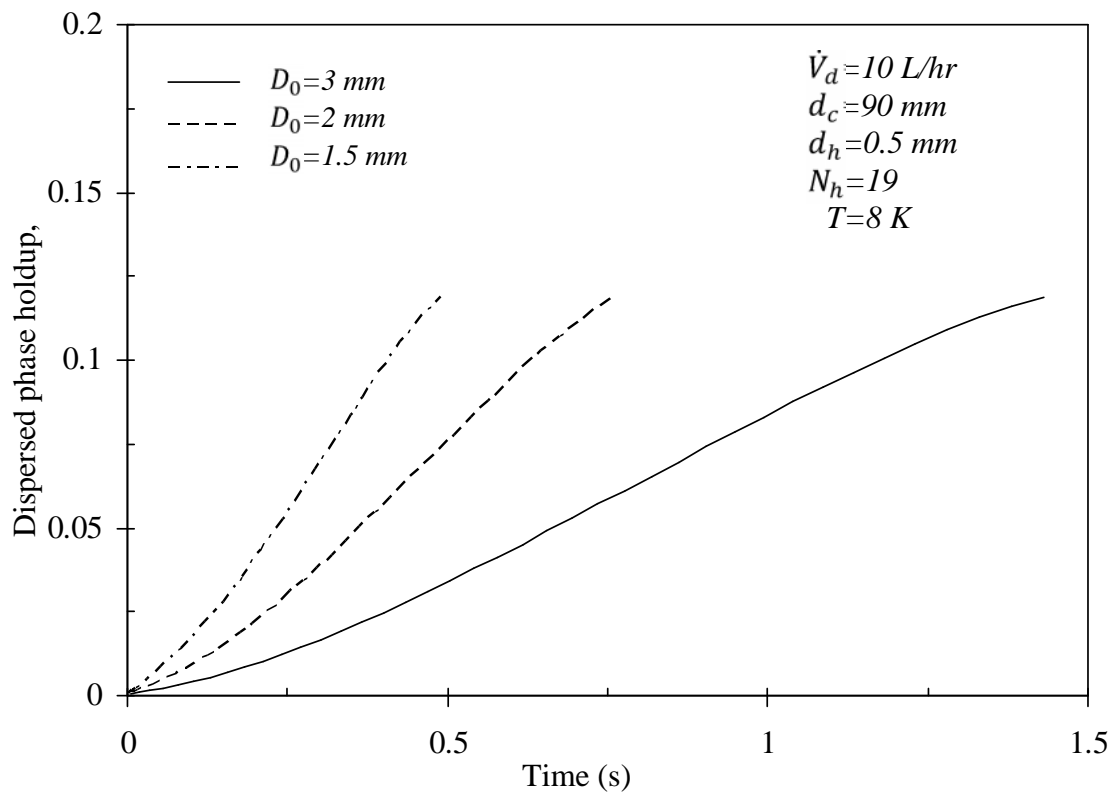
Figure 4.27 Effect of initial diameter on the dispersed phase holdup versus time.
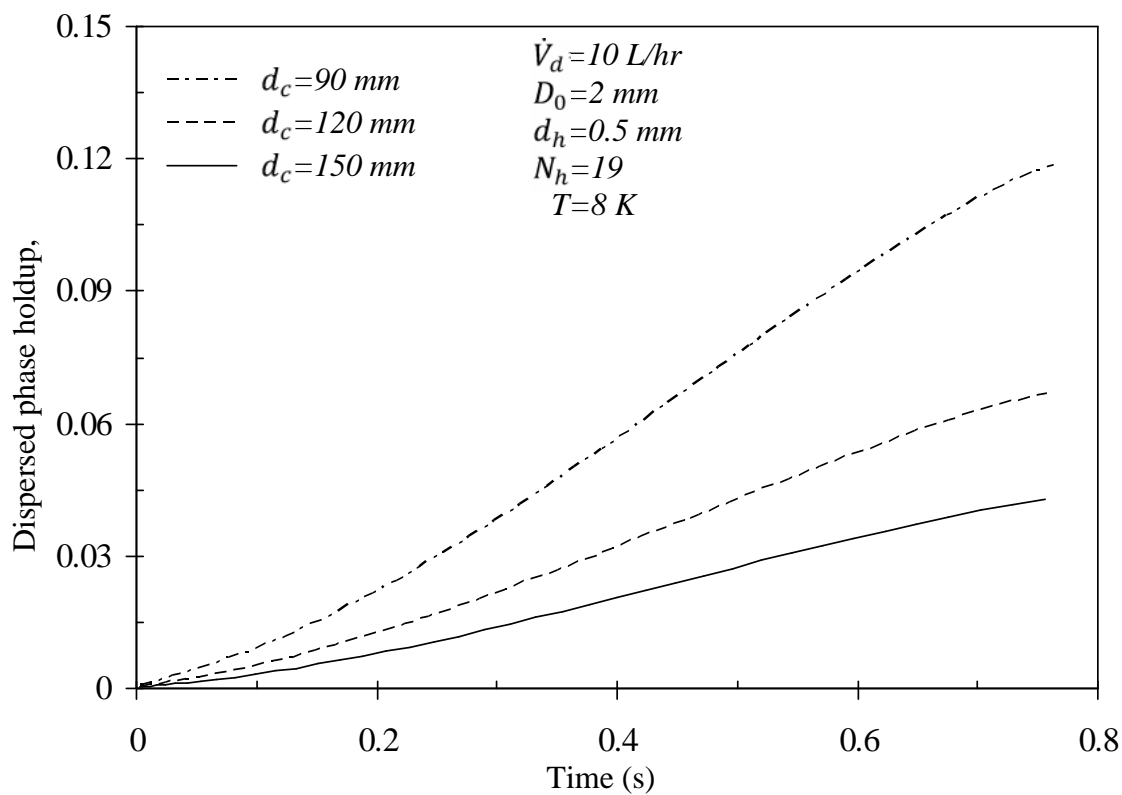
Figure 4.28 Effect of column diameter on the dispersed phase holdup versus time.
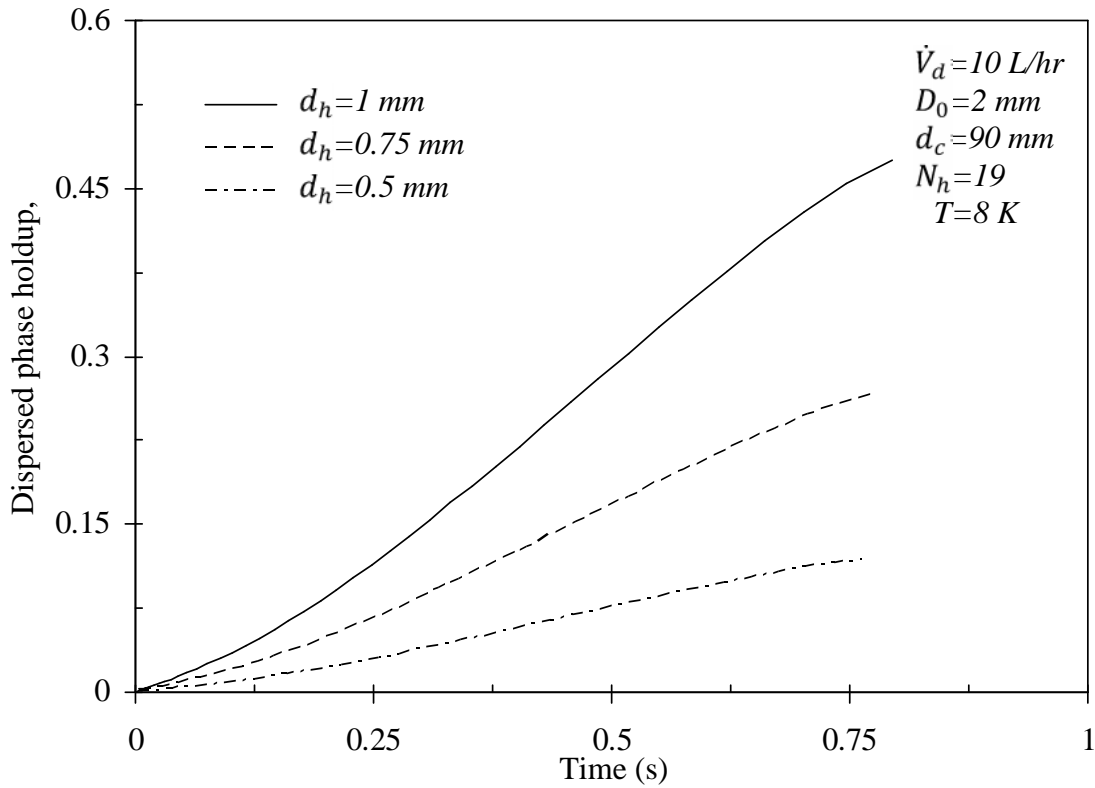
Figure 4.29 Effect of holes diameter on the dispersed phase holdup versus time.
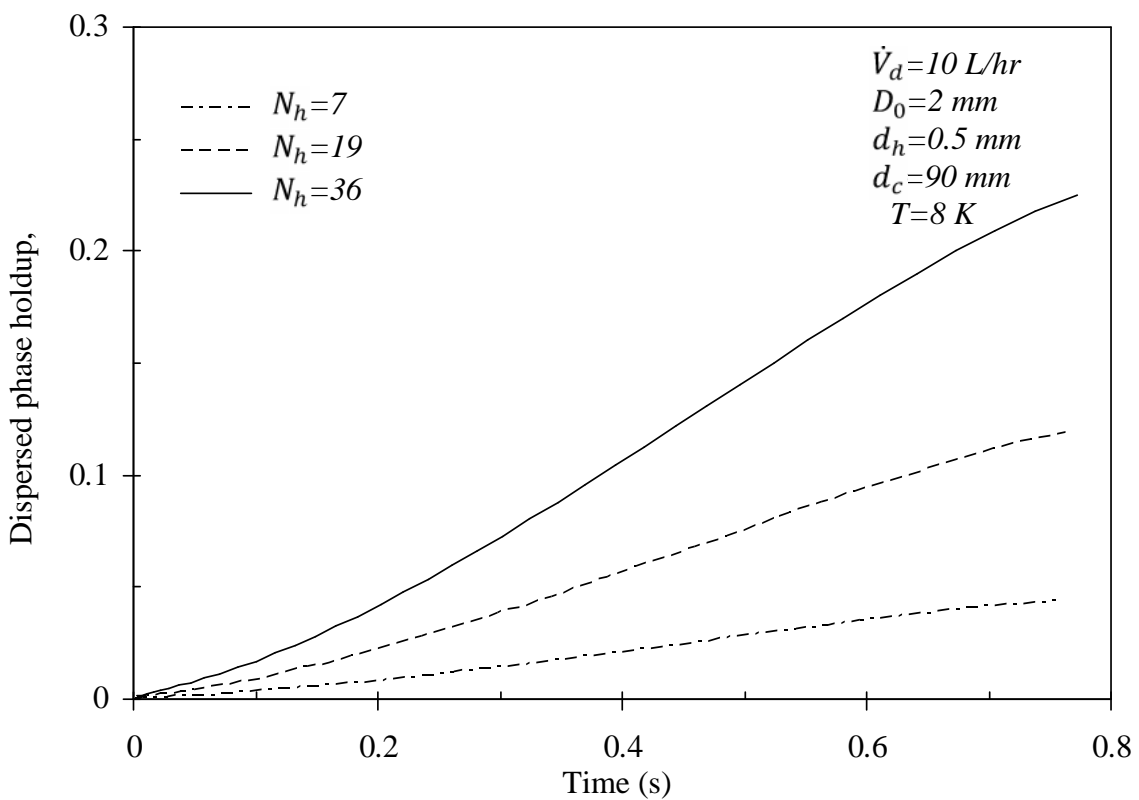
Figure 4.30 Effect of holes number on the dispersed phase holdup versus time.
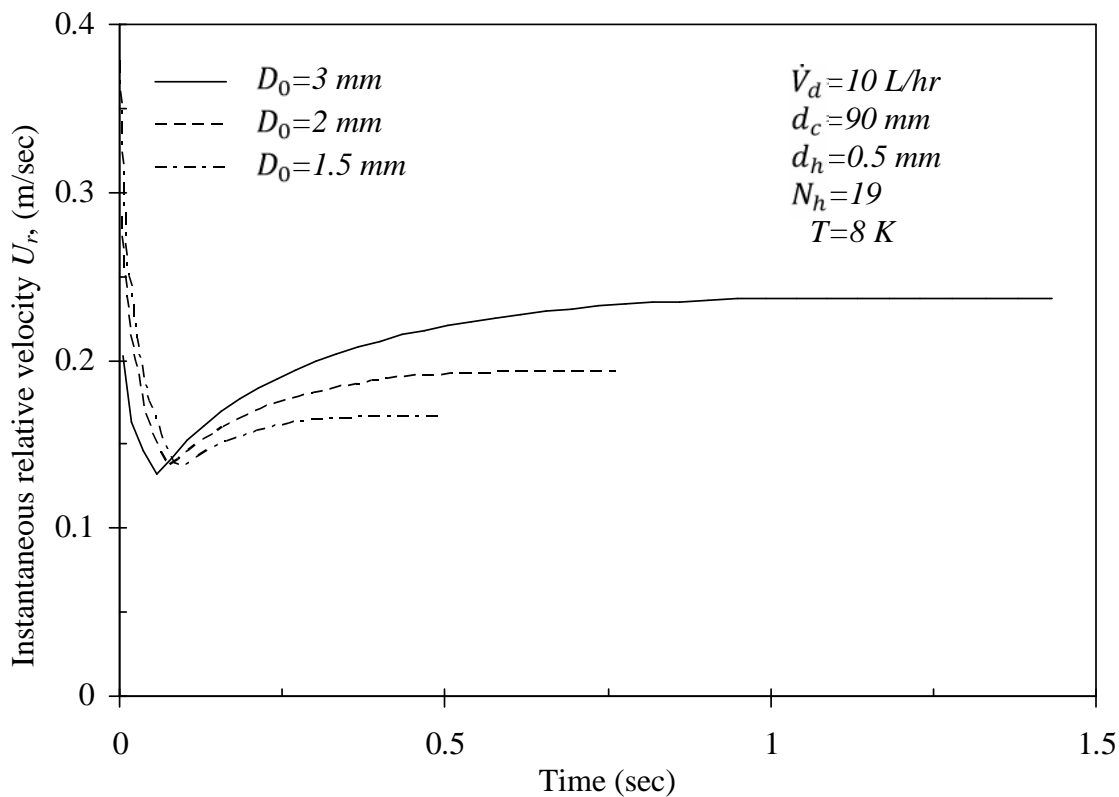
Figure 4.31 Effect of initial diameter on the instantaneous relative velocity versus time.
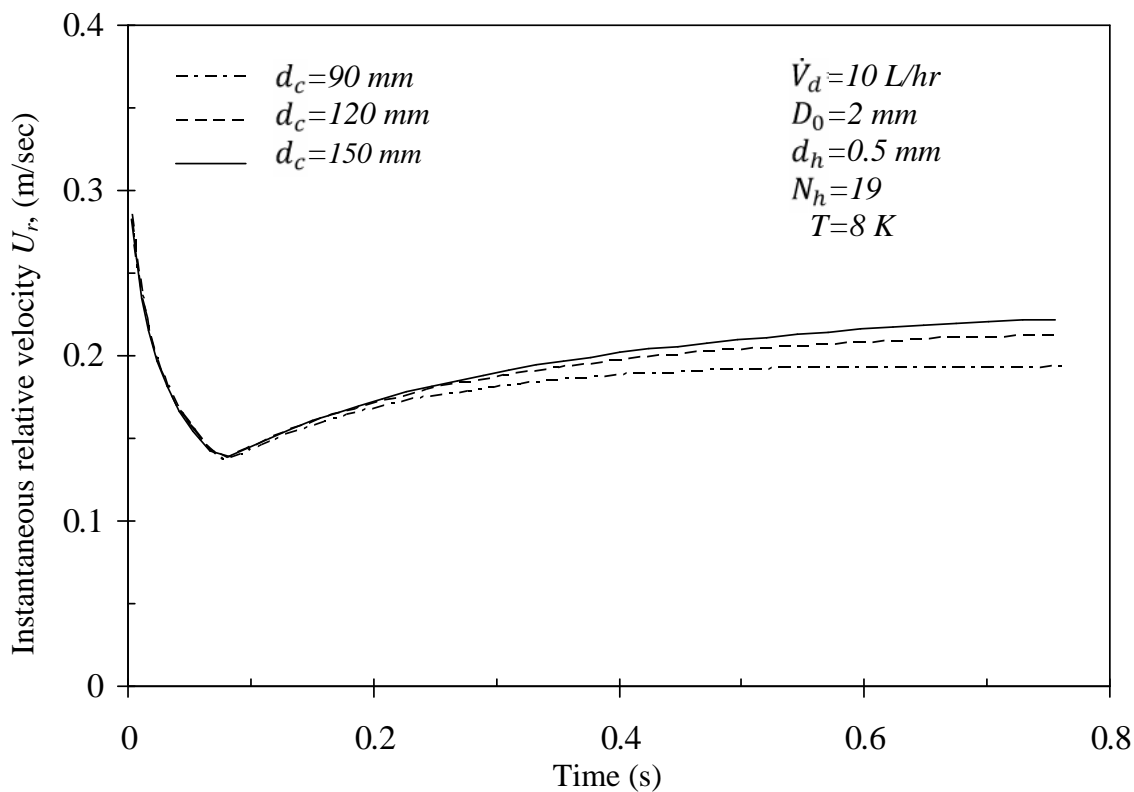
Figure 4.32 Effect of column diameter on the instantaneous relative velocity versus time.
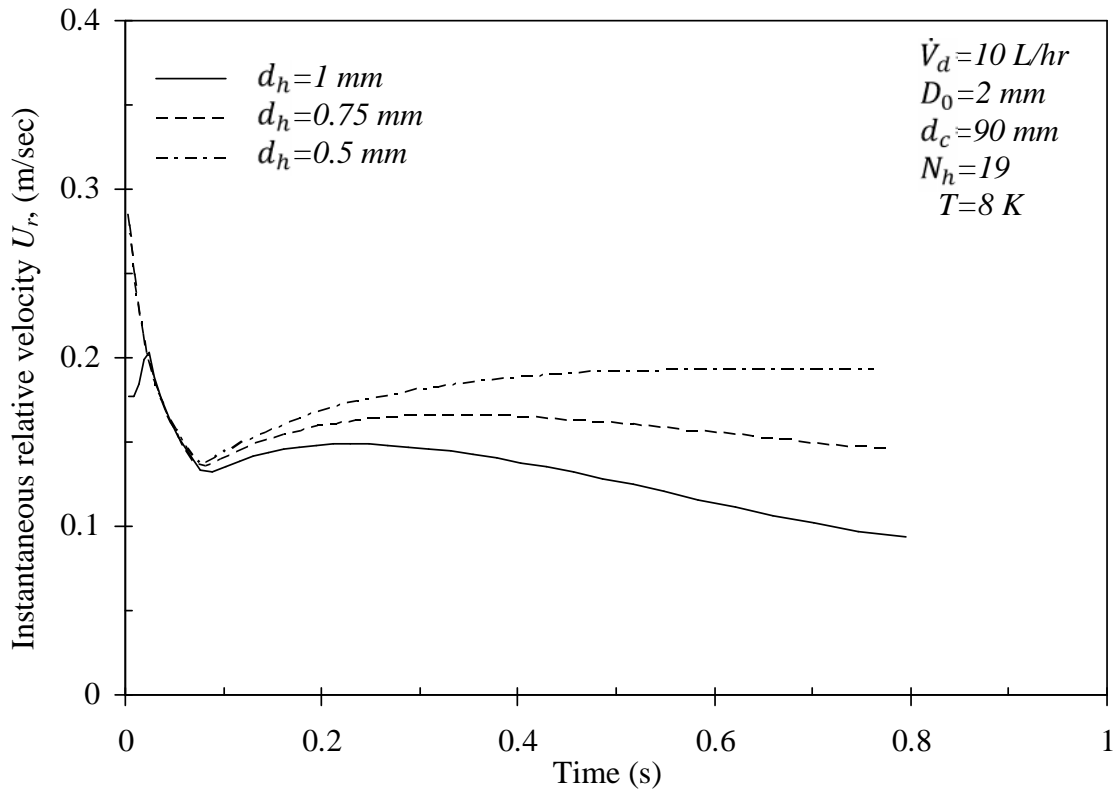
Figure 4.33 Effect of holes diameter on the instantaneous relative velocity versus time.
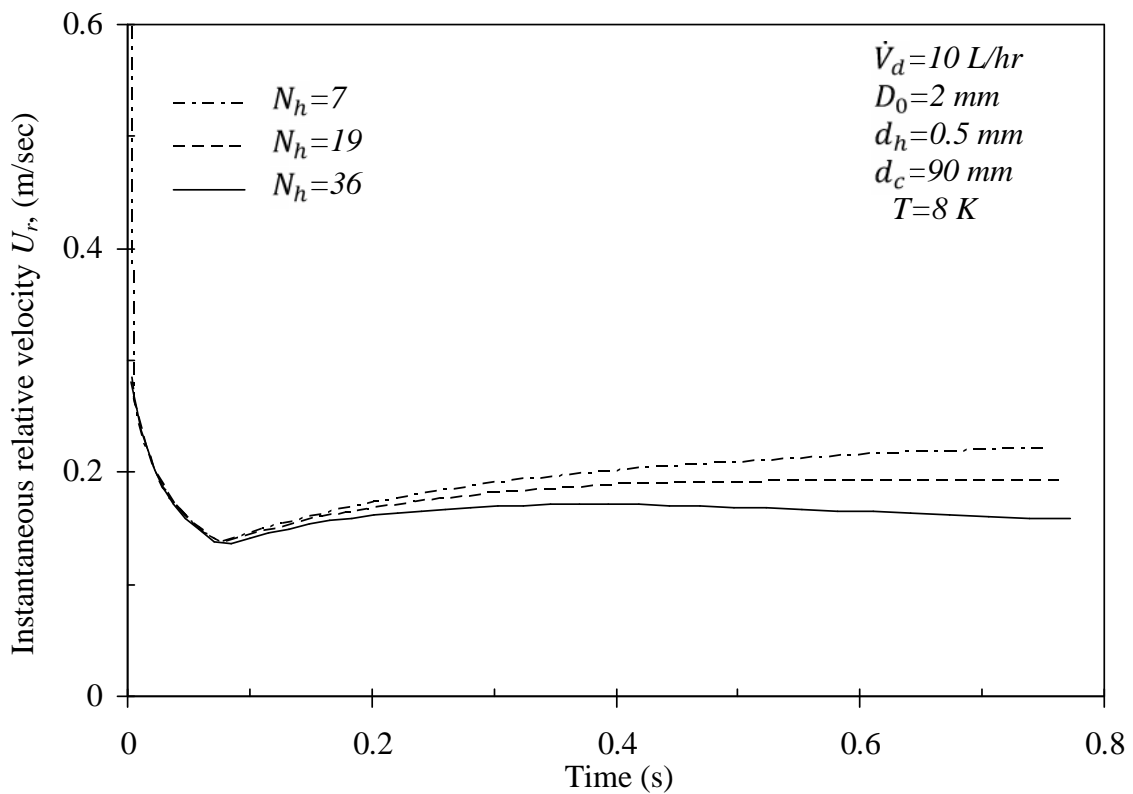
Figure 4.34 Effect of holes number on the instantaneous relative velocity versus time.

113
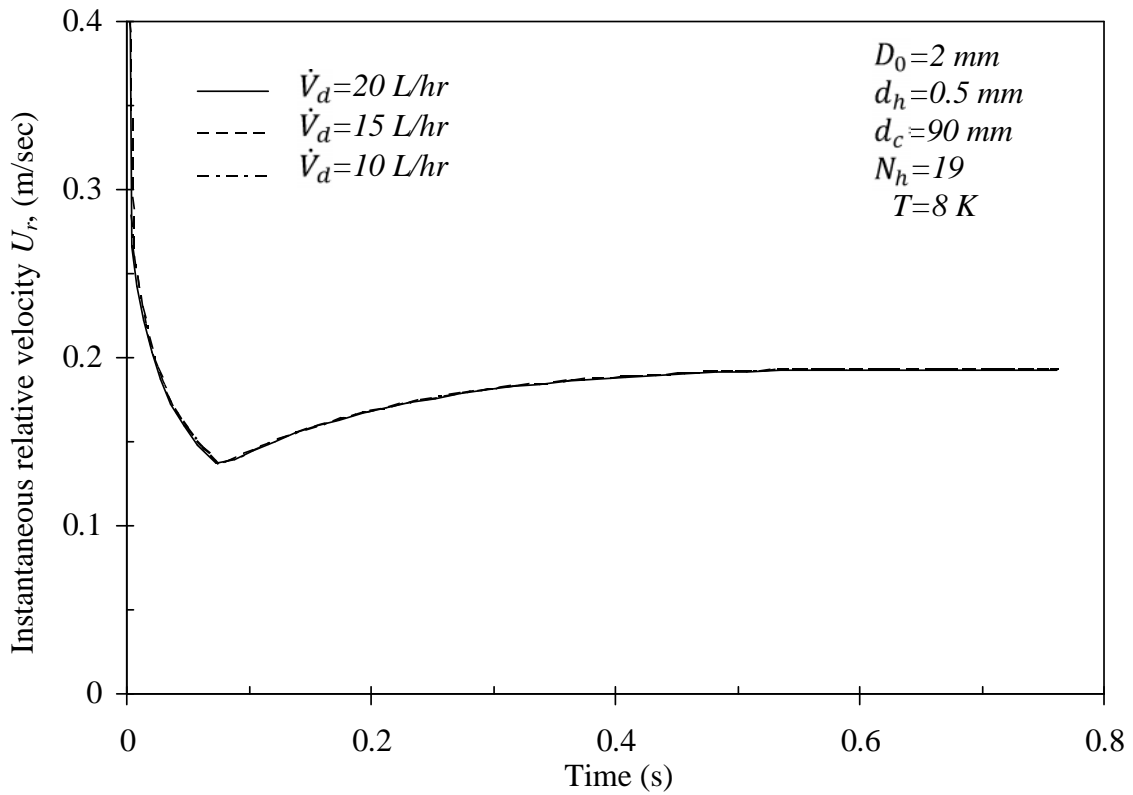
Figure 4.35 Effect of the dispersed phase volume flow rate on the instantaneous relative velocity versus time.
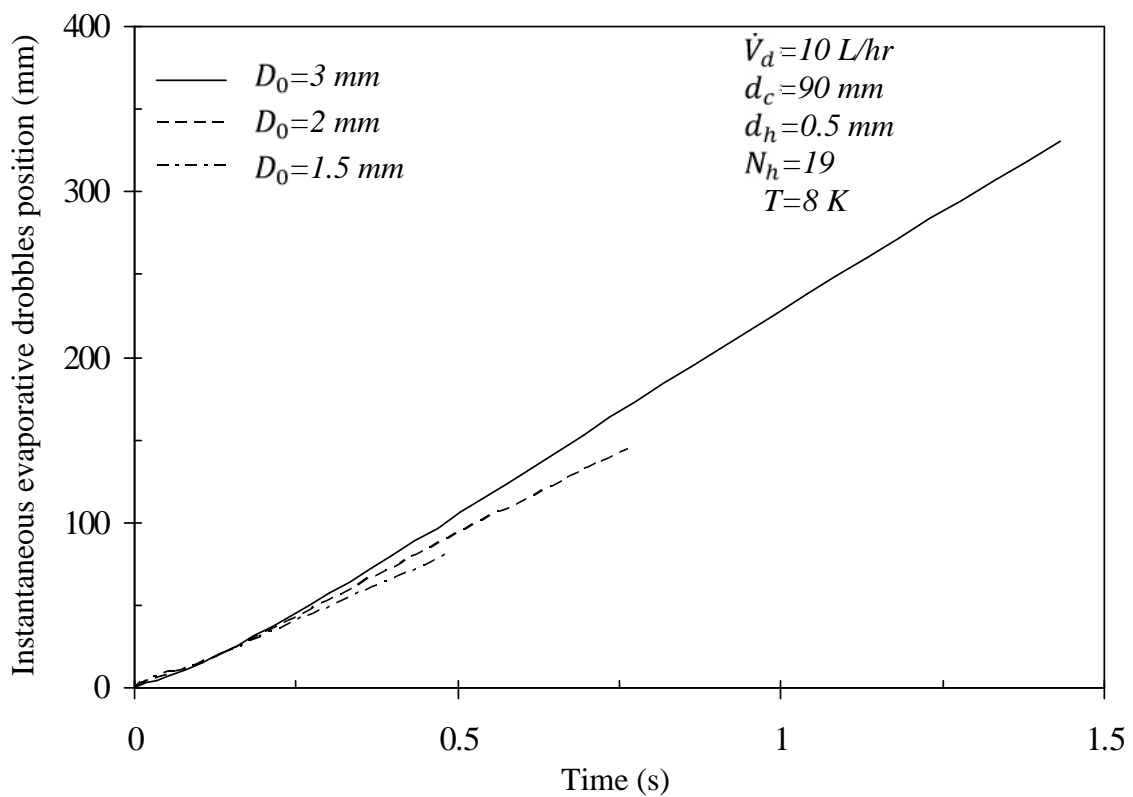
Figure 4.36 Effect of initial diameter on the instantaneous evaporative drobbles position versus time.

114
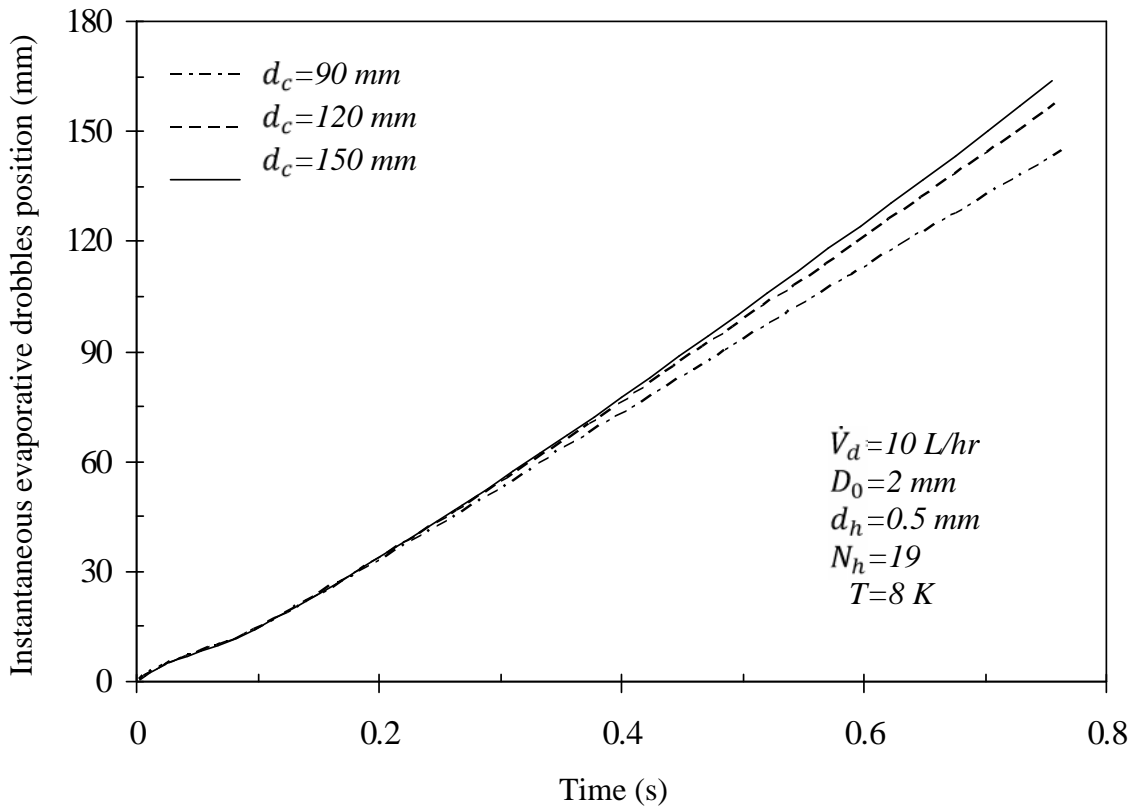
Figure 4.37 Effect of column diameter on the instantaneous evaporative drobbles position versus time.
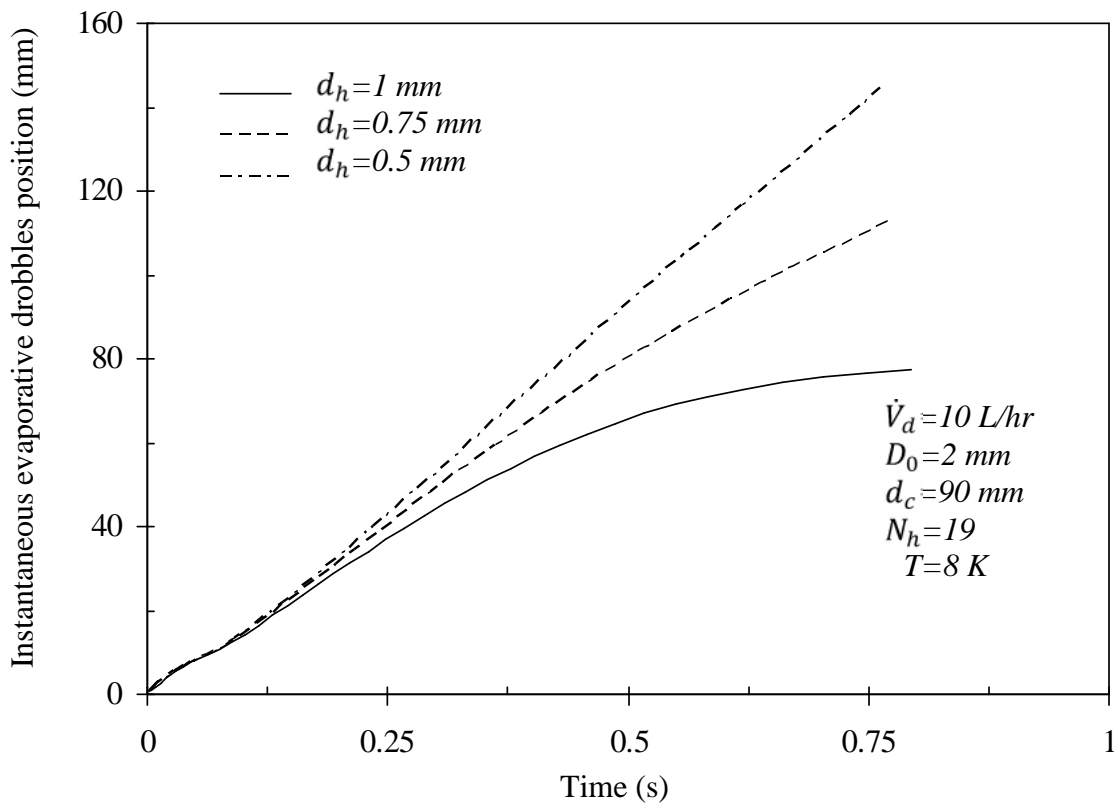
Figure 4.38 Effect of holes diameter on the instantaneous evaporative drobbles position versus time.
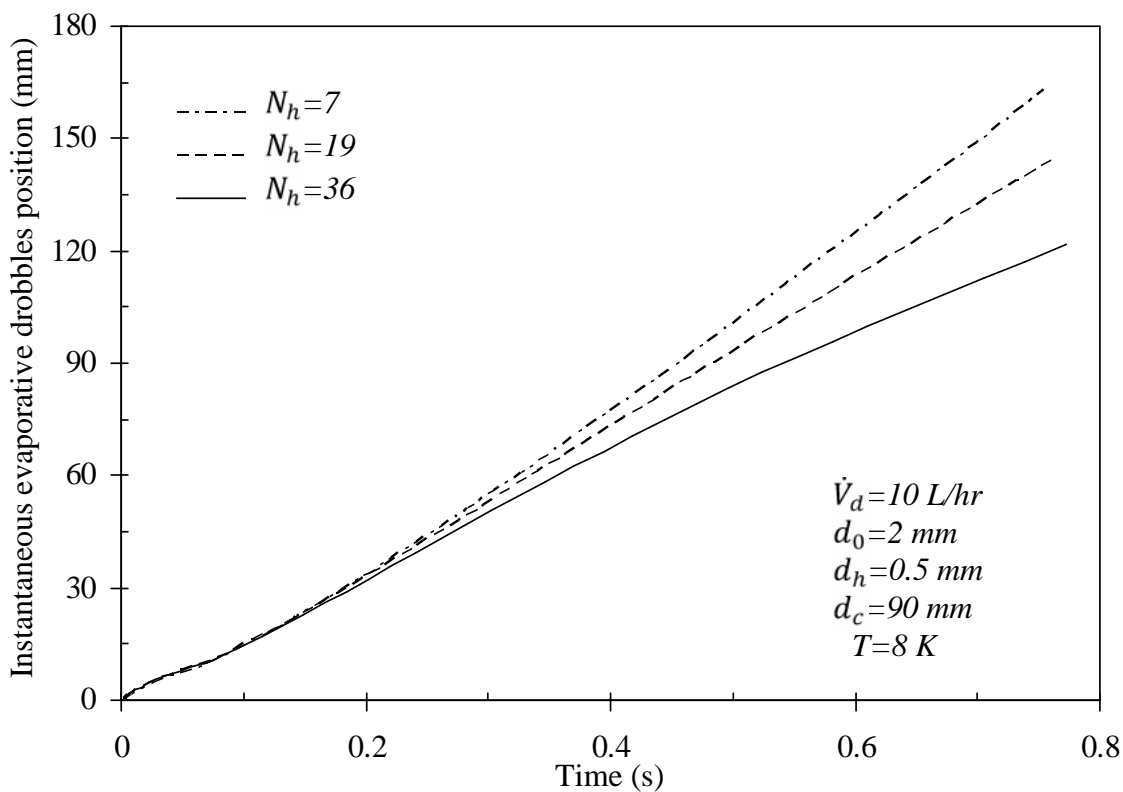
Figure 4.39 Effect of holes number the instantaneous evaporative drobbles position versus time.
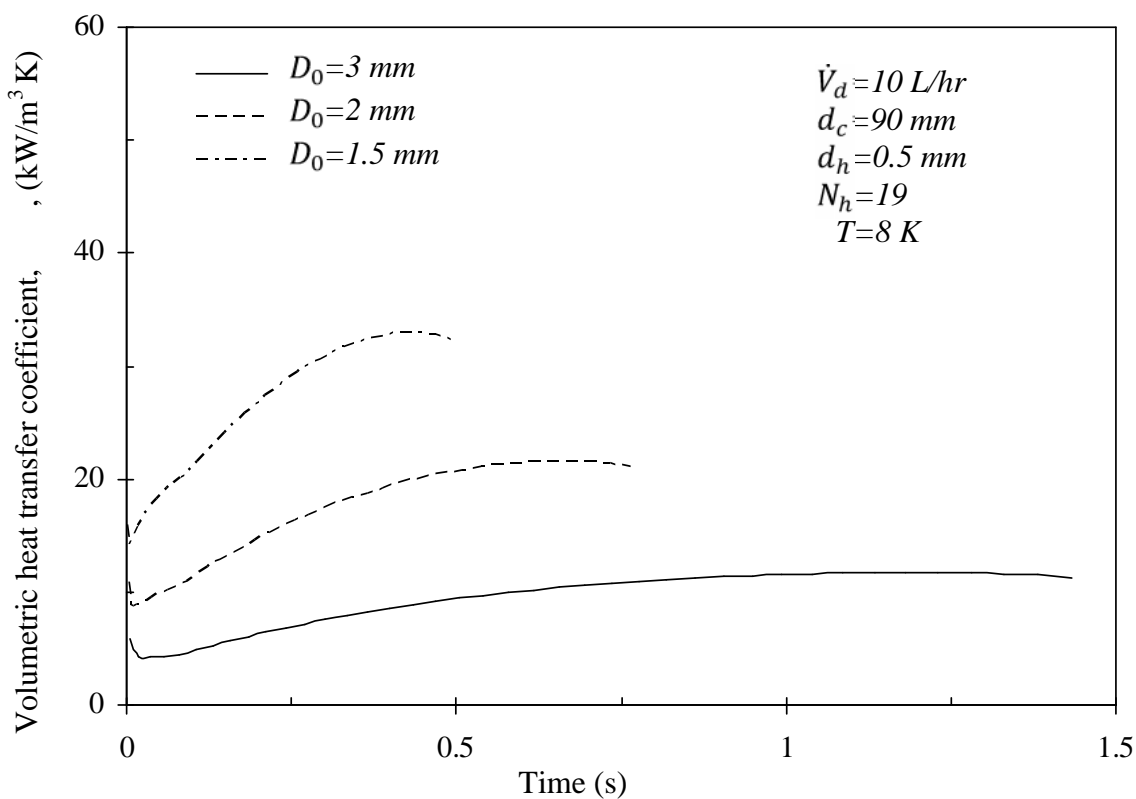
Figure 4.40 Effect of initial diameter on the average volumetric heat transfer coefficient versus time.
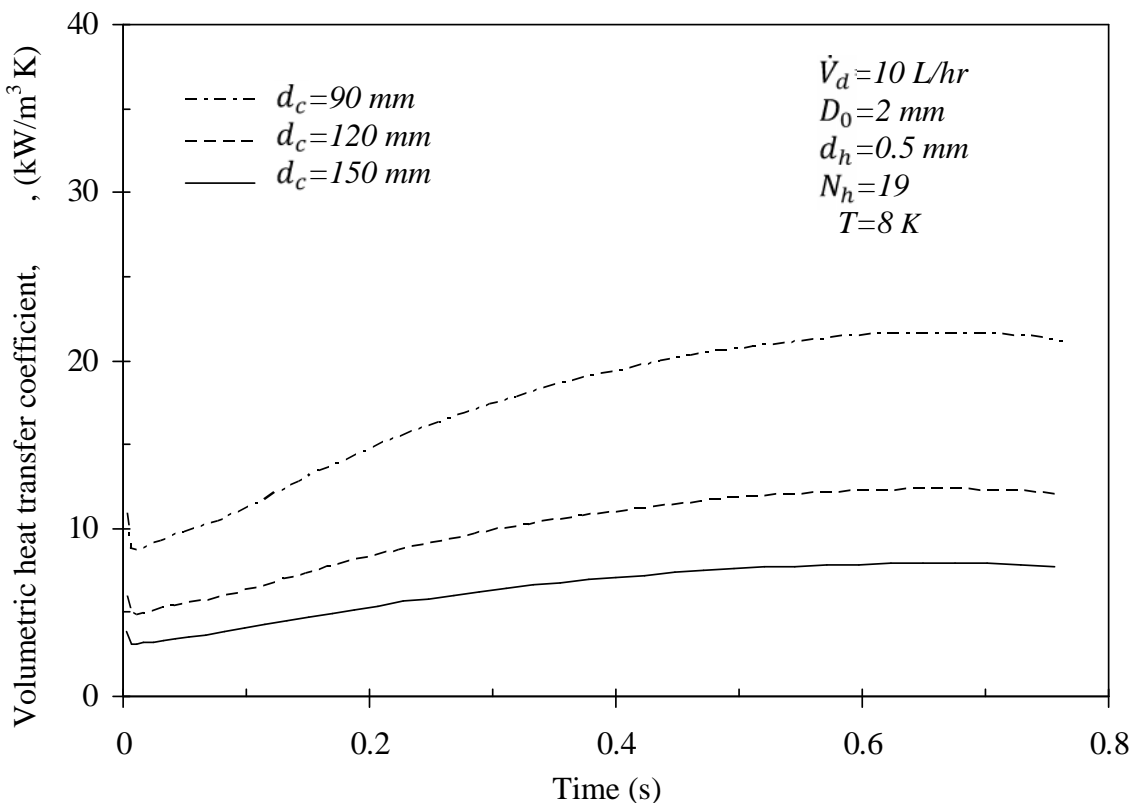
Figure 4.41 Effect of column diameter on the average volumetric heat transfer coefficient versus time.
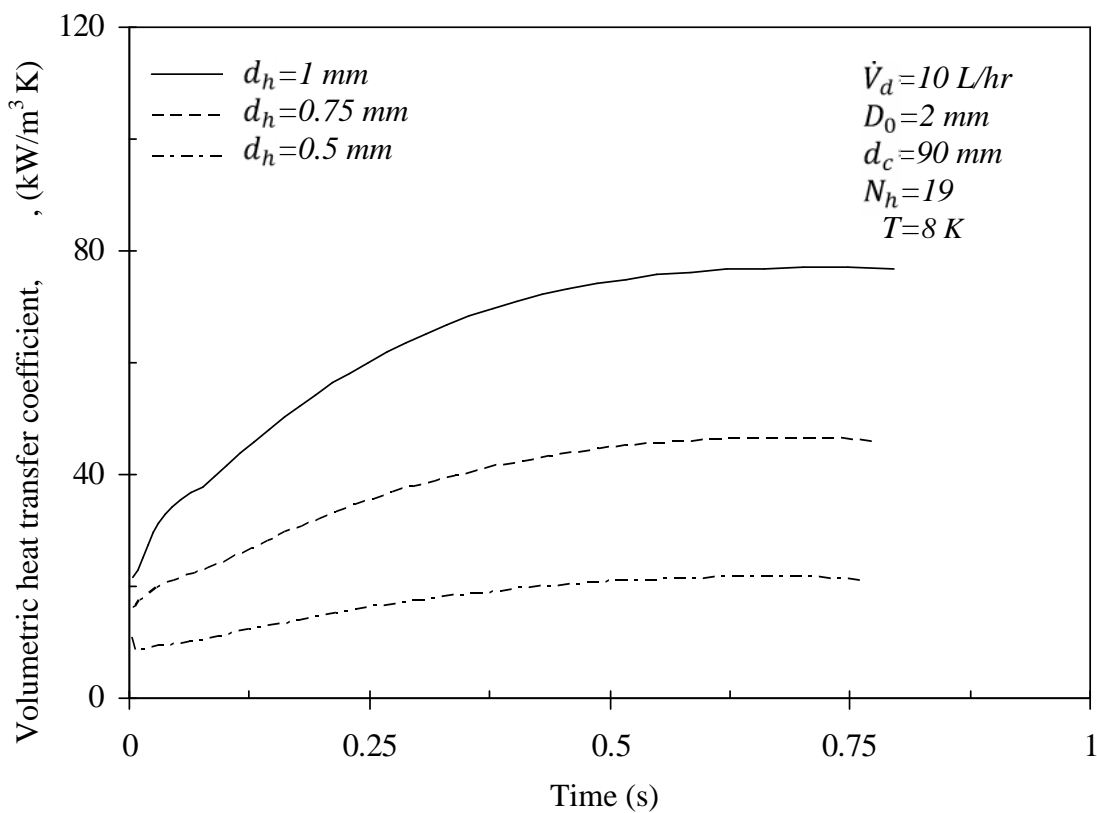
Figure 4.42 Effect of holes diameter on the average volumetric heat transfer coefficient versus time.

117
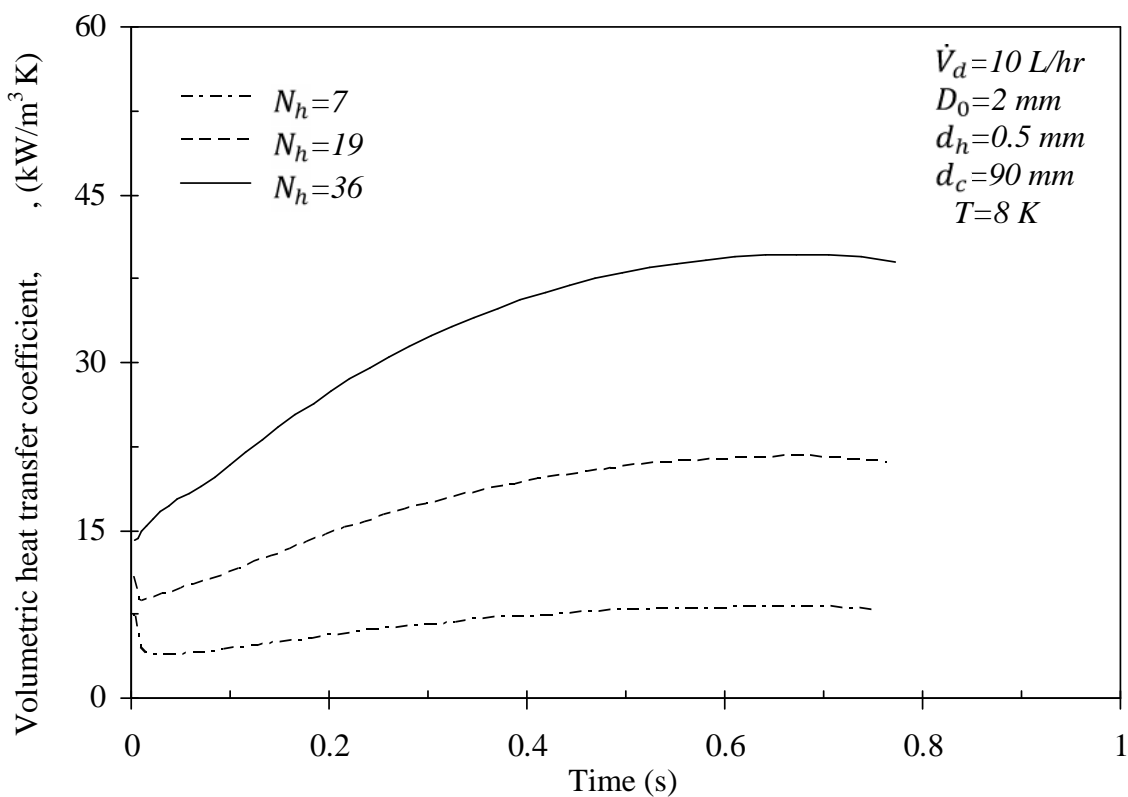
Figure 4.43 Effect of holes number on the average volumetric heat transfer coefficient versus time.
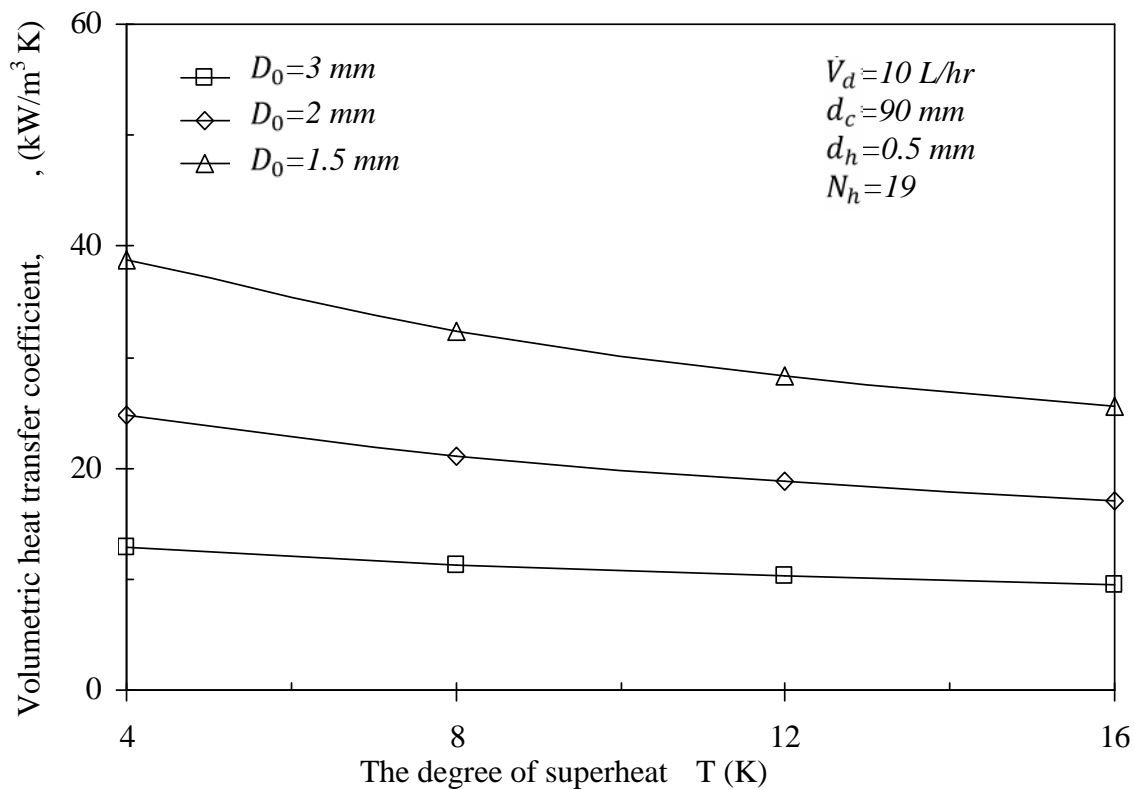
Figure 4.44 Effect of initial diameter on the average volumetric heat transfer coefficient for complete evaporation versus the degree of superheat.
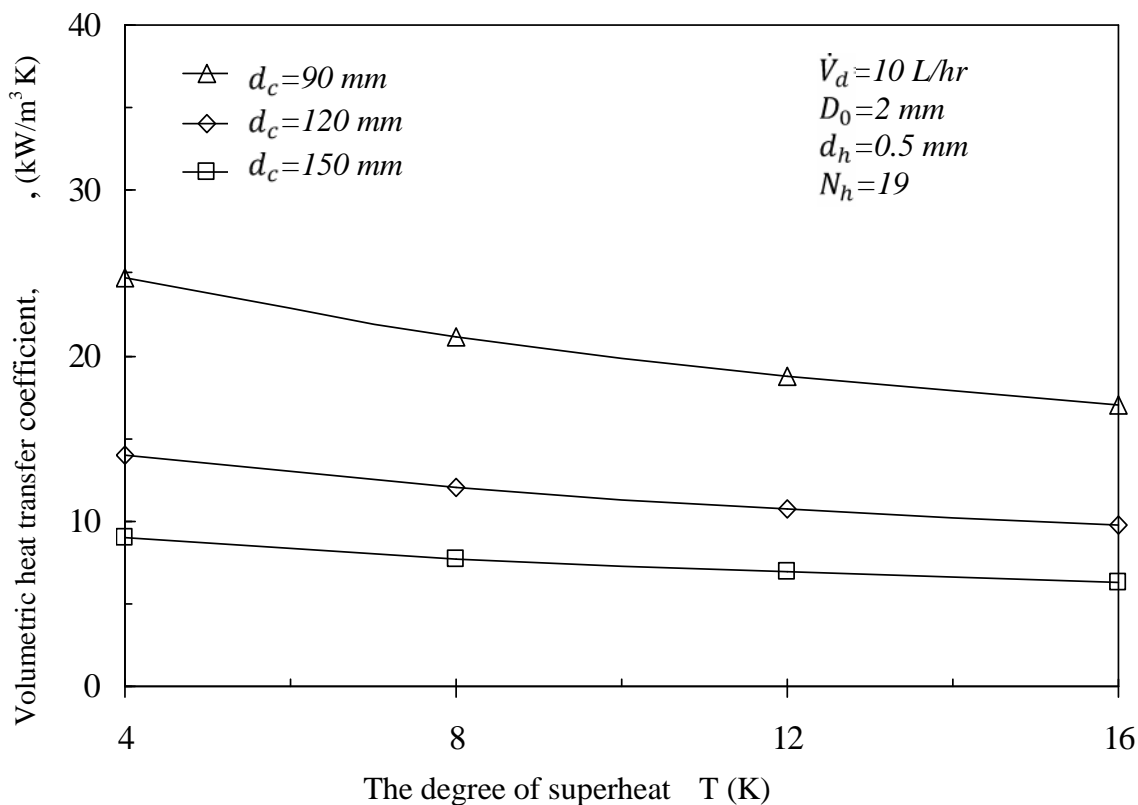
Figure 4.45 Effect of column diameter on the average volumetric heat transfer coefficient for complete evaporation versus the degree of superheat.
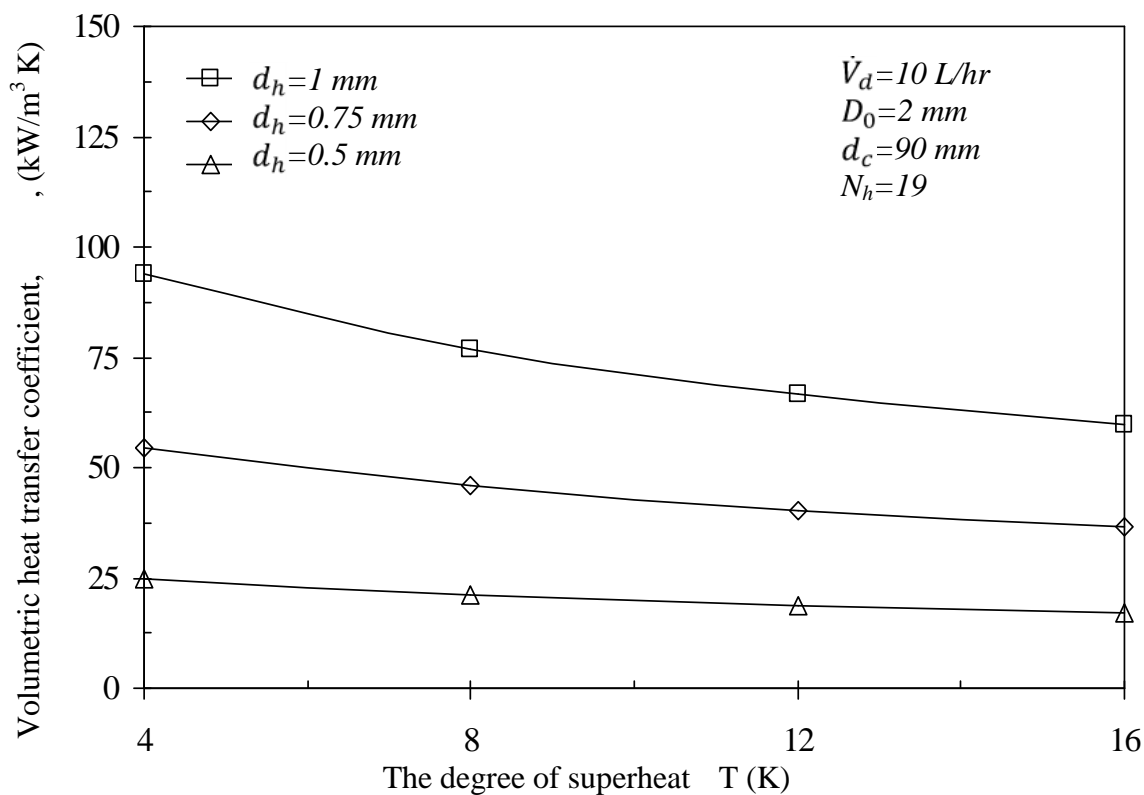
Figure 4.46 Effect of holes diameter on the average volumetric heat transfer coefficient for complete evaporation versus the degree of superheat.
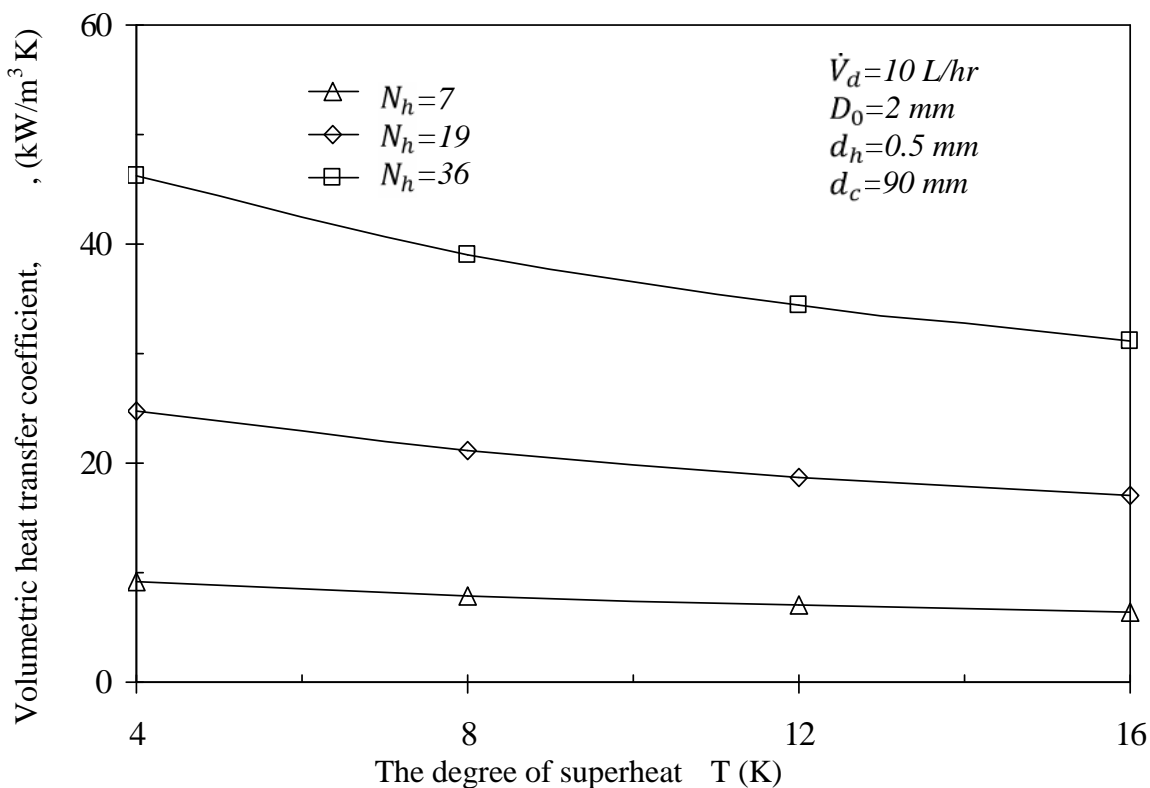
Figure 4.47 Effect of holes number on the average volumetric heat transfer coefficient for complete evaporation versus the degree of superheat.
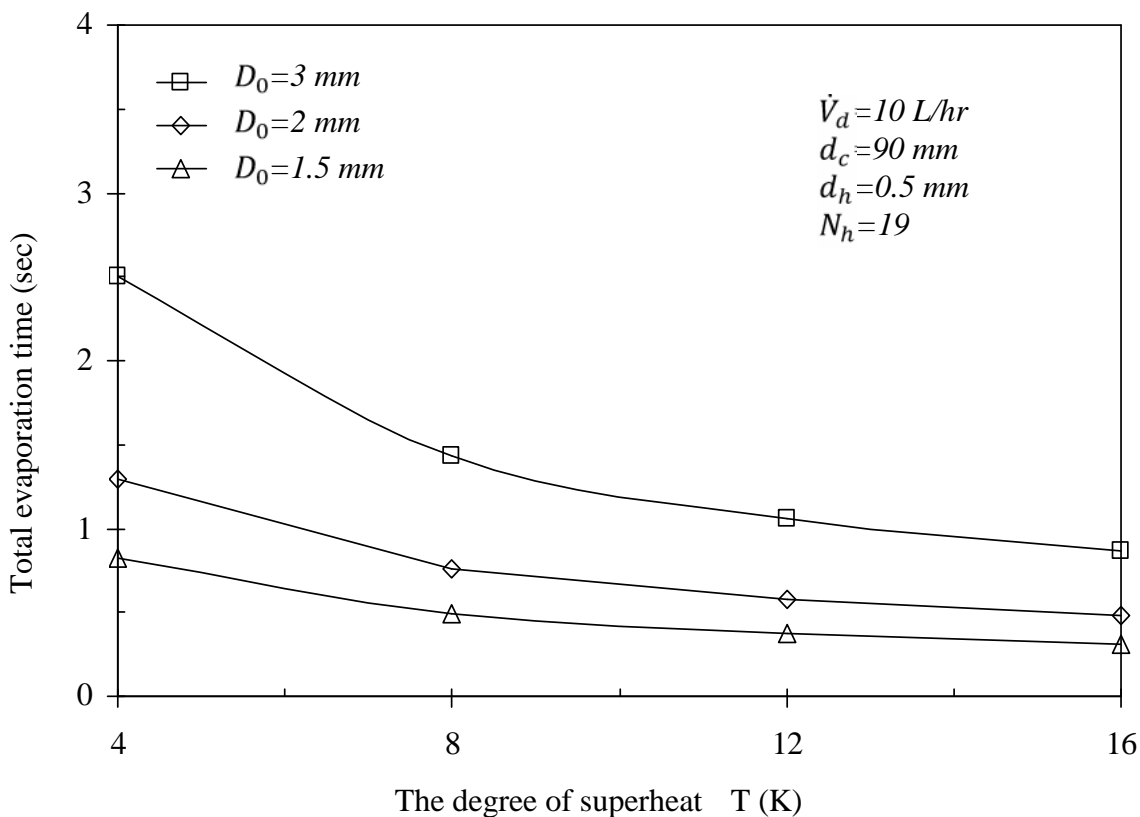
Figure 4.48 Effect of initial diameter on the total evaporation time versus the degree of superheat temperature.

120
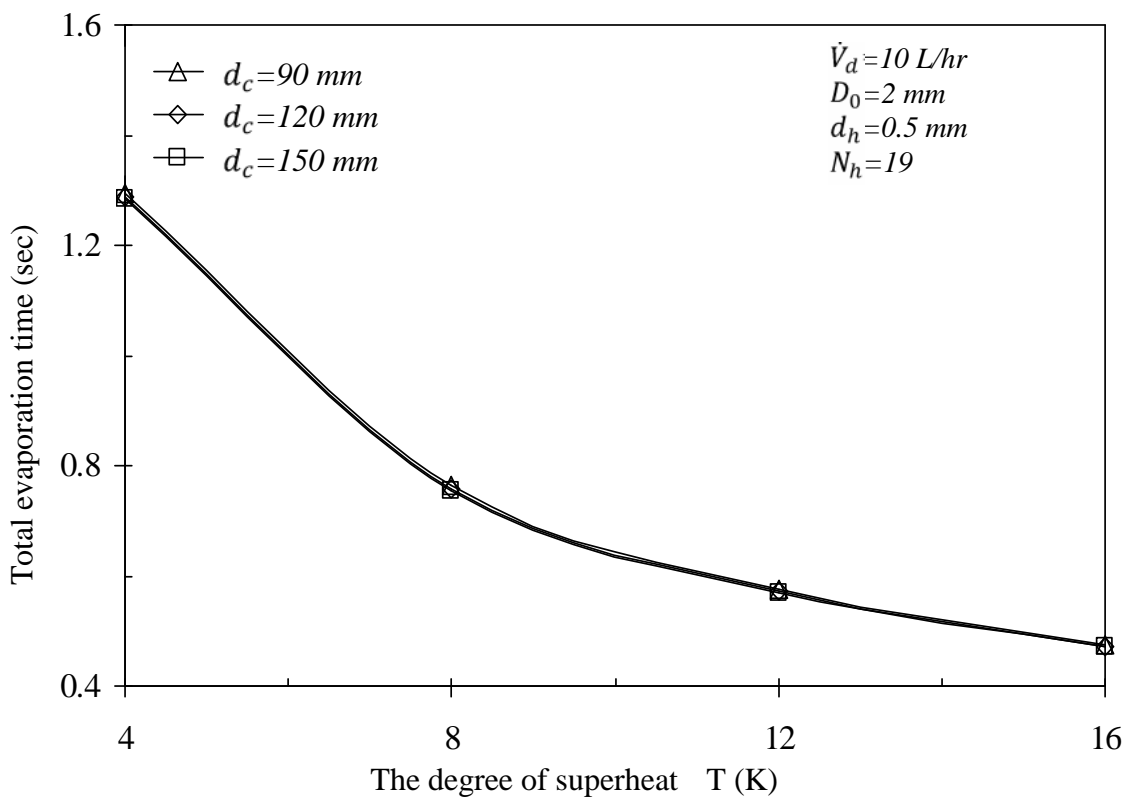
Figure 4.49 Effect of column diameter on the total evaporation time versus the degree of superheat.
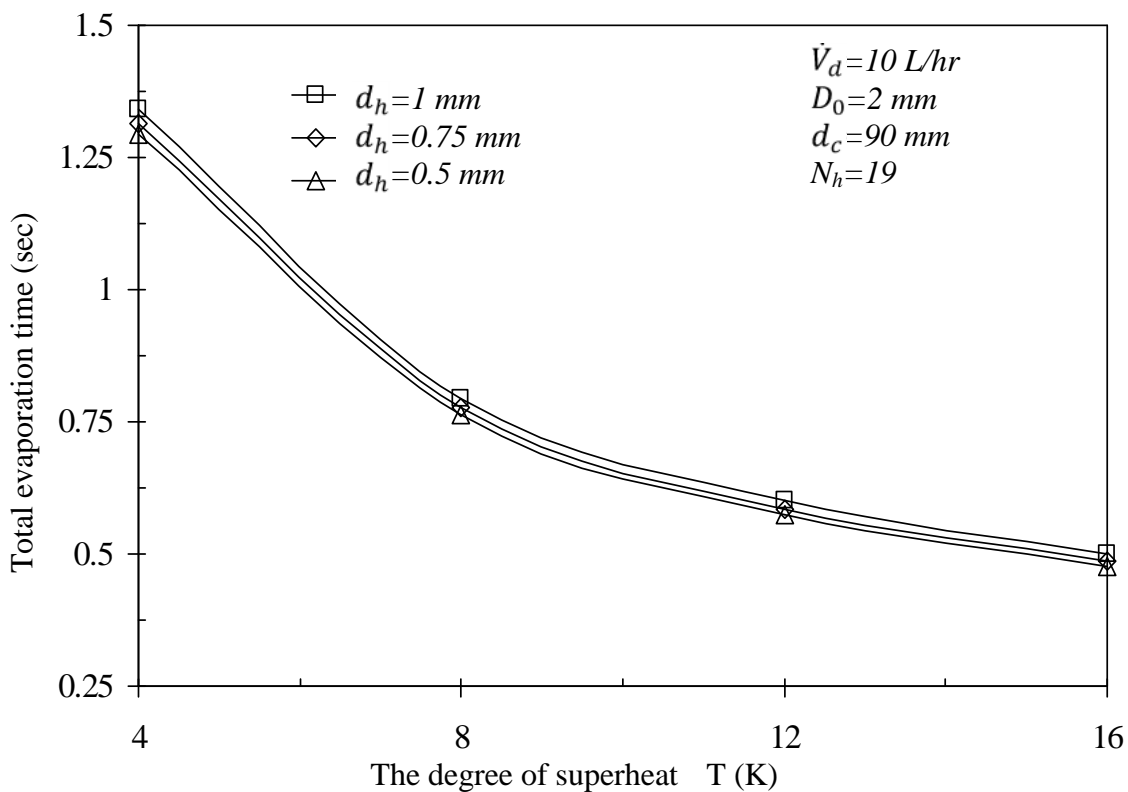
Figure 4.50 Effect of holes diameter on the total evaporation time versus the degree of superheat.
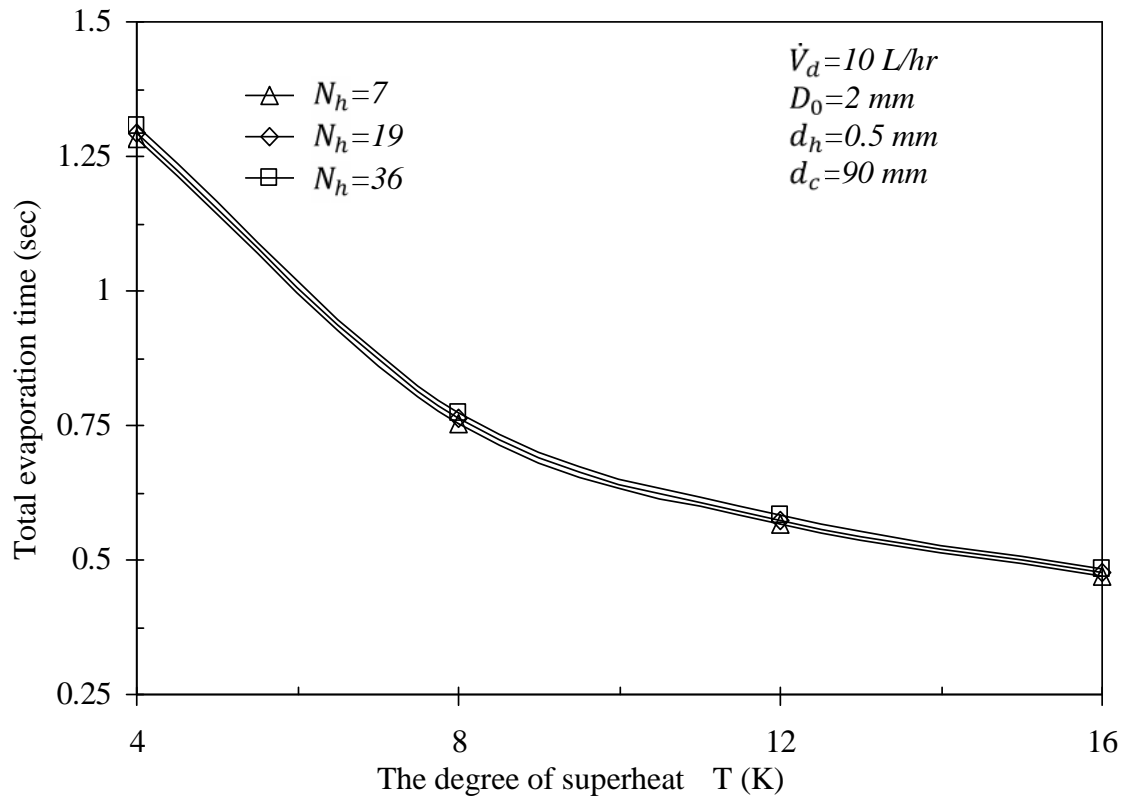
Figure 4.51 Effect of holes number on the total evaporation time versus the degree of superheat.
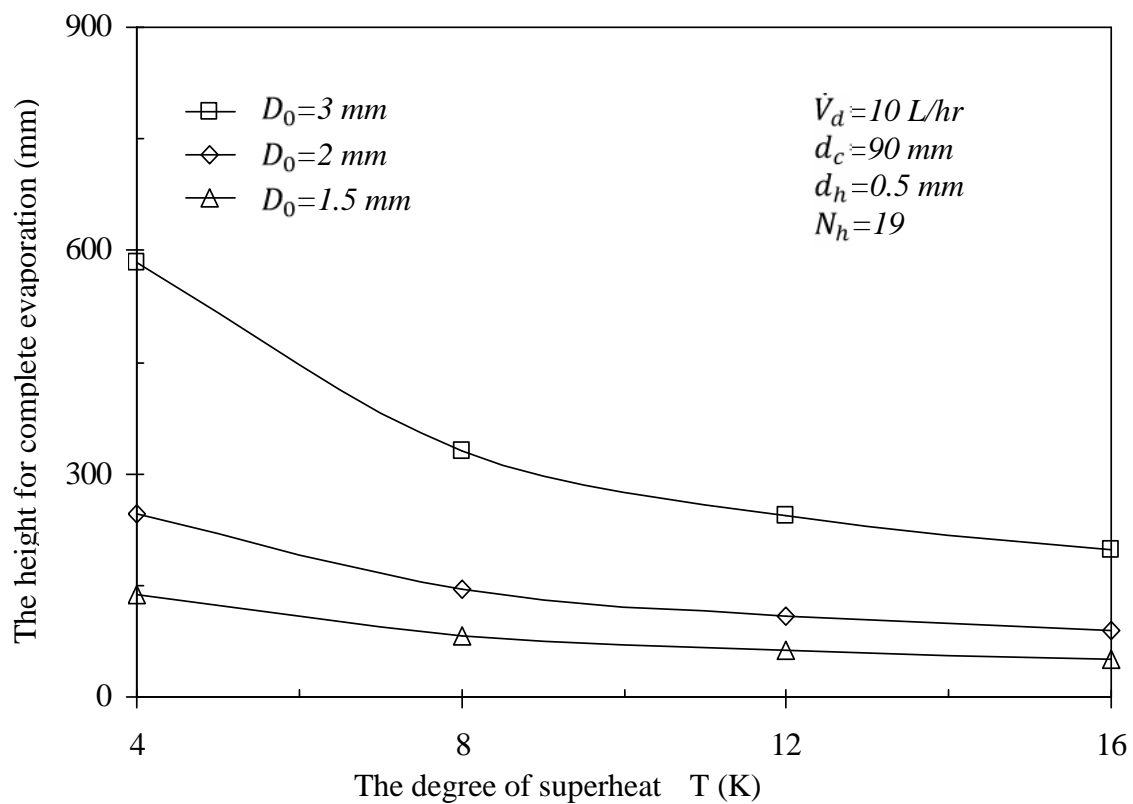
Figure 4.52 Effect of initial diameter on the height for complete evaporation versus the degree of superheat.
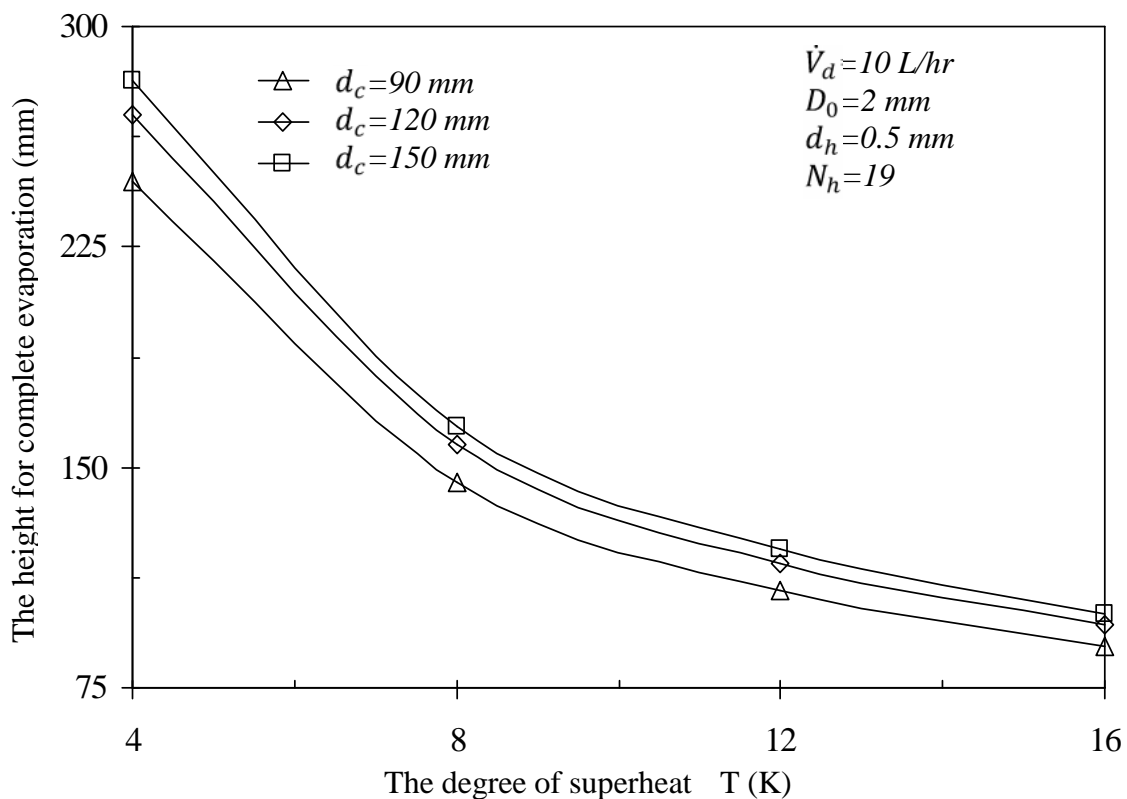
Figure 4.53 Effect of column diameter on the height for complete evaporation versus the degree of superheat.
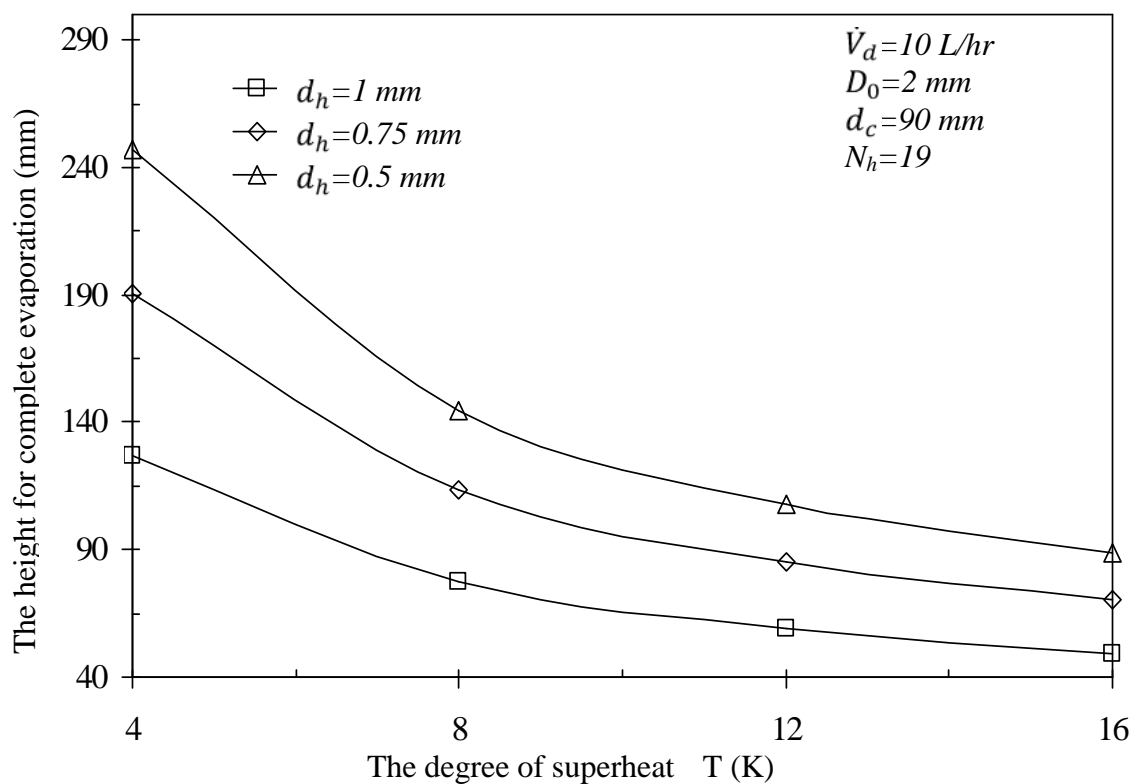
Figure 4.54 Effect of holes diameter on the height for complete evaporation versus the degree of superheat.
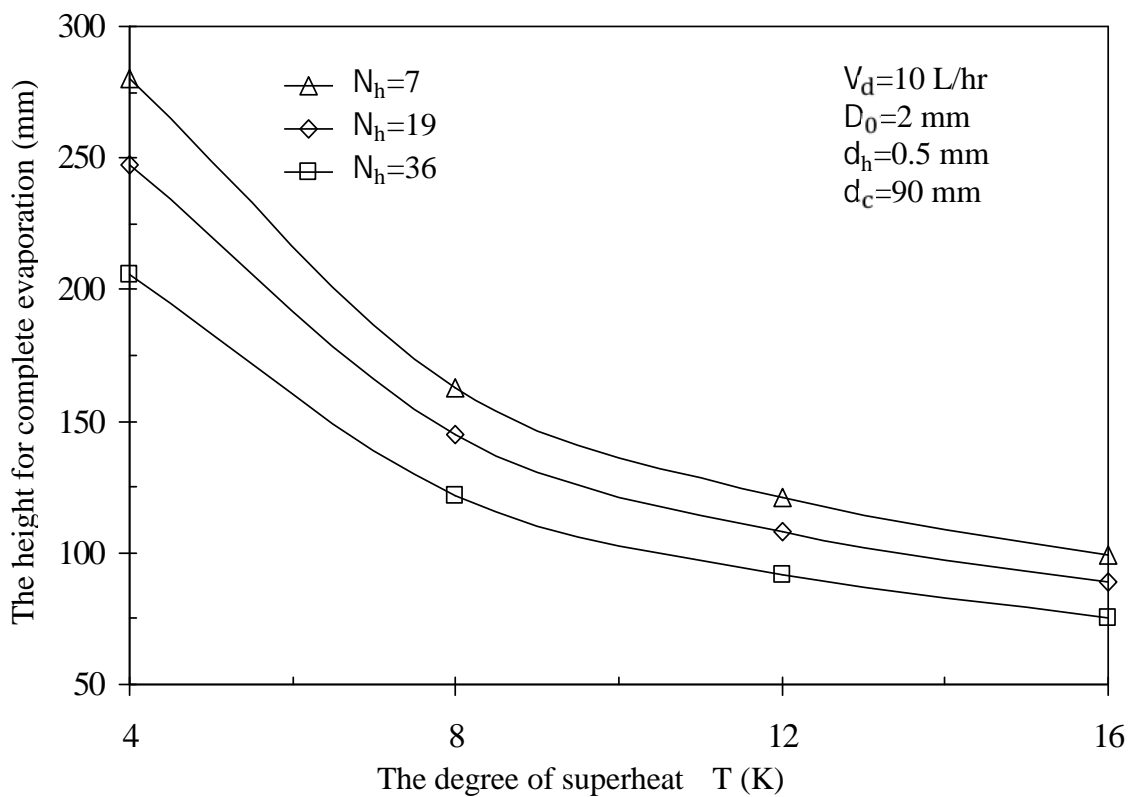
Figure 4.55 Effect of holes number on the height for complete evaporation versus the degree of superheat.
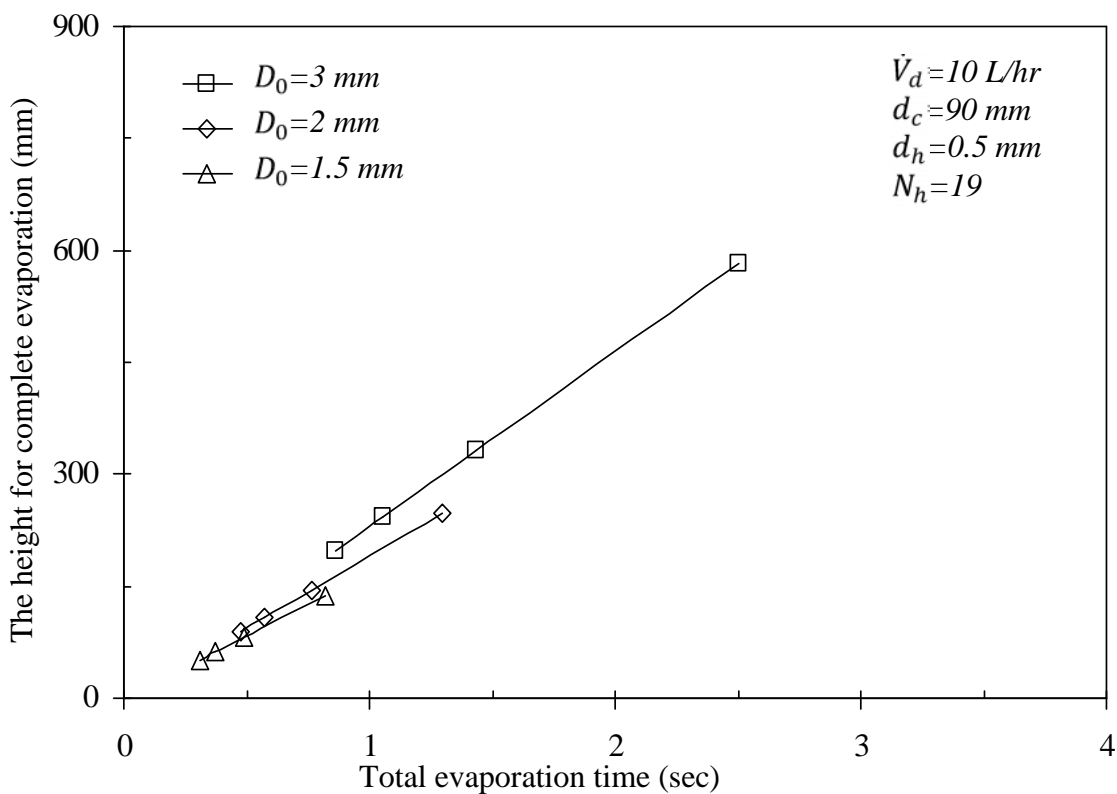
Figure 4.56 Effect of initial diameter on the height for complete evaporation versus total evaporation time.

124
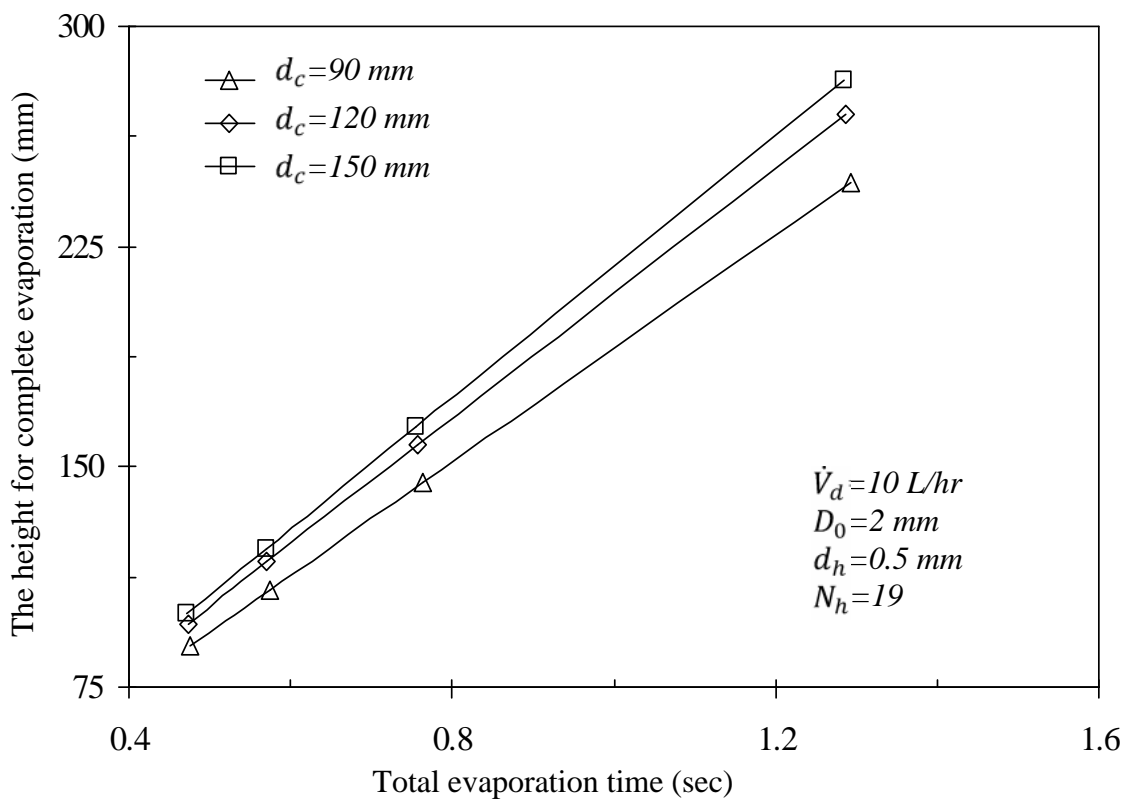
Figure 4.57 Effect of column diameter on the height for complete evaporation versus total evaporation time.
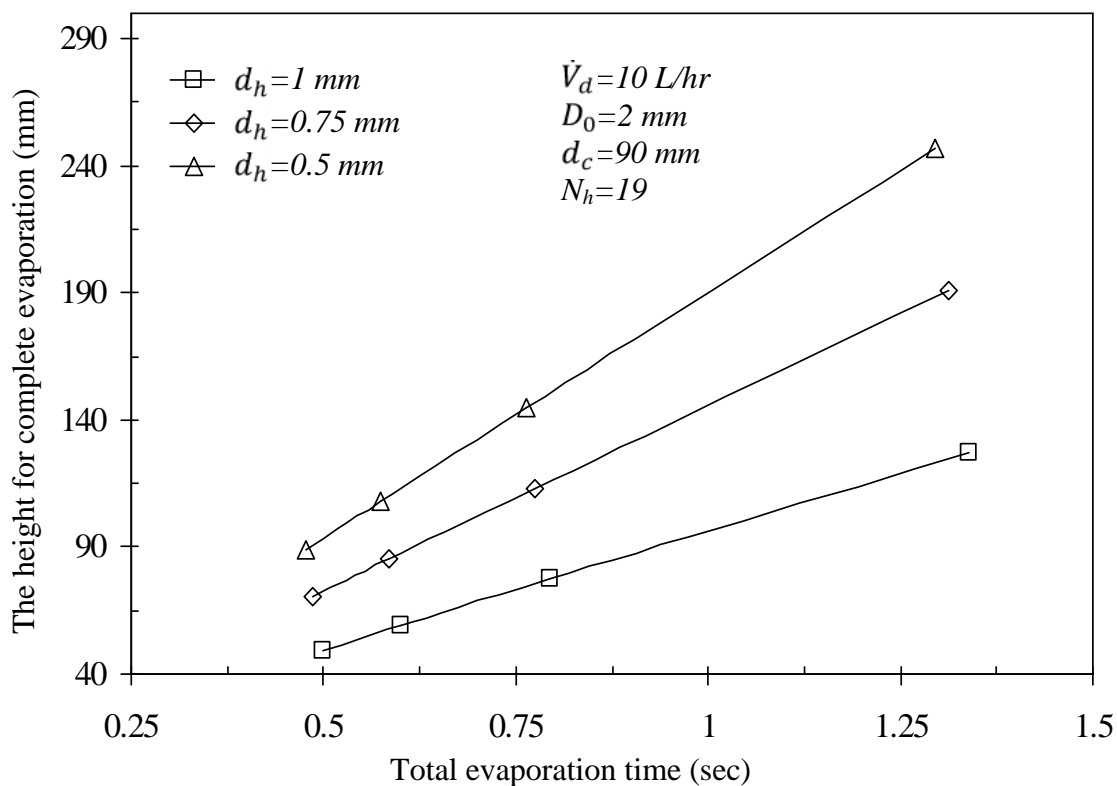
Figure 4.58 Effect of holes diameter on the height for complete evaporation versus total evaporation time.
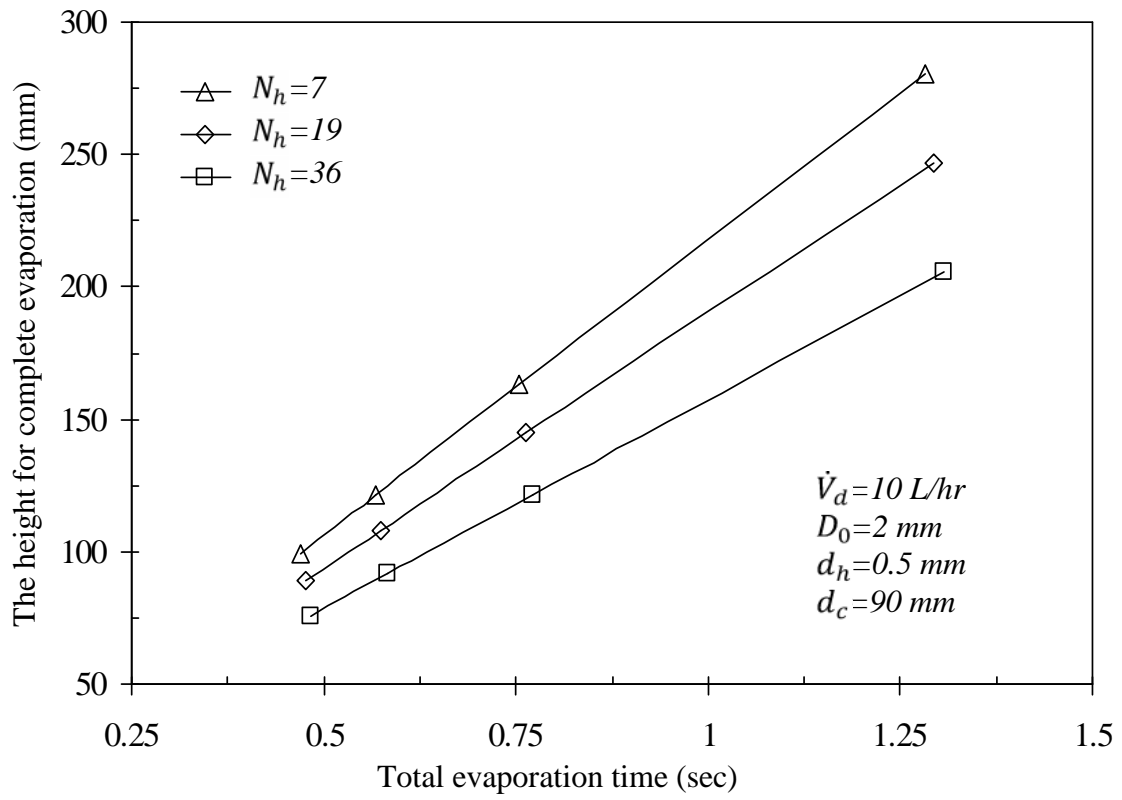
Figure 4.59 Effect of holes number on the height for complete evaporation versus total evaporation time.
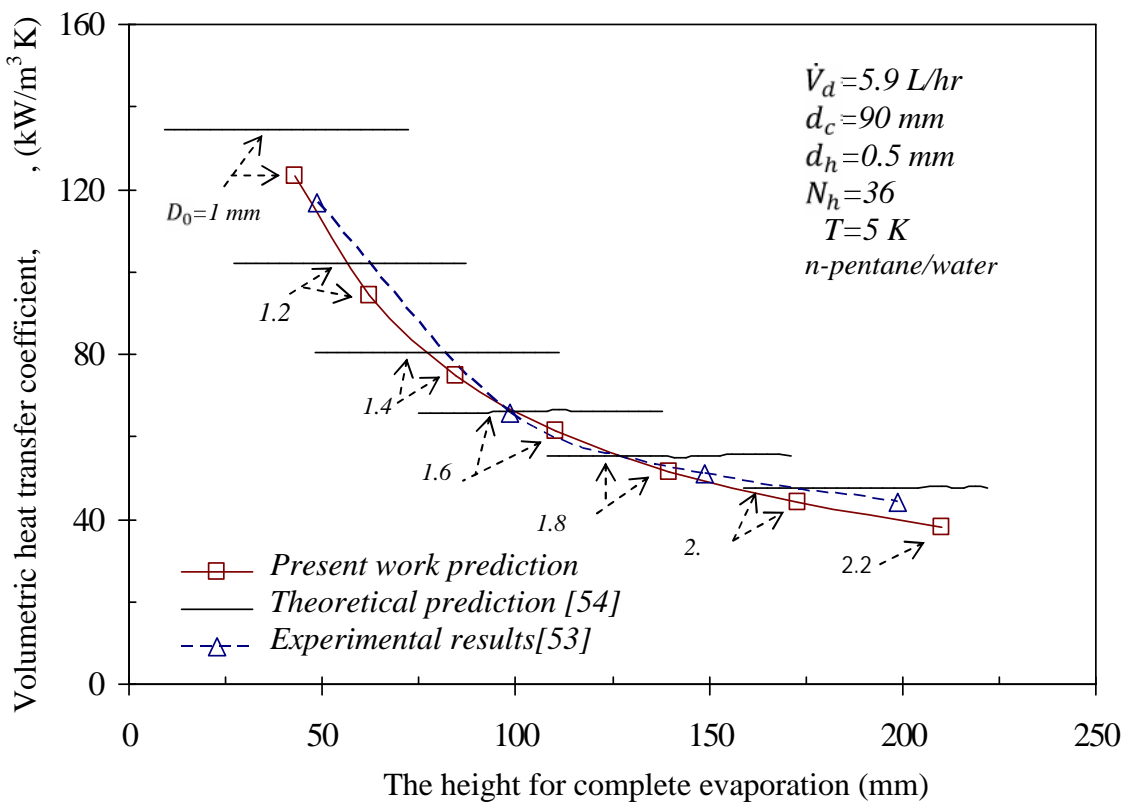
Figure 4.60: Comparison between the present predictions and other experimental and theoretical results.
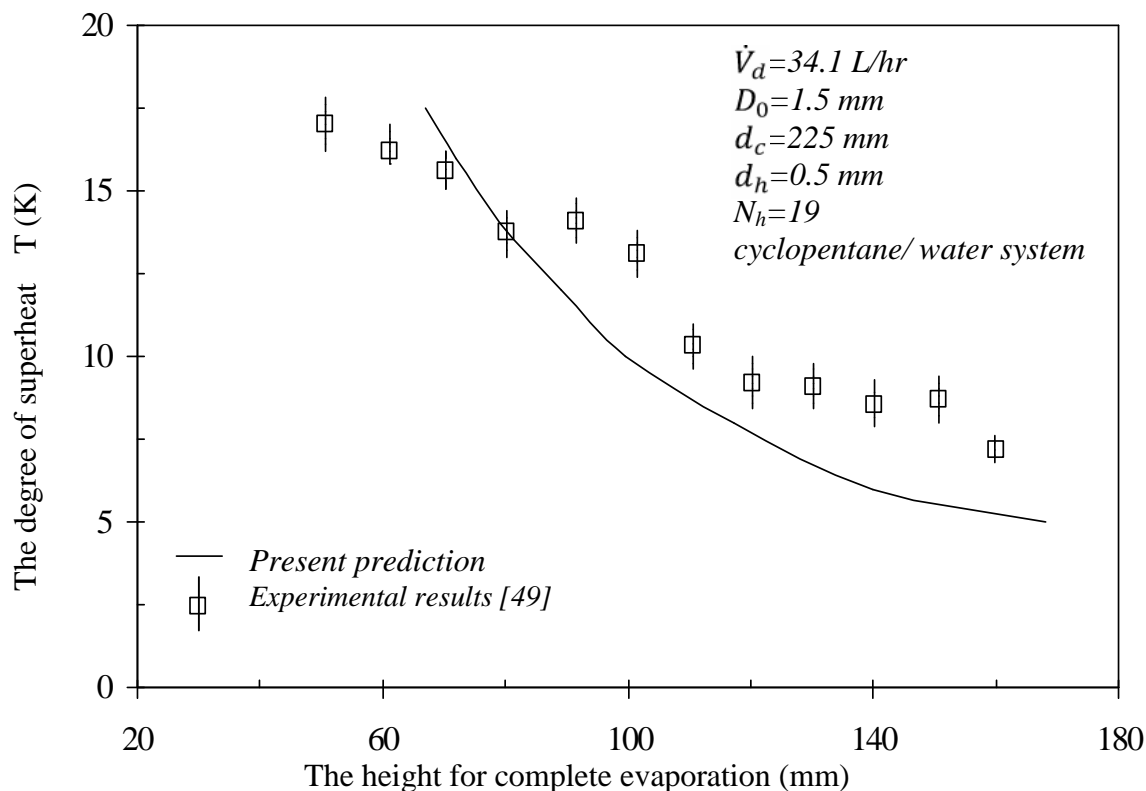
Figure 4.61: Comparison between the present predictions and other experimental results.

Chapter five

CONCLUSIONS

AND

RECOMMENDATIONS

Chapter five

Conclusions and Recommendations

5.1 Conclusions:

Direct contact evaporation of saturated droplets (n-pentane) in a column of an immiscible liquid (distilled water) is theoretically investigated. Based on the previous results and discussion the following conclusions are reached.

1. A theoretical model for direct contact evaporation of drop in an immiscible liquid using cellular model has been developed. The model gives information about the evaporation process of a single droplet bounded by a cell of continuous liquid.

2. A theoretical model for the evaporation of multidroplets based on the information of single droplets model has been developed.

3. In case where the interaction between drobbles is insignificant(single droplets case), the present analysis implies that the evaporation process is controlled by certain parameters, the major effects on the evaporation characteristics are attributed to the initial droplets diameter and the degree of superheat while the initial velocity of droplets have insignificant effect, the effects of these parameter are:

    (a) Increasing the initial droplets diameter leads to decrease the heat transfer coefficient, the time and height required for complete evaporation becomes longer.

    (b) Increasing the degree of superheat makes the evaporation process faster.

    (c) The influences of initial drop diameter and temperature difference on the heat transfer coefficient decrease with the progress of vaporization.

4. In case where there is an interaction between the adjacent drops (multidroplets case), the analysis indicated that the evaporation process is controlled by certain parameters, the effects of these parameter are:

128

(a) Increasing the degree of superheat leads to decrease the average volumetric heat transfer coefficient, decrease the time and height required for complete evaporation.

(b) Increasing the initial droplets diameter leads to decrease the average volumetric heat transfer coefficient, increase the time and height required for complete evaporation.

(c) Increasing the column diameter leads to decrease the average volumetric heat transfer coefficient, no considerable effect on the time required for complete evaporation, increase slightly, the height required for complete evaporation.

(d) Increasing the holes diameters and number leads to increase the average volumetric heat transfer coefficient, small effect on the time required for complete evaporation, decrease the height required for complete evaporation

(e) No considerable effect of the dispersed phase flow rates on the evaporation characteristics is noticed.

5. The comparison between the results of the present model with the available theoretical and experimental results gives a good agreement.

5.2 Recommendations:

The present work could be extended to include the following topics:

1. The present analysis can be extended to include another shape of drobble such as ellipsoid or other shapes of drobbles instead of spherical drobbles.

2. Developing a theoretical model when the flow around the drops obeys Stokes flow instead of potential flow.

3. Conducting experiments on direct-contact evaporation with photographing the volatile drop during its rise for the purpose of obtaining the drag coefficient of the drobbles which is needed for the calculation of the instantaneous velocity of drobble and consequently the heat transfer coefficient and other evaporation characteristics.

4. The fragmentation and coalescence phenomena can be taken into account.

5. The direct contact condensation of multidrops can be investigated.

REFERENCES

References

[1] **Bejan, A. and Kraus, A.D.**, "Heat Transfer Handbook", *John Wiley & Sons, Inc., Hoboken, New Jersey, 2003.*

[2] **Winkler, D. A.**, "A New Correlation for Direct Contact Heat Transfer Coefficients in Baffle and Perforated Plate Tower*", Ph.D. Thesis, University of Louisiana State, 1963.*

[3] **Frank K. & Boehm R. F.**, "Direct-Contact Heat Transfer", *Hemisphere Publishing, New York, 1988.*

[4] **Bruker, G. G.**, "Direct Contact Heat Transfer with Change of Phase at a High Pressure in a Steam- Water System*", Ph.D. Thesis, University of Minnesota, 1976.*

[5] **Sideman, S.**, "Direct Contact Heat Transfer between Immiscible Liquids", *Adv. Chem. Eng., Vol. 6, pp. 207-286, 1966.*

[6] **Sideman, S. and Maron, M.**, "Direct Contact Condensation", *Adv. in Heat Transfer, Vol. 15, pp. 227-281, 1982.*

[7] **Core, K. L., and Mulligan, J. C.**, "Heat Transfer and Population Characteristics of Dispersed Evaporating Droplets", *The American Institute of Chemical Engineers Journal, Vol. 36, pp. 1137-1144, 1990.*

[8] **Mori, Y. H.**, "Configuration of Gas-Liquid Two-Phase Bubbles in Immiscible Liquid Media", *Int., J. Multiphase Flow, Vol. 4, pp. 383-396, 1978.*

[9] **Mori, Y. H.**, "Classification of Configurations of Two-Phase Vapor/Liquid Bubbles in an Immiscible Liquid in Relation to Direct-Contact Evaporation and Condensation Processes", *Int. J. Multiphase Flow, Vol. 11, 571-577, 1985.*

References

[10] **Vuong, S. T., and Sadhal, S. S.**, "Growth and Translation of a Liquid – Vapor Compound Drop in a Second Liquid, Part 1,Fluid Mechanics", *J. Fluid Mechanic, Vol. 209, pp. 617-637, 1989.*

[11] **Michaelides, E. E.**, "Particles, Bubbles and Drops-Their Motion, Heat and Mass Transfer", *World Scientific Publishing Co. Pte. Ltd. ISBN 981-256-647-3, pp. 48-49, 2006.*

[12] **Simpson, H. C., Beggs, G. C. and Nazir, M.**, "Evaporation of Butane Drops in Brine", *Desalination, Vol. 15, pp. 11-23, 1974.*

[13] **Al-Jaberi, A. S.**, "Theoretical and Experimental Study of Direct-Contact Evaporation of a Volatile Drops (N-Pentane) in an Immiscible Liquid (Distilled water)", *Ph.D. Thesis, University of Basrah, Iraq, 2010.*

[14] **Vuong, S. T., and Sadhal, S. S.**, "Growth and Translation of a Liquid – Vapor Compound Drop in a Second Liquid. Part 2. Heat Transfer", *Journal of Fluid Mechanic, Vol. 209, pp. 639- 660, 1989.*

[15] **Sideman, S., and Taitel, Y.**," Direct-Contact Heat Transfer with Change of Phase: Evaporation of Drops in an Immiscible Liquid Medium", *International Journal of Heat Mass Transfer, Vol. 7, pp. 1273- 1289, 1964.*

[16] **Tochitani, Y., Mori, Y. H. and Komotori, K.**, "Vaporization of Single Liquid Drops in an Immiscible Liquid: Part I: Forms and Motions of Vaporizing drops"*, Wräme-und Stoffübertrag, Vol. 10, pp. 51-59, 1976.*

[17] **Ayyaswamy, P.S.**, "Direct-Contact Transfer Processes with Moving Liquid Droplets", *Adv. Heat Transfer, Vol. 26, pp. 1-104, 1995.*

[18] **Song, M., Steiff, A., & Weinspach, P. M.**, "Direct-Contact Heat Transfer with Change of Phase: A Population Balance Model", *Chemical Engineering Science, Vol. 54, pp. 3861-3871, 1999.*

References

[19] **Matsubara, M., Murase, H., Mori,Y. H., and Nagashima, A.**," Measurement of the Surface Tensions and the Interfacial Tensions of n-Pentane-Water and Rll3-Water Systems", *International Journal of Thermo physics, Vol. 9, No. 3, pp. 409-424,1988.*

[20] **Isenberg, J., and Sideman, S.**, "Direct Contact Heat Transfer with Change of Phase: Bubble Condensation in Immiscible Liquids", *Int. J. Heat Mass Transfer, Vol. 13, pp. 997-1011, 1970.*

[21] **Selecki, A., and Gradon, L.**, "Equation of Motion of an Evaporating Vapor Drop in an Immiscible Liquid Medium", *Int. J. Heat Mass Transfer, Vol. 19, pp. 925, 1976.*

[22] **Tochitani, Y., Nakagawa, T., Mori, Y. H., & Komotori, K.**," Vaporization of Single Liquid Drops in an Immiscible Liquid Part II: Heat Transfer Characteristics", *Wärme-Und Stofftübertragung, Vol. 10, pp. 71-79, 1977.*

[23] **Raina, G. K., Wanchoo, R. K. and Grover, P. D.**, "Direct Contact Heat Transfer with Change of Phase: Motion of Evaporating Droplets", *A.I.Ch.E. J., Vol. 30, pp. 835, 1984.*

[24] **Kendoush, A. A.**, "Theory of Convective Drop Evaporation in Direct Contact with an Immiscible Liquid", *J. Desalination, Vol. 169, pp. 33–4, 2004.*

[25] **Mahood, H. B.**,"Direct-Contact Heat Transfer of Single Volatile Liquid Drop Evaporation in an Immiscible Liquid", *J. Desalination, Vol. 222, pp. 656-665, 2008.*

[26] **Sideman, S., and Isenberg, J.**, "Direct-Contact Heat Transfer with Change of Phase: Bubble Growth in Three Phase Systems", *Desalination, Vol. 2, 207-214, 1967.*

133

References

[27] **Selecki, A. and Gradon, L.**, "Equation of Motion of an Expanding Vapour Drop in an Immiscible Liquid Medium", *Int. J. Heat Mass Transfer, Vol. 19, pp. 925-929, 1976.*

[28] **Mokhtarzadeh, M. R. & El-Shirbini, A. A.**, "A Theoretical Analysis of Evaporating Droplets in an Immiscible Liquid", *Int. J. Heat Mass Transfer, Vol. 22, pp. 27-38,1979.*

[29] **Haberman, W. L. & Morton, R. K.**, "An Experimental Study of Bubbles Moving in Liquids", *Trans. Am. Soc. Civ. Engrs, Vol. 121, pp. 227-252, 1956.*

[30] **Raina, G. K. and Grover, P. D.**, "Direct Contact Heat Transfer with Change of Phase: Theoretical Model", *The American Institute of Chemical Engineers Journal(A.I.Ch.E.),Vol. 28, pp. 515-517, 1982.*

[31] **Raina, G. K., Wanchoo, R. K. and Grover, P. D.**, "Direct Contact Heat Transfer with Phase Change: Motion Droplets of Evaporating", *The American Institute of Chemical Engineers Journal(A.I.Ch.E.),Vol. 30, pp. 835-837, 1984.*

[32] **Battya, P., Raghavan, V. R. & Seetharamu, K. N.**, "Parametric Studies on Direct Contact Evaporation of a Drop in an Immiscible Liquid", *Int. J. Heat Mass Transfer, Vol. 27, pp. 263-272,1984.*

[33] **Battya, P., Ragharan, V. R., & Seetharamu, K. N.**, "A Theoretical Correlation for the Nusselt Number In Direct Evaporation Of A Moving Drop In An Immiscible Liquid", *Wärme-Und Stoff bertragung, Vol. 19, pp. 61-66,1985.*

[34] **Raina, G. K , and Grover, P. D.**, "Direct Contact Heat Transfer with Change of Phase: Theoretical Model Incorporating Sloshing Effects", *The American Institute of Chemical Engineers Journal, Vol. 31, pp. 507-510,1985.*

References

[35] **Mokhtarzadeh, M. R. and EI-Shirbini, A. A.**, "Dynamics and Heat Transfer to a Butane Bubble-Droplets in Immiscible Liquids", *Wärme-Und Stoff bertragun, Vol. 20, pp. 69-75, 1986.*

[36] **Tadrist, L., Diso, I. S., Santini, R. & Pantaloni, J.**, "Vaporization of a Liquid by Direct Contact in Evaporation in another Immiscible Liquid Part I: Vaporization of a Single Droplet Part II:Vaporization of Rising Multidroplets", *Int. J. Heat Mass Transfer, Vol. 30, pp.* 1773-1785,1987.

[37] **Shimizu, Y., & Mori, Y. H.**, "Evaporation of Single Drops in an Immiscible Liquid at Elevated Pressure: Equipment and Preliminary Results", *Experimental in fluids, Vol. 6, pp. 73-79, 1988.*

[38] **Shimizu, Y., & Mori, Y. H.**, "Evaporation of Single Drops in an Immiscible Liquid at Elevated Pressure: Experimental Study with N-Pentane and R 113 Drops in Water", *Int. J. Heat Mass Transfer, Vol. 31, pp. 1843-1851, 1988.*

[39] **Shimizu, Y., and Mori, Y. H.**, "Direct Contact Heat Transfer to Bubble with Simultaneous Translation and Growth", *Numerical Heat Transfer, Part A, Vol. 15, pp. 509-524, 1989.*

[40] **Shimaoka, H., and Mori, Y. H.**, "Evaporation of Single Liquid Drops in an Immiscible Liquid: Experiments With N-Pentane Drops in Water and Preparation of New Heat Transfer Correlation", *Exp. Heat Transfer, Vol. 3, pp. 159-172, 1990.*

[41] **Wanchoo, R. K., Raina, G. K. & Savyasachi, T. V.**, "Evaporation of a Two-Phase Drop in an Immiscible Liquid: A Parametric Study", *Heat Recovery Systems & CHP, Vol. 12, pp. 105-111, 1992.*

[42] **Celata, G., Cumo, M., D.,Annibale, F., Gugliermetti, F., and Ingui, G.**, "Direct Contact Evaporation of Nearly Saturated R 114 in Water", *Int. J. Heat Mass Transfer, Vol. 38 ,pp. 1495– 1504, 1995.*

[43] **Song, M. A., and Weinspach, P. M.**, "Nusselt Number of Direct-Contact Evaporation of a Moving Ellipsoidal Drop in an Immiscible Liquid", *Chemical Engineering Communications, Vol. 145, pp. 73-87, 1996.*

[44] **Dammel, F., and Beer, H.**, "Heat Transfer from a Continuous Liquid to an Evaporating Drop: a Numerical Analysis", *Int. J. Thermal Sciences, Vol. 42, pp. 677- 686. 2003.*

[45] **Sideman, S., Hirsch, G., and Gat, Y.**, "Direct Contact Heat Transfer with Change of Phase: Effect of the Initial Drop Size in Three-Phase Heat Exchangers", *A.I.Ch.E. J., Vol. 11, pp. 1081-1087, 1965.*

[46] **Sideman, S., and Gat, Y.**, "Direct-Contact Heat Transfer with Change of Phase: Spray-Column Studies of a Three-Phase Heat Exchanger", *A.I.Ch.E. J., Vol. 12, pp. 296-303, 1966.*

[47] **Suratt, W. B., and Hart, G. K.**, "Testing of direct heat exchangers for geothermal brines", *AIChE-ASME Heat Transfer Conference, Salt Lake City, Utah, 1977.*

[48] **Plass, S. B., Jacobs, H. R., Boehm, R. F.**, "Operation Characteristics of a Spray Column Type Direct-Contact Preheater", *AIChE Symp., Ser. 189, pp. 227–23, 1979.*

[49] **Smith, R. C., Rohsenow, W. M., & Kazimi, M. S.**, "Volumetric Heat Transfer Coefficient for Direct Contact Evaporation", *Transactions of ASME, J. Heat Transfer, Vol. 104, pp. 264-270,1982.*

References

[50] **Wallis, G. B.**, "One-Dimensional Two-Phase Flow", *McGraw-Hill, New York, 1969.*

[51] **Battya, P., Raghavan, V. R., and Seetharamu, K. N.**, "A Theoretical Analysis of Direct Contact Evaporation in Spray Columns", *Int. Comm. Heat Mass Transfer, Vol. 10, pp. 533-543, 1983.*

[52] **Hetsroni, G.**, "Handbook of Multiphase Systems", *McGraw-Hill, New York, 1982.*

[53] **Seetharamu, K. N., & Battya, P.**, "Direct-Contact Evaporation between Two Immiscible Liquids in a Spray Column", *Transactions of the ASME, J. Heat Transfer, Vol. 111, pp. 780-785, 1989.*

[54] **Mori, Y. H.**, "An Analytic Model of Direct-Contact Heat Transfer in Spray-Column Evaporators", *the American Institute of Chemical Engineers Journal, Vol. 37, pp .539-546, 1991.*

[55] **Ay, H., Johnson, R. R., and Yang, W-J.**, "Direct-Contact Heat Transfer between A Rising Dispersed Phase in A Counterflow Stream", *Numerical Heat Transfer, Part A, Vol. 26, pp. 667-682, 1994.*

[56] **Song, M., and Steiff, A.**, "Simulation of Vaporization Height by Considering the Size Distribution of Drobbles in Drobble Columns", *Chemical Engineering Processing, Vol. 34, pp. 87-95.1995.*

[57] **Marrucci, G.**, "Rising Velocity of a Swarm of Spherical Bubbles", *Industrial and Engineering Chemistry (Fundamentals), Vol. 4, pp. 224-225, 1965.*

[58] **Song, M., Steiff, A., & Weinspach, P.-M.**, "The Analytical Solution for a Mode of Direct Contact Evaporation in Spray Columns", *Int. comm., Heat Mass Transfer, Vol. 23, pp. 263-272, 1996.*

References

[59] **Song, M., Steiff, A., & Weinspach, P.M.**, "Parametric Analysis of Direct Contact Evaporation Process in A Bubble Column", *Int. J. Heat Mass Transfer, Vol. 41, pp. 1749-1758, 1998.*

[60] **Peng, Z., Yiping, W., Cuili, G., & Kun, W.**, "Heat Transfer in Gas–Liquid–Liquid Three-Phase Direct-Contact Exchanger", *Chemical Engineering Journal, Vol. 84, pp. 381–388, 2001.*

[61] **Zung, J. T.**, "Evaporation Rate and Lifetime of Clouds and Sprays in Air-The Cellular Model", *Journal of chemical physics, Vol. 46, pp. 2064-2070, 1967.*

[62] **Kendoush , A. A.**, "Hydrodynamic Model for Bubbles in a Swarm", *Chemical Engineering Science, Vol. 56, pp. 235- 238, 2001.*

[63] **Ehara, N., Nojima, K., & Mori, Y. H.**, "Bubble Swarms in Power-Law Liquids at Moderate Reynolds Numbers: Drag and Mass Transfer", *Chemical Engineering Research and design, Vol. 86, Vol. 14, pp. 39–53, 2008.*

[64] **Ehara, N., Nojima, K., & Mori, Y. H.**, "Visualization Study of Evaporation of Single N-Pentane Drops in Water", *Experiments in Fluids, Vol. 14, pp. 97-103, 1993.*

[65] **Hanchi, S., Oualli, H., & Askovic, R.**, "On the Heat Transfer to an Accelerated Translating Droplet", *Theoret. Appl. Mech., Vol. 31, No .2, Belgrade, pp. 85-99, 2004.*

[66] **Cliff, R., Grace, J. R. & Weker, M. E.**, "Bubbles, Drops and Particles**",** *Academic Press, New York, pp. 7 & 325, 1978.*

[67] **Kendoush, A. A.**, "The Drag Force on A Growing Bubble", *The 11th International Topical Meeting on Nuclear Reactor Thermal-Hydraulics*

(NURETH-11),Popes' Palace Conference Center, Avignon, France, October 2-6, 2005.

[68] **Wanchoo, R. K.**, "Forced Convection Heat Transfer around Large Two-Phase Bubbles Condensing In An Immiscible Liquid", *Heat Recovery Systems & CHP, Vol. 13, No. 5, pp. 441-449, 1993.*

[69] **Kreyszig, E.**, "Advanced Engineering Mathematics", 8th edition, *John Wiley & Sons, ISBN 0-471-33328-X (paperback)*, *1999.*

[70] **Hildebrand, F. B.**, "Introduction to Numerical Analysis", 2nd edition, *Dover Publications, Inc. ,New York, pp.567 , 1987.*

[71] **Patankar, S. V.**, "Numerical Heat Transfer and Fluid Flow", *Taylor & Francis, ISBN 978-0891165224, 1980.*

[72] **Hirsch, C.**, "Numerical Computation of Internal and External Flows", *John Wiley & Sons, ISBN 978-0471924524, 1990.*

[73] **Alvarado, F. L. and Klein, S. A.**, "Engineering Equation Solver", *F-Chart Software Professional Edition, V 7.124-3D, 2004.*

APPENDICIES

APPENDIX-A

Upwind Scheme

To illustrate the method, consider the following one-dimensional linear wave equation

$$\frac{\partial u}{\partial t} + a\frac{\partial u}{\partial x} = 0$$

It describes a wave propagating in the *x*-direction with a velocity *a*. The preceding equation is also a mathematical model for one-dimensional linear advection. Consider a typical grid point *i* in the domain. In a one-dimensional domain, there are only two directions associated with point *i* - left and right. If *a* is positive the left side is called *upwind* side and right side is the *downwind* side. Similarly, if *a* is negative the left side is called *downwind* side and right side is the *upwind* side. If the finite difference scheme for the spatial derivative $\partial u/\partial x$ contains more points in the upwind side, the scheme is called an *upwind-biased* or simply an *upwind scheme.*

First-Order Upwind Scheme

The simplest upwind scheme possible is the first-order upwind scheme. It is given by[70]

$$(1) \qquad \frac{u_i^{n+1} - u_i^n}{\Delta t} + a\frac{u_i^n - u_{i-1}^n}{\Delta x} = 0 \quad \text{for} \quad a > 0$$

$$(2) \qquad \frac{u_i^{n+1} - u_i^n}{\Delta t} + a\frac{u_{i+1}^n - u_i^n}{\Delta x} = 0 \quad \text{for} \quad a < 0$$

Defining

$$a^+ = \max(a, 0), \qquad a^- = \min(a, 0)$$

and

$$u_x^- = \frac{u_i^n - u_{i-1}^n}{\Delta x}, \qquad u_x^+ = \frac{u_{i+1}^n - u_i^n}{\Delta x}$$

The two conditional equations (1) and (2) can be combined and written in a compact form as

$$(3) \qquad u_i^{n+1} = u_i^n - \Delta t \left[a^+ u_x^- + a^- u_x^+ \right]$$

Equation (3) is a general way of writing any upwind-type schemes. The upwind scheme is *stable* if the following *Courant–Friedrichs–Lewy condition* (CFL) condition is satisfied[71].

$$c = \left| \frac{a \Delta t}{\Delta x} \right| \leq 1.$$

A Taylor series analysis of the upwind scheme discussed above will show that it is first-order accurate in space and time. The first-order upwind scheme introduces severe numerical diffusion in the solution where large gradients exist.

APPENDIX-B

Computer program for steady state direct contact evaporation of liquid drop

in an immiscible liquid

Program symbols

Symbol	definition
nmu	number of nodes in μ direction
ny	number of nodes in y direction
y_0	initial y =0
Pe0	initial Peclet number
x	The radius ratio of cell radius to actual radius, (R_{cell}/R)
y_t	Final y,$((R_{cell} -R)/R)$
ph(i,j)	Dimensionless temperature, (i,j)
holdup	$((R /R_{cell})**3)$
k_j	parameter,((beta/pi)*(nmu-1.)+1.)
E	parameter, ((1-holdup)/(1-holdup**(5/3.)))
a11	Parameter, (0.5*pe0*E*(1.-1./(1+y)**3)*mu -2./(1+y))
a22	Parameter , (0.5*pe0*E*(1.+0.5/(1+y)**3)*(1.-mu**2) /(1+y)+2.*mu/(1+y)**2)
a33	Parameter , (-(1.-mu**2)/(1.+y)**2)
a11p	Parameter, (max(a11,0.))
a11n	Parameter, (min(a11,0.))
a22p	Parameter, (max(a22,0.))
a22n	Parameter, (min(a22,0.))
d1	Parameter,(a11p/dy -a11n/dy +a22p/dmu -a22n/dmu +2/dy**2-2*a33/dmu**2.)
d2	Parameter,(-a11p/dy -1./dy**2)
d3	Parameter,(a11n/dy -1./dy**2.)
d4	Parameter,(-a22p/dmu +a33/dmu**2.)
d5	Parameter,(a22n/dmu+a33/dmu**2.)
dph/dy(1,j)	Gradient of temperature

Flow chart

Start

Read data dy, dmu, Pe_0, x, $beta_0$, beta

Calculate y_0, y_t, holdup, ny, nmu

Assume initial ph (i,j)=0.0

Calculate kj and apply boundary conditions, equation (3.56)

Calculate ph (i,j) using iteration method
$Ph(i,j)=-1/d_1*(d_2*ph(i-1,j)+d_3*ph(i+1,j)+d_4*ph(i,j-1)+d_5*ph(i,j+1))$

Calculate dph/dy(1,j),using equation(3.67)

Calculate Nu,using equation(3.54)

Beta=beta+ beta

Is
Beta 180^0

Yes

No

Stop

143

APPENDIX-C

Computer program for direct contact evaporation of single liquid drop in an immiscible liquid

Program symbols

Symbol	definition
nmu	number of nodes in μ direction
ny	number of nodes in y direction
y_0	initial y =0
Pe0	initial Peclet number
y_t	Final y,((R_{cell} -R)/R)
ph(i,j)	Dimensionless temperature, (i,j)
holdup	((R /R_{cell})**3)
k_j	parameter,((beta/pi)*(nmu-1.)+1.)
E	parameter, ((1-holdup)/(1-holdup**(5/3.)))
a11	Parameter, (0.5*pe0*E*(1.-1./(1+y)**3)*mu -2./(1+y))
a22	Parameter , (0.5*pe0*E*(1.+0.5/(1+y)**3)*(1.-mu**2) /(1+y)+2.*mu/(1+y)**2)
a33	Parameter , (-(1.-mu**2)/(1.+y)**2)
a11p	Parameter, (max(a11,0.))
a11n	Parameter, (min(a11,0.))
a22p	Parameter, (max(a22,0.))
a22n	Parameter, (min(a22,0.))
d1	Parameter,(a11p/dy -a11n/dy +a22p/dmu -a22n/dmu +2/dy**2-2*a33/dmu**2.)
d2	Parameter,(-a11p/dy -1./dy**2)
d3	Parameter,(a11n/dy -1./dy**2.)
d4	Parameter,(-a22p/dmu +a33/dmu**2.)
d5	Parameter,(a22n/dmu+a33/dmu**2.)
pes	parameter, (pe0*U$^+$(im)*E)
dBtao	gradient of dimensionless radius, dB/dtao
a1	Parameter, B(im)**2.
a2	Parameter, (0.5*pes*(1.-1./(1.+y)**3)*mu +1./(1+y)**2.*dBtao)*B(im)

144

a3	Parameter, 0.5*pes*(1.+0.5/(1.+y)**3) *(1.-mu**2)/(1.+y)*B(im)
a4	Parameter, -2./(1.+y)
a5	Constant, -1.
a6	Parameter, -(1.-mu**2)/(1.+y)**2
a7	Parameter, 2.*mu/(1.+y)**2
a8	a2+a4
a8p	max(a8,0.)
a8n	min(a8,0.)
a9p	max(a9,0.)
a9n	min(a9,0.)
ak	Parameter, a8p/dy -a8n/dy +a9p/dmu-a9n/dmu-2*a5/dy**2 -2*a6/dmu**2
dtao	dimensionless time step, c1*a1/ak
dphyp	(ph(i+1,j)-ph(i,j))/dy
dphyn	(ph(i,j)-ph(i-1,j))/dy
dphmup	(ph(i,j+1)-ph(i,j))/dmu
dphmun	(ph(i,j)-ph(i,j-1))/dmu
dphdy2	(ph(i+1,j)+ph(i-1,j)-2*ph(i,j))/dy**2.
dphdmu2	(ph(i,j+1)+ph(i,j-1)-2*ph(i,j))/dmu**2.
zeta	vaporization ratio
dph/dy(1,j)	Gradient of temperature at drobble surface
B	dimensionless radius, R /R_0
B_f	R_f /R_0

Flow chart

Start

Read data dy, dmu, C1,   T, $beta_0$, d_0, U_0

Read data (properties of dispersed and continuous phase)

Calculate DRD, DRC, St, Ja, Pe_0, Fr_0

Calculate R_f and B_f using equation (3.57)

Calculate $R_{cell} = 3*R_f$

im=1

Calculate
$y_{cell} = (R_{cell} - R(im))/R(im)$

Calculate ny = $y_{cell}/dy + 1$

Calculate
holdup=$(R(im)/R_{cell})**3$

Calculate E, Pes

assume ph(i,j)=0
(initial value)

Calculate ph (i,j) for steady state using iteration method
$Ph(i,j) = -1/d_1*(d_2*ph(i-1,j) + d_3*ph(i+1,j) + d_4*ph(i,j-1) + d_5*ph(i,j+1))$

Calculate kj and apply boundary conditions, equation (3.56)

Calculate dtao= C1*a1/ak

2

1

146

②   ①

Calculate new ph (i,j) using explicit method,
phn(i,j)=ph(i,j)-dtao/a1*((a8p*dphyn+a8n*dphyp)+(a9p*dphmun +
a9n*dphmup)+ a5*dphdy2+a6*dphdmu2)

Calculate dph/dy(1,j),using equation(3.67)

Calculate Nu,using equation(3.54)

Calculate new velocity $U^+(im+1)$, using Runge-Kutta method(3.59)

Calculate new radius B(im+1), using Runge-Kutta method(3.68)

Calculate new zeta, using equation (3.60)

Calculate new beta, using equation (3.61)

Is
B B_f

No

Yes

Calculate h(im), Roa(im)

Calculate y_{cell}, ny

im=im+1

Calculate final time, t_f

③

```
        ( 3 )
          |
          v
+-------------------------------------+
| Calculate dU_r/dt, using three point formula |
+-------------------------------------+
          |
          v
+-------------------------------------+
|   Calculate Z, using equation (3.87)   |
+-------------------------------------+
          |
          v
       ( Stop )
```

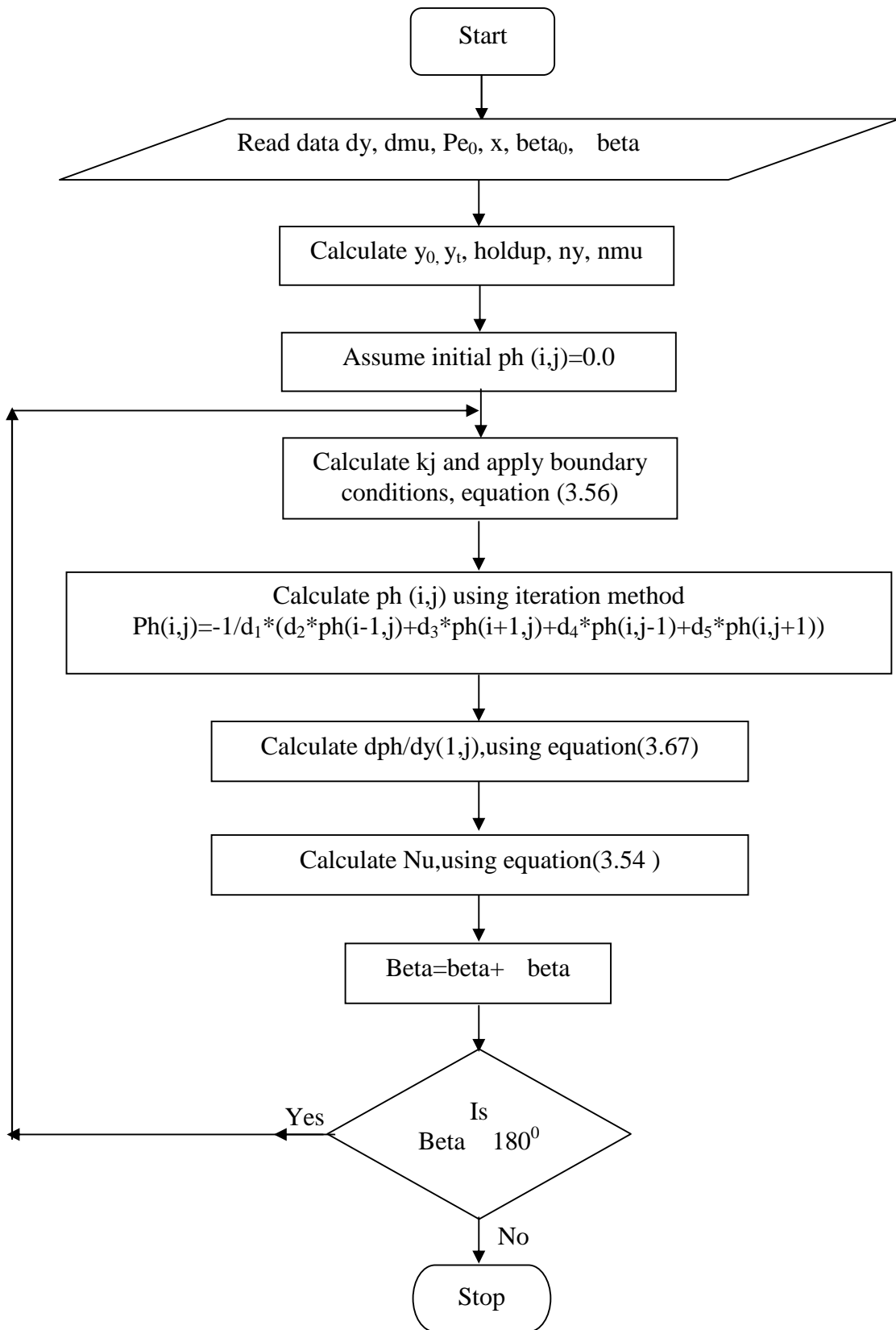Calculate dU_r/dt, using three point formula

Calculate Z, using equation (3.87)

Stop

APPENDIX-D

Computer program for direct contact evaporation of multidrops in an immiscible liquid

Program symbols

Symbol	definition
nmu	Number of nodes in µ direction
ny	Number of nodes in y direction
d_h	Hole diameter
d_c	Column diameter
N_h	Hole number
Q_d	Dispersed phase volume flow rate
y_0	Initial y =0
Pe0	Initial Peclet number
y_t	Final y,((R_{cell} -R)/R)
ph(i,j)	Dimensionless temperature, (i,j)
holdup	((R /R_{cell})**3)
k_j	Parameter,((beta/pi)*(nmu-1.)+1.)
E	Parameter, ((1-holdup)/(1-holdup**(5/3.)))
a11	Parameter, (0.5*pe0*E*(1.-1./(1+y)**3)*mu -2./(1+y))
a22	Parameter , (0.5*pe0*E*(1.+0.5/(1+y)**3)*(1.-mu**2) /(1+y)+2.*mu/(1+y)**2)
a33	Parameter , (-(1.-mu**2)/(1.+y)**2)
a11p	Parameter, (max(a11,0.))
a11n	Parameter, (min(a11,0.))
a22p	Parameter, (max(a22,0.))
a22n	Parameter, (min(a22,0.))
d1	Parameter,(a11p/dy -a11n/dy +a22p/dmu -a22n/dmu +2/dy**2-2*a33/dmu**2.)
d2	Parameter,(-a11p/dy -1./dy**2)
d3	Parameter,(a11n/dy -1./dy**2.)
d4	Parameter,(-a22p/dmu +a33/dmu**2.)
d5	Parameter,(a22n/dmu+a33/dmu**2.)

pes	parameter, (pe0*U^+(im)*E)
dBtao	gradient of dimensionless radius, dB/dtao
a1	Parameter, B(im)**2.
a2	Parameter, (0.5*pes*(1.-1./(1.+y)**3)*mu +1./(1.+y)**2.*dBtao)*B(im)
a3	Parameter, 0.5*pes*(1.+0.5/(1.+y)**3) *(1.-mu**2)/(1.+y)*B(im)
a4	Parameter, -2./(1.+y)
a5	Constant, -1.
a6	Parameter, -(1.-mu**2)/(1.+y)**2
a7	Parameter, 2.*mu/(1.+y)**2
a8	a2+a4
a8p	max(a8,0.)
a8n	min(a8,0.)
a9p	max(a9,0.)
a9n	min(a9,0.)
ak	Parameter, a8p/dy -a8n/dy +a9p/dmu-a9n/dmu-2*a5/dy**2 -2*a6/dmu**2
dtao	dimensionless time interval, c1*a1/ak
dphyp	(ph(i+1,j)-ph(i,j))/dy
dphyn	(ph(i,j)-ph(i-1,j))/dy
dphmup	(ph(i,j+1)-ph(i,j))/dmu
dphmun	(ph(i,j)-ph(i,j-1))/dmu
dphdy2	(ph(i+1,j)+ph(i-1,j)-2*ph(i,j))/dy**2.
dphdmu2	(ph(i,j+1)+ph(i,j-1)-2*ph(i,j))/dmu**2.
dph/dy(1,j)	Gradient of temperature at drobble surface
zeta	vaporization ratio
B	dimensionless radius, R /R_0
B_f	R_f /R_0

Flow chart

```
┌──────────┐
│  Start   │
└──────────┘
     │
     ▼
/ Read data dy, dmu, C1,    T, beta₀, d₀, d_c, d_h,   /
/ N_h, Q_d                                            /
     │
     ▼
/ Read data (properties of dispersed and continuous   /
/ phase)                                               /
     │
     ▼
┌─────────────────────────────────────┐
│ Calculate U₀ , using equation (3.76)│
└─────────────────────────────────────┘
     │
     ▼
┌─────────────────────────────────────┐
│ Calculate N_d, using equation (3.77)│
└─────────────────────────────────────┘
     │
     ▼
┌─────────────────────────────────────────┐
│ Calculate DRD, DRC, St, Ja, Pe₀, Fr₀    │
└─────────────────────────────────────────┘
     │
     ▼
┌──────────────────────────────────────────────┐
│ Calculate R_f  and B_f using equation (3.57)  │
└──────────────────────────────────────────────┘
     │
     ▼
┌─────────────────────────────────────────────────────────┐
│ Calculate R_cell ,using equation (3.78) and utilizing   │
│ equation(3.79), R_cell =(4/3.*  *N_d)**(-1/3.)          │
└─────────────────────────────────────────────────────────┘
     │
     ▼
   <  im=1  >
     │
     ▼
┌──────────────────────────────────┐
│ Calculate                        │
│ y_cell =(R_cell-R(im))/R(im)     │
└──────────────────────────────────┘
     │
     ▼
┌──────────────────────────────────┐
│ Calculate ny = y_cell/dy +1      │
└──────────────────────────────────┘
     │
     ▼
┌──────────────────────────────────┐
│ Calculate                        │
│ holdup=(R(im)/R_cell)**3         │
└──────────────────────────────────┘
     │
     ▼
┌──────────────────────────────────┐
│ Calculate E, Pes                 │
└──────────────────────────────────┘
     │
     ▼
┌──────────────────────────────────┐
│ assume ph(i,j)=0                 │
│ (initial value)                  │
└──────────────────────────────────┘
     │
     ▼
┌────────────────────────────────────────────────────────────────────────┐
│ Calculate ph (i,j) for steady state using iteration method             │
│ Ph(i,j)=-1/d₁*(d₂*ph(i-1,j)+d₃*ph(i+1,j)+d₄*ph(i,j-1)+d₅*ph(i,j+1))    │
└────────────────────────────────────────────────────────────────────────┘
     │
     ▼
    (1)
```

Equations rendered:

- Calculate U_0, using equation (3.76)
- Calculate N_d, using equation (3.77)
- Calculate DRD, DRC, St, Ja, Pe_0, Fr_0
- Calculate R_f and B_f using equation (3.57)
- Calculate R_{cell}, using equation (3.78) and utilizing equation (3.79), $R_{cell} = (4/3.* \ *N_d)**(-1/3.)$
- $im=1$
- Calculate $y_{cell} = (R_{cell}-R(im))/R(im)$
- Calculate $ny = y_{cell}/dy + 1$
- Calculate $holdup = (R(im)/R_{cell})**3$
- Calculate E, Pes
- assume $ph(i,j)=0$ (initial value)
- Calculate $ph(i,j)$ for steady state using iteration method
$$Ph(i,j) = -1/d_1 * (d_2 * ph(i-1,j) + d_3 * ph(i+1,j) + d_4 * ph(i,j-1) + d_5 * ph(i,j+1))$$

```
                                  ( 1 )
                                    │
     ┌──────────────────────────────┐
     │                              ▼
     │          ┌──────────────────────────────────┐
     │          │   Calculate kj and apply boundary │
     │          │   conditions, equation (3.56)     │
     │          └──────────────────────────────────┘
     │                            │
     │                            ▼
     │          ┌──────────────────────────────────┐
     │          │   Calculate dtao= C1*a1/ak        │
     │          └──────────────────────────────────┘
     │                            │
     │                            ▼
     │   ┌──────────────────────────────────────────────────┐
     │   │ Calculate new ph (i,j) using explicit method,     │
     │   │ phn(i,j)=ph(i,j)-dtao/a1*( (a8p*dphyn+a8n*dphyp)+  │
     │   │ (a9p*dphmun + a9n*dphmup)+ a5*dphdy2+a6*dphdmu2 )  │
     │   └──────────────────────────────────────────────────┘
     │                            │
     │                            ▼
     │        ┌──────────────────────────────────────┐
     │        │  Calculate dph/dy(1,j),using equation(3.67) │
     │        └──────────────────────────────────────┘
     │                            │
     │                            ▼
     │        ┌──────────────────────────────────────┐
     │        │  Calculate Nu,using equation(3.54)     │
     │        └──────────────────────────────────────┘
```

Calculate new ph (i,j) using explicit method,
$phn(i,j)=ph(i,j)-dtao/a1*((a8p*dphyn+a8n*dphyp)+(a9p*dphmun + a9n*dphmup)+ a5*dphdy2+a6*dphdmu2)$

Calculate dph/dy(1,j),using equation(3.67)

Calculate Nu,using equation(3.54)

Calculate new velocity $U^{+}(im+1)$, using Runge-Kutta method(3.59)

Calculate new radius B(im+1), using Runge-Kutta method(3.68)

Calculate new zeta, using equation (3.60)

Calculate new beta, using equation (3.61)

Is B B_f — No

Yes

Calculate h(im), Roa(im)

Calculate y_{cell}, ny

im=im+1

(2)

```
        ( 2 )
          |
          v
  +---------------------------+
  | Calculate final time, t_f |
  +---------------------------+
          |
          v
  +------------------------------------------+
  | Calculate dU_r/dt, using three point formula |
  +------------------------------------------+
          |
          v
  +------------------------------------+
  | Calculate Z, using equation (3.87) |
  +------------------------------------+
          |
          v
      (  Stop  )
```

تهدف الدراسة ألحاليه   نظري   لعملية التبخر بالتماس المباشر
لقطرات، تنمو بسبب تغير طورها، في مائع آخر لا يمتزج معها. تستهدف المحاولة الحالية
الحصول على توضيح أساسي لعمليات الانتقال (   ) المصاحبة للعملية.

تم تطوير نموذج رياضي لتمثيل العملية باستخدام النموذج الخلوي (cellular model)
بناء هذا النموذج على معادلات الاستمرارية

.

يهدف   الحصول على مميزات عملية التبحر بالتماس
(   )   طة بخلية كروية من المائع الأخر المحيط بها، واستخدام هذه
المميزات لتطوير نموذج رياضي للحصول على مميزات عن تبخر مجموعة من القط

.

تم تحليل ديناميكية الـ
ثم حلها سوي بطريقة عددية. أيضا تم حل معادلة الطاقة، المتضمنة سرعة الجريان الكامن
والتي أُخذ بنظر الاعتبار فيها التأثير بين القطرات المتجاورة، حلاً عددياً باستخدام تقنيات
. أجريت الحسابات لقطرات من البنتان الطبيعي المتبخرة في الماء.

تم عرض النتائج لحالتين :
بدلالة السرعة النسبية و الارتفاع   القطرة، وزاوية
. وقد بينت النتائج لهذه الحالة إن العوامل الرئيسية المؤثرة
على عملية التبخر هي القطر الابتدائي   وفرق درجات الحرارة بين المائعين.

وقد عُبر عن النتائج النظرية للحالة الثانية بدلالة نسبة حجم الطور المنثور إلى
المستمر،السرعة النسبية والارتفاع
والزمن والارتفاع اللازمين لإكمال عملية التبخر. أيضا اجري تحليل مفصل لدراسة تأثير

عدة عوامل مهمة على مميزات عملية التبخر، مثل القطر الابتدائي، فرق درجات الحرارة بين المائعين،

.

إضافة لذلك، قورنت نتائج النموذج الحالي للحالتين مع نتائج نظرية متو

بين النتائج   .   وكذلك قورنت النتائج الحالية مع نتائج عملية لباحثين آخرين وكان التقارب بين النتائج جيد.

نظرية

بر امتزاجي

كلية الهندسة

الهندسة الميكانيكية

من قبل

عمار علي عجيمي

(ماجستير هندسة ميكابيكية)

2011